Plasma-assisted development of plant-based biomaterials for wound-healing applications

Ph.D. Thesis

Jesus Romo Rico

December 2023

For the Degree of Doctor of Philosophy

In College of Science and Engineering

James Cook University

Supervisors:

Prof. Mohan Jacob, Dr. Smriti M. Krishna, Prof. Johnathan Golledge and Prof. Krasimir Vasilev

DECLARATION

I declare that this Ph.D. thesis is my own work and has not been submitted in any form for another degree or diploma at any university or institute of tertiary education. Information derived from the published and unpublished work of other have been acknowledged in the text and a list of references is given.

Jesus Romo Rico
December 2023

STATEMENT OF ACCESS TO THIS THESIS

I, the undersigned, the author of this work, understand that James Cook University will make this work available for use within the University, and via the Australian Digital Thesis Network, for use elsewhere.

I understand that as an unpublished work, a thesis has significant protection under the Copyright Act. I do not wish to place any restriction on access to this thesis. However, any use of its content must be acknowledged and could be potentially be restricted by future patents.

Jesus Romo Rico

December 2023

ACKNOWLEDGMENTS

First and foremost, I would like to express my sincere gratitude to my supervisor, Prof. Mohan Jacob, for his unwavering support and invaluable contribution to my growth as a researcher.
I am also deeply thankful to my advisors, Dr. Smriti Krishna and Prof. Jon Golledge, for their significant assistance and insightful ideas that have greatly enriched my candidature.
I would like to extend my thanks to Prof. Krasimir Vasilev for giving me the opportunity to collaborate with him and his esteemed research group at Flinders University. Without their contribution, none of my achievements would have been possible.
I am grateful to the College of Science and Engineering department and the College of Medicine and Dentistry at James Cook University for their support. I would also like to thank all my colleagues and JCU personnel who have played a role in the development of this project.
I am truly appreciative of Dr. Pacific Huynh, Dr. Shiv, and Dr. James for generously sharing their laboratory experience with me.
Special recognition goes to the Krasi's research group at Flinders University, particularly Dr. Richard Bright and Dr. Andrew Hayles for all the time and ideas we shared inside and outside of the lab. Also, many thanks to Dr. Neethu, Dr. Dennis, and Dr. Khan, for their valuable contribution.
I would like to express my sincere thanks to Dr. Katya Bazaka for her contribution to my literature review. Her comments and revisions were immensely valuable during this stage of my project.
I am deeply grateful to my beloved family and friends who have stood by me with unwavering love and support, always present during the best and the most challenging times. To Jesus, Lourdes, Sebastian, Gabriela, Guadalupe, Santiago, Martin, Javier, Angel, Cecilia, Miguel, Alejandro, Jano, Osiris, Gaspar, Pablo, JD, Riccardo, Ale, and Juan, my apologies if I have unintentionally omitted any names. I want you all to know that I am sincerely thankful to each one of you.
I consider myself incredibly fortunate to have met all my friends in Townsville, who have made my life easier and happier during the time we have spent together.
I would like to express my deepest appreciation to Evgenia, she has played an integral role in all my research and life projects, offering dedication and patience. I hold her in the highest regard and I am profoundly grateful for her influence and presence during the past years. Her support and contributions have made a lasting impact, for which I am forever thankful.

Lastly, I would like to acknowledge Simeon, who always believed in me and taught me invaluable lessons that I could not have learned elsewhere. Wherever he may be, I am certain he would be proud of my accomplishments.

ABSTRACT

Plant secondary metabolites (PSMs) are volatile molecules with medicinal and antibacterial properties which can be integrated into medical device surfaces by radiofrequency plasma-enhanced chemical vapor deposition (RF-PECVD). This thesis presents the RF-PECVD fabrication of plasma polymers (PP) and graphene (Gr) derived from oregano secondary metabolites (OSMs). The biocompatibility, antibacterial and wound-healing properties were in-depth investigated and correlated with the surface properties of PP-OSMs and Gr.

PP films were fabricated using OSMs at different RF power levels. The resulting films were smooth and super hydrophilic. The films had bactericidal properties against Gram-negative *P. aeruginosa* and antifouling properties against Gram-positive *S. aureus*. They also supported fibroblast growth and proliferation without significant cytotoxicity. In addition, PP-OSMs are shown to have good adhesion and spread of fibroblasts. The findings suggest PP-OSMs films have potential in medical applications, such as wound dressings, due to their antibacterial and biocompatible properties.

Moreover, we investigated the wound-healing properties of oregano-based plasma polymer (OPP) and found that it has the potential as a wound-healing interface for dressings and bandages. This study provides an *in vitro* evaluation of the biocompatibility and immune responses to OPP using RAW 264.7 macrophage-like cells and human foreskin fibroblasts. OPP did not activate the pro-inflammatory responses of RAW macrophages and showed potential anti-inflammatory and antioxidant properties on macrophages treated with LPS. OPP promoted wound closure faster than the control samples. The study suggests that OPP provides mammalian cell support, anti-inflammatory activity, antioxidant properties, enhanced cell proliferation, as well as antibacterial and antifouling properties previously reported. The results suggest that OPP is a strong candidate as a wound-healing interface for dressings and bandages.

The study focused on depositing graphene on CoCr substrates using RF-PECVD and OSMs as Gr precursors. With the increasing power and temperature, in the company of hydrogen gas, RF-PECVD can defragment OSM molecules and recombine them into carbon nanostructures such as graphene and its allotropes. The presence of graphene was confirmed using various spectroscopy techniques, and biocompatibility tests showed that CoCr-Gr had similar viability, adhesion, and morphology of RAW macrophages compared to CoCr alone. CoCr-Gr also had

a significant bactericidal and antifouling effect against *P. aeruginosa* and *S. aureus*. The results suggest that CoCr-Gr has potential applications as an antibacterial coating for implantable devices.

CONTENTS

LIST OF FIGURES

Chapter 2.

Chapter 3.

Chapter 4.

Chapter 5.

LIST OF TABLES

LIST OF PUBLICATIONS

Potential of plant secondary metabolite-based polymers to enhance wound healing. Acta Biomaterialia, Volume 147, 2022, Pages 34-49, ISSN 1742-7061, https://doi.org/10.1016/j.actbio.2022.05.043. *Jesus Romo-Rico, Smriti Murali Krishna, Kateryna Bazaka, Jonathan Golledge, and Mohan V. Jacob.*

Plasma polymers from oregano secondary metabolites: An antibacterial and biocompatible plant-based polymers. Plasma Processes and Polymers, Volume 19, 2022, 19:e2100220, ISSN 1612-8850, https://doi.org/10.1002/ppap.202100220. *Jesus Romo-Rico, Smriti Murali Krishna, Jonathan Golledge, Andrew Hayles, Krasimir Vasilev, and Mohan Jacob.*

In Vitro Study of the Wound healing Properties of an Oregano Based Plasma Polymer, ACS Biomaterials Science & Engineering, 2023, Under review. *Jesus Romo-Rico, Richard Bright, Neethu Ninan, Smriti Murali Krishna, Krasimir Vasilev, Jonathan Golledge, and Mohan Jacob.*

Antimicrobial graphene-based coatings for biomedical implant applications. Carbon Trends, Volume 12, 2023, 100282, ISSN 2667-0569, https://doi.org/10.1016/j.cartre.2023.100282. *Jesus Romo-Rico, Richard Bright, Smriti Murali Krishna, Krasimir Vasilev, Jonathan Golledge, Mohan V. Jacob.*

STATEMENT OF THE CONTRIBUTION OF OTHERS

Nature of Assistance	Contribution	Names, Titles and Affiliation of Co-Contributors
Intellectual support	Project Supervision	***Professor Mohan Jacob*** (Associate Dean, Research Education, College of Science and Engineering, James Cook University, Townsville) ***Professor Jonathan Golledge*** (Head of the Queensland Research Centre for Peripheral Vascular Disease, James Cook University, Townsville) ***Professor Krasimir Vasilev*** (Matthew Flinders Professor, Flinders University) ***Dr Smriti Krishna*** (Research officer, Baker Heart and Diabetes Institute) ***Richard Bright, PhD candidate*** (Flinders University) ***Andrew Hayles, PhD candidate*** (Flinders University) ***Dr Neethu Ninan, Research Associate*** (Flinders University) ***Professor Katia Bazaka*** (Australian National University)
Financial support	Research Funding Stipend Support	***College of Science and Engineering*** (James Cook University) ***Cooperative Research Centre for Developing Northern Australia***
Data Collection	Laboratory Assistance	***Richard Bright, PhD candidate*** (Flinders University) ***Andrew Hayles, PhD candidate*** (Flinders University) ***Dr Neethu Ninan, Research Associate*** (Flinders University) ***Dr Pacific Huynh, Postdoctoral fellow*** (Icahn School of Medicine Mount Sinai)
		Richard Bright, PhD candidate (Flinders University) ***Andrew Hayles, PhD candidate*** (Flinders University)

Data Analysis	Assistance with statistical analysis	***Dr Neethu Ninan, Research Associate*** (Flinders University) ***Dr Pacific Huynh, Postdoctoral fellow*** (Icahn School of Medicine Mount Sinai) ***Professor Mohan Jacob*** (Associate Dean, Research Education, College of Science and Engineering, James Cook University, Townsville) ***Professor Krasimir Vasilev*** (Matthew Flinders Professor, Flinders University) ***Dr Smriti Krishna*** (Research officer, Baker Heart and Diabetes Institute)

Chapter 1

Introduction

1.1. Introduction

Chronic wounds are wounds that fail to heal within a reasonable amount of time. They are often associated with underlying health conditions such as diabetes, obesity, and peripheral arterial disease. Chronic wounds can cause pain, discomfort, and reduced mobility, which can significantly impact the quality of life of the patients. They also represent a substantial burden to healthcare systems worldwide, with significant costs associated with their treatment and management. One of the challenges of managing chronic wounds is biofilms, which are communities of microorganisms that can form on the wound surface and impair wound-healing. Additionally, the emergence of antibiotic-resistant bacteria has further complicated the treatment of chronic wounds. Oxidation and inflammation are other challenges caused by a variety of factors, including environmental toxins, stress, poor diet, infections, and chronic diseases such as diabetes and cardiovascular disease. These factors can lead to the production of reactive oxygen species (ROS), which can damage cells and tissues and trigger inflammation. Antioxidants are molecules that can neutralize ROS and prevent their harmful effects. They can act as physical barriers that prevent ROS from being generated or accessing important biological sites. By inhibiting ROS, antioxidants can reduce inflammation by preventing the activation of pro-inflammatory cytokines and pathways. This has led to a growing interest in the development of wound-healing materials, derived from plant secondary metabolites (PSMs), which have been shown to have wound-healing properties.

PSMs are natural compounds found in plants that have been shown to have antioxidant, anti-inflammatory, and antimicrobial properties. They can be incorporated into wound dressings through various fabrication techniques, such as electrospinning, gelation, emulsification, and plasma polymerization among others. The use of PSMs in wound dressings is an emerging area of research that has the potential to reduce the healthcare costs associated with chronic wounds, as well as improve the quality of life of patients. Oregano is a popular herb that has been used for centuries in traditional medicine to treat respiratory infections, skin conditions, and digestive disorders. Oregano contains secondary metabolites, which are volatile molecules that are responsible for its health benefits. The antimicrobial properties of oregano are attributed to

the presence of phenolic monoterpene carvacrol (CR). Depending on the species of oregano, the content of CR can be as high as 90%. CR disrupts bacterial membrane permeability, which leads to the leakage of important ions like Na+ and K+, inhibits enzyme activity, and causes irreparable damage to bacteria.

Plasma technology is a promising method for the fabrication of wound-healing materials, including those incorporating PSMs with antibacterial properties. PSMs contain monoterpenes that can inhibit bacterial growth by disrupting membrane function and ion transport. One method for incorporating PSMs onto wound dressings is the use of RF-PECVD, which allows for the formation of plasma polymers from PSMs by partially or fully fragmenting and reconstituting them as highly crosslinked polymeric coatings on surfaces. The RF-PECVD technique can be optimized to retain the functional groups of PSMs in the coatings, allowing for flexibility in application and tuning of the final properties of the resulting polymeric surface. Moreover, RF-PECVD can be modified to create graphene nanostructures from PSMs precursors, the increment in temperature and plasma power facilitates the creation of sp2 bonding of carbon nanostructures. Graphene-based coatings have been used in wound-healing applications and have been shown to inhibit the growth of a wide range of bacteria.

The use of RF-PECVD for fabricating of Oregano-derived materials is a feasible technique that allows to obtain green materials that can be used in wound-healing applications such as wound dressings and implants. In this project, we fabricated plasma polymers and graphene coatings using RF-PECVD and oregano secondary metabolites as precursor material and studied their wound-healing properties.

1.2. Research gap

The constant increasing of chronic wounds in an aging population have brought the attention to the scientific community to develop materials that can help chronic wounds to heal. For example, wound dressings with tailored properties to suit specific wound-healing process like oxidation, inflammation and infection. Though Oregano oil exhibited wound-healing properties, there is no attempt reported to develop an Oregano-derived plasma polymer that can be used in wound-healing by retaining the medicinal values and utilise it as a coating in wound dressings or implants. The use of RF-PECVD to fabricate polymer films from Oregano oil in commercial wound dressings is a promising alternative strategy to enhance wound-

healing by the inhibition of pro-inflammatory cytokines, reducing reactive oxygen species and infection.

1.3.Research objectives

This project aims to fabricate, characterize and study the wound-healing properties of plasma polymers and graphene coatings using RF-PECVD and oregano secondary metabolites.
The following objectives will be carried out:

- Synthesis of the oregano-based plasma polymers and graphene using RF-PECVD.
- Characterization of the plasma fabricated materials using advanced techniques.
- Study the wound-healing properties of oregano-based plasma polymers and graphene.

1.4.Thesis organization

The presented thesis consists of 6 chapters. A brief abstract is provided at the beginning of each chapter to maintain consistency and coherence when reading the thesis in sequential order. The thesis is formatted based on the published articles (without any change) and articles under peer review.

Chapter 1 presents the rational and objectives of this study.

Chapter 2 reviewed the literature on how plant secondary metabolites-based polymers can enhance wound-healing. We highlighted the anti-inflammatory and antioxidant mechanisms, as well as the antibacterial properties and potential against antibiotic resistance bacteria. This study was published as Potential of plant secondary metabolite-based polymers to enhance wound-healing. *Jesus Romo-Rico, Smriti Murali Krishna, Kateryna Bazaka, Jonathan Golledge, and Mohan V. Jacob. Acta Biomaterialia, 2022*

Chapter 3 presented the fabrication of PP-OSMs. The surface and chemical characterization shows smooth roughness, super hydrophilic properties and the retention of the functional groups of OSMs on the PP-OSMs. The biocompatibility and antibacterial properties of PP-OSMS were evaluated. Our findings suggest PP-OSMs as a potential wound-healing agent against bacterial infection. This chapter was published as Plasma polymers from oregano

secondary metabolites: An antibacterial and biocompatible plant-based polymers. *Jesus Romo-Rico, Smriti Murali Krishna, Jonathan Golledge, Andrew Hayles, Krasimir Vasilev, and Mohan Jacob. Plasma Processes and Polymers, 2022.*

Chapter 4 studied the wound-healing properties of an oregano-based plasma polymer (OPP). The results showed that OPP had anti-inflammatory and antioxidant properties, did not cause any pro-inflammatory responses or activate ROS, and promoted wound closure faster than the control samples in an *in vitro* wound-healing assay. These findings suggest that OPP has potential as a wound-healing interface for dressings and bandages due to its multiple beneficial properties, such as supporting mammalian cell growth and promoting wound closure. *In Vitro* Study of the Antioxidant Activity and the Wound Closure Assessment of an Oregano-Based Plasma Polymer. *Jesus Romo-Rico, Richard Bright, Neethu Ninan, Smriti Murali Krishna, Jonathan Golledge, Krasimir Vasilev, and Mohan Jacob.*

Chapter 5 describes the fabrication of graphene onto a medical grade CoCr alloy surface using *Origanum vulgare* as a precursor material by RF-PECVD at high power and high temperature. The deposition was confirmed by Raman spectroscopy, X-Ray photoelectron spectroscopy (XPS), and scanning electron microscopy (SEM). The biocompatibility and antibacterial properties of the resulting CoCr-Gr were investigated. CoCr-Gr was found to be biocompatible, as it promoted cell adhesion and spreading of RAW 267.4 Macrophage-Like cells. CoCr-Gr was also effective in inhibiting the attachment of *P. aeruginosa* and was antibacterial against *S. aureus* and *P. aeruginosa*. These results suggest that CoCr-Gr could be a promising antibacterial coating material for implantable medical devices. Antimicrobial graphene-based coatings for biomedical implant applications. *Jesus Romo-Rico, Richard Bright, Smriti Murali Krishna, Jonathan Golledge, Krasimir Vasilev, and Mohan Jacob.*

Chapter 6 reports the overall conclusion of this thesis and presents future work recommendations.

Chapter 2

Literature Review

The potential of plant secondary metabolite-based polymers to enhance wound-healing

Chapter 2 reviews the scientific background on how plant secondary metabolites (PSMs) based polymers can promote wound-healing and methods of incorporating PSMs-based polymers into wound dressings. To achieve this objective, the wound-healing process and the causes of chronic wounds are described in this chapter. The anti-inflammatory and antioxidant mechanisms by which PSMs may promote wound-healing are also discussed. The antibacterial mechanisms and the advantages of PSMs over antibiotics are also covered in this chapter.

Chapter 2 was published as *Jesus Romo-Rico, Smriti Murali Krishna, Kateryna Bazaka, Jonathan Golledge, and Mohan V. Jacob*. Potential of plant secondary metabolite-based polymers to enhance wound-healing. Acta Biomaterialia, Volume 147, 2022, ISSN 1742-7061, https://doi.org/10.1016/j.actbio.2022.05.043.

The potential of plant secondary metabolite-based polymers to enhance wound-healing

Graphical abstract

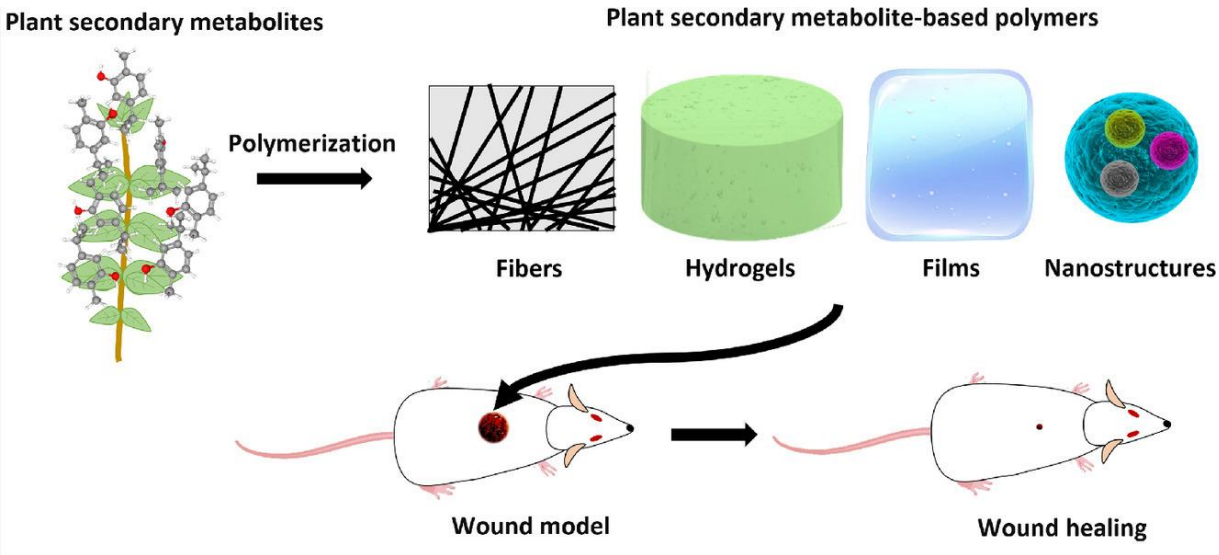

Abstract

There is a global epidemic of non-healing wounds. Chronic inflammation, overexpression of pro-inflammatory cytokines, oxidative stress and bacterial infection are implicated in delayed wound-healing. Natural extracts are a rich source of bioactive molecules called plant secondary metabolites (PSMs) that include terpenes and phenols. These molecules may facilitate wound-healing through their antioxidant, anti-inflammatory, and antibacterial activity. After briefly outlining the process of wound-healing and how it is compromised in chronic wounds, this review focuses on investigating how PSMs-based polymers may improve wound-healing. Best methods for incorporating PSMs into wound dressings are reviewed and critically compared. The existing body of literature strongly suggests that PSMs-based polymers incorporated into wound dressings could have clinical value in aiding wound-healing.

Statement of significance

Chronic wounds develop by the persistence of inflammation, oxidative stress and infection. Chronic wounds affect the worldwide population, by reducing the quality of life of patients with significant cost to healthcare systems. To help chronic wounds to heal and overcome this burden, materials with anti-inflammatory, antioxidant and antibacterial properties are required. Plant secondary metabolites (PSMs) are volatile materials that have all these properties. PSMs-

based polymers can be fabricated by polymerization techniques. The present review provides an overview of the state-of-the-art of the wound-healing mechanisms of PSMs. Current developments in the field of PSMs-based polymers are reviewed and their potential use as wound dressings is also covered.

2.1. Introduction

Dressings have been applied to wounds since ancient times and their evolution has been constant [1]. Wound dressings have many functions such as absorbing exudate, retaining moisture, decreasing microbial contamination, and potentially delivering wound-healing agents to the wound milieu. A large range of different types of wound dressings has been developed, including films, hydrogels, foams, hydrocolloids, alginates, gauzes, hydro-fibers and tissue-engineered skin, among others [2-5]. Gauzes, for example, are the most common wound dressings used to protect the wound from external contamination and maintain appropriate levels of moisture. Tissue-engineered skin has been proposed to support cell proliferation, migration and differentiation, and to reduce the risk of infection to accelerate wound-healing [6-9].

Chronic wounds reduce the quality of life of patients and represent a burden to healthcare systems worldwide [10]. Chronic wounds affect the quality of life of approximately 2% of the global population [11]. In developed countries like the USA, the total Medicare expenses for all types of wounds range from 3.8% to 13.3% of the total budget [12]. In Wales, wounds account for 5.5% of the National Health System (NHS) spending [13]. Developing countries, too, spend ~3% of their total healthcare expenditure on chronic wounds [14]. Therefore, there is an urgent need to develop novel wound dressings that not only promote wound-healing but also help reduce healthcare costs associated with delayed wound-healing.

The incorporation of plant secondary metabolites (PSMs) in wound dressings is an emerging topic of research that is driven by their wound-healing properties. PSMs have been proposed to inhibit inflammation and promote cell proliferation and wound remodelling [15]. PSMs have been included as dressings through topical application or by polymerization techniques, such as electrospinning, gelation, emulsification, homogenization, film hydration, supercritical impregnation¸ solution casting, and encapsulation. [16-21]. Despite the available literature about the different uses of PSMs and their applications, to our knowledge, we are the first authors to publish an extensive review that summarizes the wound-healing mechanisms of

PSMs along with the most relevant methods of fabrication of PSMs-based derived polymers for wound dressings.

Nevertheless, the incorporation of PSMs into wound dressings remains a relatively novel approach to promoting wound-healing and limiting wound infection that has a strong potential to address some of the persisting challenges of wound management. In this review, we briefly discuss the mechanisms involved in wound-healing, biofilm formation, antibiotic resistance, and their impact on wound-healing. We summarize the properties by which PSMs have been proposed to promote wound-healing, with a focus on their antioxidant and anti-inflammatory properties. The review also describes methods by which PSMs have been or may be incorporated into wound dressings.

2.2. Wound-healing

Normal wound-healing is usually described by three overlapping stages, namely hemostasis/inflammation, proliferation, and remodelling/maturation. These stages are regulated by a cascade of different factors and mediators [22, 23]. In the first stage, hemostasis is triggered by the constriction of blood vessels to stop blood loss. Platelets aggregate to form a fibrin network or clot. Different types of cells such as neutrophils, monocytes, keratinocytes and fibroblasts migrate to the wound site. Neutrophils kill bacteria and degrade damaged cells. Monocytes transform into macrophages and engulf debris, bacteria and remaining neutrophils. Macrophages stimulate fibroblasts to form granulation tissue. They also stimulate endothelial cells to promote re-epithelialization and angiogenesis. In the proliferation/reconstruction phase, fibroblasts continue to form granulation tissue over the wound site and transform into myofibroblasts to promote contraction of the wound edges. The last stage, remodelling and maturation starts with apoptosis and the removal of dead cells. Collagen deposition starts to build up leading to contraction of the wound edges until the scar and epidermis mature and the wound finally heals (Figure. 2.1 A) [24].

A comparison between cell composition within the normal and impaired wounds follows. In acute wounds, the wound-healing process occurs without any interruption, whereas in impaired wounds, the wound-healing process is delayed by different factors such as persistent inflammation, oxidation, and/or infection. If any of the above elements fail, the wound can become chronic. A chronic wound is essentially a non-healing wound. Chronic inflammation, oxidative stress, bacterial infection and a deficit of cell proliferation have been implicated in impaired wound-healing (Figure. 2.1 B) [25]. Chronic inflammation contributes to the

formation of excess reactive oxygen species (ROS), causing further molecular damage and tissue injury [26]. ROS promote inflammation and the formation of free radicals (e.g., nitride oxide (NO), superoxide (SO), anion (O_2*-), hydrogen peroxide (H_2O_2) and hydroxyl (OH*)) and the release of pro-inflammatory cytokines such as interleukin (IL)-1, IL-6, tumor necrosis (TNF)-α and interferon (IFN)-γ. Antioxidant and free radical scavengers attenuate inflammation by downregulating pro-inflammatory cytokines through the inhibition of ROS [27].

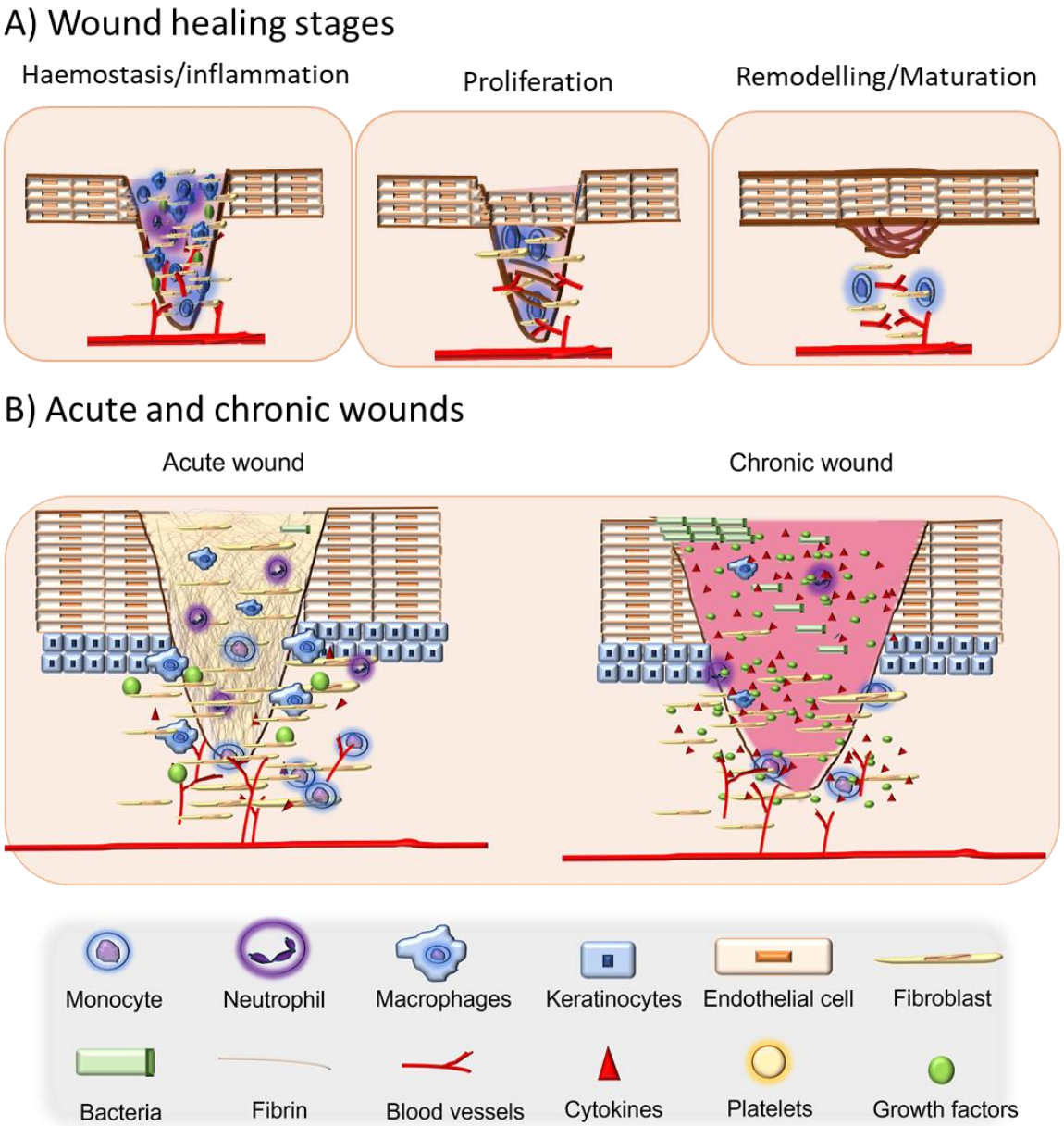

Figure 2. 1. A) Wound-healing stages: haemostasis and inflammation, proliferation and remodelling/maturation. B) A comparison between cell composition within normal and impaired wounds.

Wound infection occurs when bacteria, viruses or other microorganisms evade the immune system of the host and colonize the wound, leading to pain, wound contamination, slow re-epithelization and bad odour [26]. An infected wound compromises the general health of the patient. The overgrowth of bacteria within the wound may evolve into a structure community, *i.e.* a biofilm, which is held together by extracellular polymeric substances and is attached to the wound bed [28].

2.3. Antibiotic resistance and biofilms

The efficacy of antibiotics has diminished over time due to bacterial survival mechanisms, including genetic mutations and bacterial ability to form highly resistant biofilm communities. Antibiotic resistance (AR) and biofilms play a major role in chronic wounds. Approximately 60% of chronic wounds are associated with AR and biofilms. In the United States alone, AR affects nearly 3 million people and more than 35,000 people die as a consequence of developing antibiotic-resistant infections [29]. AR can develop via the repeated administration of antibiotics whereas biofilm infection is more likely to develop in diabetic patients due to metabolic dysfunction, and dysregulation of inflammatory and immune responses. Therefore, to overcome AR and biofilm-infected wounds it is important to know what they are and how to treat them.

AR arise when a bacterium evolves through chromosomal mutation or by the acquisition of mobile genetic elements (free-floating RNA). AR bacteria also eliminate antibiotics through free efflux pumps. Additionally, plasmid and bacteriophages transfer genes to the bacterial population through horizontal gene transfer (HGT). HGT has two main mechanisms, conjugation and transduction. In conjugation, AR genes are transferred allowing bacteria to evolve resistance whereas during transduction, bacteriophages transfer AR genes to bacteria (Figure. 2.2 A) [30]. Another mechanism of bacterial survival is the development of biofilms. Biofilms are microbial congregations generally formed by single or multispecies of microorganisms including bacteria, fungi and protists enclosed within a matrix of extracellular polymeric substances (EPS) adherent to an abiotic or biotic surface [31, 32]. EPS have a major role in biofilm formation, development and survival. EPS facilitate the development of microbial resistance through intracellular interactions termed quorum sensing (QS). QS benefits microorganisms within the biofilm by enhancing access to nutrients and increasing resistance to antibiotics. Biofilm formation is often described in four steps, namely surface

attachment, microcolony formation, biofilm maturation, dispersal and detachment [32]. In *Caulobacter crescentus*, a model microorganism widely used to study biofilm formation, mechano-sensing of the surface is induced by a flagellar motor that acts as a sensor for stimulating polysaccharide adhesin and surface adherence [33, 34]. Bacterial cells aggregate and proliferate in the wound. Subsequently, biofilms mature with ongoing bacterial proliferation (Figure. 2.2 B) [35]. Mature biofilms are more difficult to eradicate, leading to a greater potential for chronic wound development.

Many strategies have been implemented to treat biofilms, from aggressive and intensive antibiotic administration to cold plasmas, ultrasounds, electromagnetic currents and photothermal techniques. However, these techniques are difficult to implement *in vivo* and require expensive equipment [36]. Likewise, the administration of antibiotics is generally ineffective leading to antibiotic-resistance (AR). There is wide evidence of the use of PSMs against AR bacteria and biofilms [37]. The mechanisms of how PSMs can contribute to wound-healing including antibacterial mechanisms are discussed in the following sections.

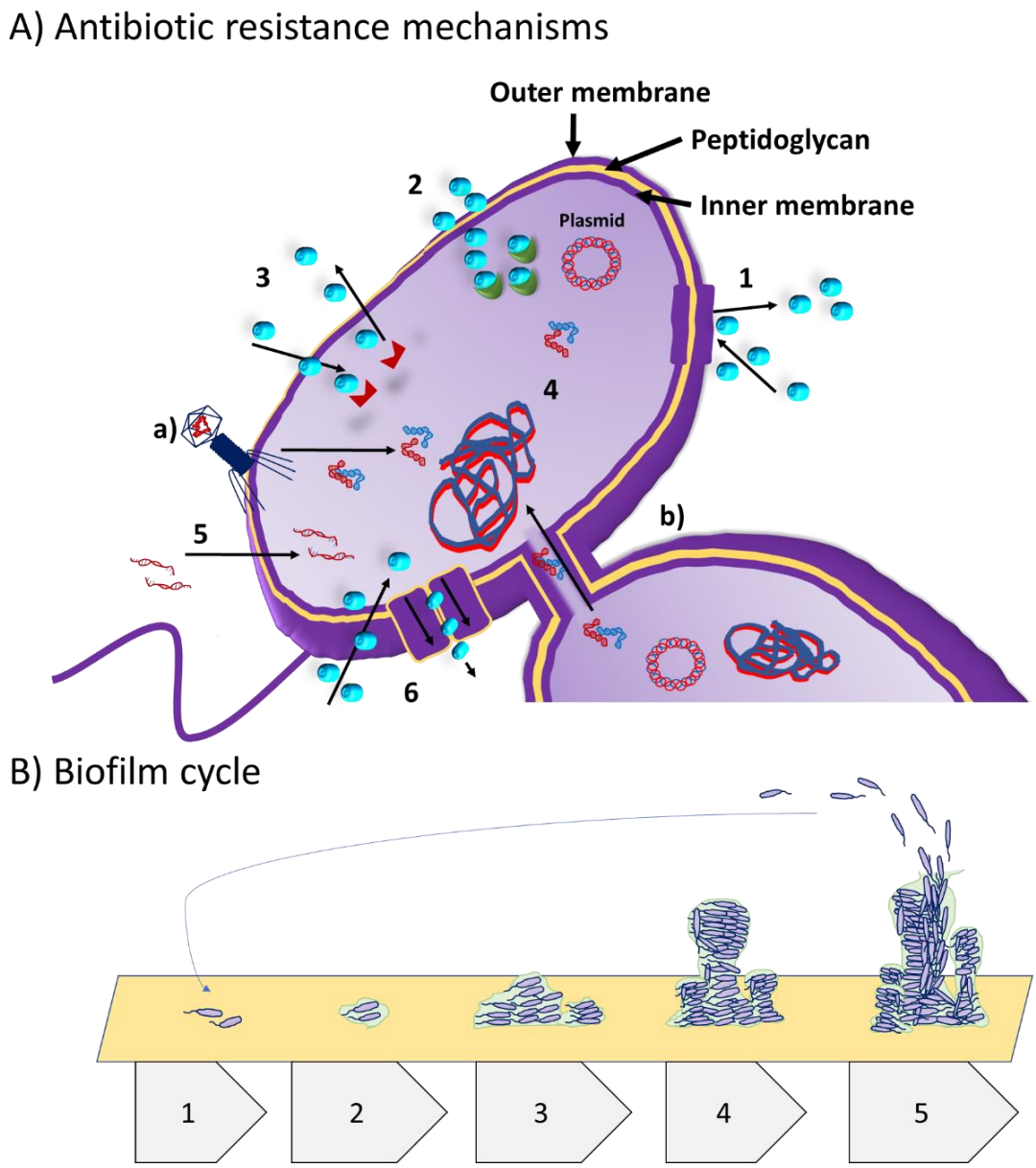

Figure 2. 2. A) Representation of antibiotic resistance mechanisms in a gram-negative bacterium: 1. Cell wall modification, 2. Antibiotic inactivation by enzymes, 3. Drug target modification, 4. Chromosomal mutation by a) Bacteriophage AR gene transduction and b) conjugation by pilus tube, 5. Free-floating RNA and 6. Efflux pumps. B) Biofilm cycle: 1. Planktonic bacteria move freely around the surface, then bacteria attach to the surface, and a microcolony formation of biofilm starts, biofilm grows and maturates d), then bacteria detach and disperse along the surface.

2.4. Mechanisms by which PSMs may promote wound-healing

PSMs, such as those found in essential oils and herb extracts, are bioactive molecules with strong wound-healing potential. Terpenes and phenols in particular display biological activity

that is highly relevant to wound-healing [38], namely anti-oxidant, anti-bacterial, anti-fungal and anti-inflammatory properties [38-44].

2.4.1 Antioxidant and anti-inflammatory effects of PSMs

Antioxidants act as physical barriers that prevent ROS generation or ROS access to important biological sites. The inhibition of ROS reduces inflammation by preventing the activation of pro-inflammatory cytokines (e.g., TNF-α, IL-1β, IL-6) and pro-inflammatory pathways (e.g., NF-kb, MAPK), see (Figure. 2.3 A, B). The antioxidant and anti-inflammatory properties of PSMs are listed in **Table 2.1**.

In a study by Cheng *et al.* [45], the monocyte/macrophage-like cells (RAW264.7 cells) were pre-treated with oregano essential oil (OEO) for 12h and subsequently incubated with lipopolysaccharide (LPS) for 12h. It was shown that LPS increased mRNA levels of pro-inflammatory cytokines such as TNF-α, IL-1β, and IL-6 (Figure. 2.3 C), whereas OEO inhibited the mRNA expression of the pro-inflammatory cytokines. Furthermore, OEO-treated cells showed decreased production of inflammatory mediators in the AKT, MAPKs and NF-κβ pathways. Additionally, oxidative stress activator nicotinamide adenine dinucleotide phosphate (NADPH) oxidase 2 was inhibited in OEO treated cells [46]. In other studies, essential oils from *Origanum vulgare* collected at different locations of Tunisia were reported to scavenge 2,2-diphenyl-1-picrylhydrazyl (DPPH) radicals. These effects were correlated with the percentage of phenolic compounds present in the oils collected from the different regions [47]. Different extracts of oregano with high content of carvacrol showed inhibition of ROS and NO production in an LPS activated macrophage cell line (RAW 264.7 cells) [48-50]. Additionally, oregano extract promoted downregulation of cyclooxygenases activity (COX-1 and COX-2) and reduced mitochondrial dehydrogenase activity [48-50]. Kivrak *et al.* [51], recently published a detailed report of the antioxidant activity of different types of lavender and lavandin extracts with high content of linalyl acetate and linalool. It was shown that the extracts rich in linalyl acetate and linalool were more effective in scavenging of DPPH, ABTS and β-carotene. This result suggests the potential antioxidant properties of *Lavandula angustifolia* and its extracts.

Table 2. 1. Examples of anti-inflammatory effects of PSMs.

PSMs	Inflammatory agent	Model	Mechanism of action	Reference

	Fe^{2+}	SH-SY5Y cells	↓ TNF-α[a)], IL-1β[b)], IL-6 ↓MAPK[c)]/JNK[d)]-NF-κβ[e)]	[52]
Oregano oil Carvacrol Thymol	LPS[f)]	RAW 264.7 cells	↓ TNF-α, IL-1β, IL-6 ↓ MAPK, NF-κβ, AKT[g)] ↓ NOX2[h)], ROS[i)]	[45]
Lavender oil Linalool	LPS	Monocytes THP-Cells	↓ Phosphor- NF-κβ ↓TLR4[j)]	[53]
	Croton oil	Mice, edema model	↓Edema formation ↓MPO[k)] ↓Nitric oxide	[54]
Tea Tree oil Terpinen-4-ol	LPS, TLR/4, TLR2/4	Human monocytes	↓ IL-1β, IL-6, IL-10 ↓ NF-κβ, MAPK	[55]
Rosa laevigata	LPS	RAW 264.7 cells	↓ NF-κβ, TNF-α, IL-1β, ↓IL-6 and IL-10	[56]
18β glycyrrhetinic acid Isoliquiritigenin Ursolic acid	LPS	RAW 264.7 cells	↓ ICAM-1, TNF-α, COX-2, iNOS, NF-κβ	[57]
Malaxis acuminata	N/A	Enzyme 5-lipoxygenase	Anti-hyaluronidase activity Anti-5-LOX activity	[58]
Eupafolin	LPS	RAW 264.7 cells	↓ p38 MAPK, ERK1/2, JNK, AKT and p65	[59]
Zygophyllum album	DCFH-DA[l)] assay	Human skin fibroblast	↓NO	[60]

Abbreviations: a) Tumor necrosis factor-alpha, b) interleukin, c) mitogen-activated protein kinase, d) c-Jun N-terminal Kinase, e) nuclear factor kappa light chain enhancer of activated B cells, f) lipopolysaccharide, g) protein kinase b (Akt), h) nicotinamide adenine dinucleotide phosphate oxidase isoform 2, i) reactive oxygen species, j) toll-like receptor, k) myeloperoxidase, l) 20,70-dichlorofluorescein-diacetate.

In a study by Huang *et al.* [53], human monocyte (THP) cells were first activated with LPS and subsequently treated with lavender essential oil (LEO). Protein levels of phosphor-NF-κβ and membrane toll-like receptor 4 (TLR4) were increased by LPS stimuli and decreased after

treatment with LEO. Linalool and linalyl acetate are the major components of LEO. The authors also reported an increase in the expression of the cytoprotective heat shock protein (HSP)-70 after LEO and LPS treatment, however, there were no changes in HSP70 expressions between the treatment groups. The authors speculated that this result could be associated with the contribution of signalling molecules produced by both treatments. However, this pathway is not well elucidated yet [53]. The influence of tea tree oil (TTO) and terpinen-4-ol was evaluated on human monocytes cell line [55]. Monocytes were treated with LPS, TLR/4, and TLR2/4 activators. Terpinen-4ol showed major activity on the reduction of pro-inflammatory cytokines, specifically on levels of TNF-α, IL-1β, IL-6, and IL-10 by the inhibition of NF-κβ, p38, and ERK MAPK pathways. These pro-inflammatory markers were not inhibited by pure TTO, suggesting the anti-inflammatory potential of terpinen-4ol.

The anti-inflammatory properties of PSMs from traditional medicine plants (TCMP) have been also studied. For example, *Rosa laevigata* leaves have been used in TCMP, particularly in skin treatments, burns and ulcers. The inflammatory properties of this plant and its components have been studied in LPS-stimulated RAW 264.7 cells. *Rosa laevigata* compounds are able to downregulate TNF-α, IL-1β, IL-6, and IL-10 production after 8h LPS treatment [56]. The anti-inflammatory effect of other TCMP, such as *Glycyrrhiza glabra* and *Eriobotrya japonica* and their components have been investigated in LPS-treated RAW 264.7 cells. 18β glycyrrhetinic acid, Isoliquiritigenin and ursolic acid are the secondary metabolites of *Glycyrrhiza glabra* and *Eriobotrya japonica* that inhibited ICAM-1, TNF- α, COX-2 and iNOS through the suppression of NF-κβ expression [57].

Studies on the anti-inflammatory potential of a terrestrial orchid, *Malaxis acuminata*, demonstrated an inhibition of the 5-lipoxygenase (5-LOX) pathway [58]. 5-LOX. 5-LOX catalyzes the conversion of arachidonic acid to pro-inflammatory leukotrienes that are mediators of inflammatory and allergic reactions [61]. *M. acuminata* showed inhibition against hyaluronidase enzyme responsible for hyaluronic acid degradation, leading to inflammation and delayed wound-healing [62].

In other studies, Eupafolin, a major compound from *Artemisia princeps* Pampanin presented anti-inflammatory properties against LPS-challenged RAW 264.7 macrophages by the inhibition of p38 MAPK, ERK1/2, JNK, AKT and p65 and the nuclear translocation of p65 and c-fos [59]. The PSMs of a halophyte plant, *Zygophyllum album*, showed high anti-inflammatory activity by the inhibition of NO release in RAW 264.7 cells under oxidative stress [60].

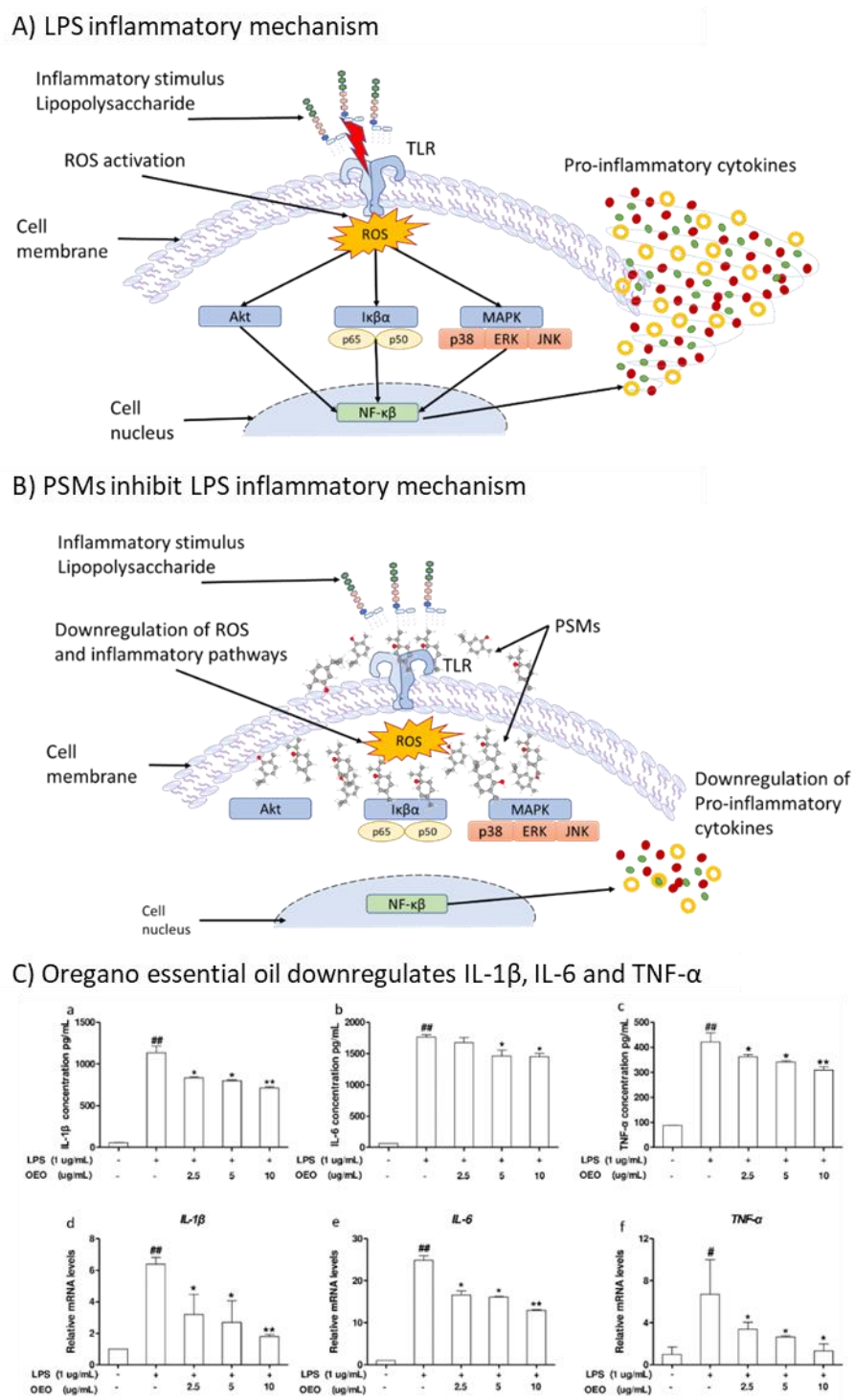

Figure 2. 3. A) Schematic representation of inflammatory and oxidant mechanisms induced by LPS. B) Anti-inflammatory and antioxidant mechanisms promoted by PSMs. C) Oregano essential oil (OEO) inhibits LPS induced mRNA levels of pro-inflammatory cytokines expression in murine macrophage cells (RAW264.7 cells). (a–c) Cells were pretreated with OEO for 12 h, then incubated with 1 µg/mL LPS for 12 h. (d–f) Cells were pretreated with OEO for 12 h, then incubated with 1 µg/mL LPS for 1 h. Reproduced under terms of the CC-BY license [45]. Copywrite 2018. Chuanshang Cheng, Yi Zou, and Jian Peng, published by MDPI.

2.4.2 Antibacterial effects of PSMs

The antibacterial properties of PSMs are attributed to their wide variety of phenolic monoterpenes [63]. PSMs cause damage to the bacteria cell membrane and interrupt quorum sensing, thus inhibiting biofilm formation. PSMs also inhibit ATP generation, disturb ion transport and kill bacteria. Studies assessing the antibacterial properties of PSMs include comparisons of the effects of different types of PSMs against different bacteria strains, see Table 2.2. PSMs have also been reported to have antifungal properties against *Candida albicans*, *Candida tropicalis* and *Candida parapsilosis* [64-70]. In addition, PSMs inhibit the proliferation of multidrug-resistant pathogens [71, 72]. Monoterpenes derived from oregano, tea tree, and clove oils (carvacrol and thymol, terpinen-4-ol, and eugenol, respectively) act as antibacterial agents against a wide variety of pathogenic bacteria. These monoterpenes attack the cell membrane causing leakage of various substances, such as ions, ATP, nucleic acids and amino acids. The mechanism of OEO against bacterial infection of different pathogens, including Methicillin-resistant *Staphylococcus aureus* (MRSA), proposes that OEO destroys the bacterial cell membrane causing leaking of Na^+, K^+ and irreparable damage to bacteria. Additionally, recent studies have shown that when carvacrol reaches bacterial DNA its genetic composition alters preventing it from replication, transcription and translation [73-76]. Terpinen-4-ol induced leakage of K^+ ions from *E. coli* and inhibition of respiration in exponential and stationary phase cell suspensions of *E. coli* [77]. Eugenol increased permeability in the cytoplasmic membrane of *Salmonella typhi*, affecting membrane-embedded proteins and inducing the inhibition of the respiratory system and alteration of ion transport activities of bacterial cells (Figure. 2.4 A) [78]. The antibacterial mechanism of PSMs is highly effective against bacterial colonization, biofilm formation and AR bacteria (Figure. 2.4 B) [79]. Polo *et al.* reported the synthesis of calcium phosphate microparticles grafted with vanillin essential oil (VEO) at different concentrations [80]. (Figure. 2.4 C) shows healthy *E. coli* on uncoated commercially available bone regenerator material, Surgibone ®, (Figure. 2.4 D-F) shows antibacterial properties of this material enhanced with VEO against *E. coli*. Moreover, thymol/carvacrol was loaded into polythioether nanoparticles via thiol alkene photopolymerization in miniemulsion [81]. (Figure. 2.4 G) represents the loading of thymol/carvacrol, H) shows the multifunctional monomers used to generate the nanoparticles and SEM images of them, and I) illustrates the antibacterial properties of the material at different concentrations of carvacrol/thymol against various bacterial strains. Overall, these results suggest the enhancement of antibacterial properties when including PSMs in different

materials. Among the wound-healing properties of PSMs, antibacterial properties have been the most studied. While most of the studies are on the wound-healing applications of PSMs as essential oils, our interest is focused on the potential use of PSMs in medical devices as a polymer film for wound-healing purposes.

Table 2. 2. Plant secondary metabolites and their activity against different types of bacteria.

Plant secondary metabolites	Pathogens	Reference
Eugenol	*Candida albicans*	[65-69, 78]
	Escherichia coli	
	Enterobacter aerogenes	
	Proteus vulgaris	
	Salmonella typhi	
	Staphylococcus aureus ATCC25923	
	Enterococcus faecalis ATC29212	
	Escherichia coli ATCC25922	
	Candida albicans ATCC90028	
Oregano oil (carvacrol and thymol)	*Candida albicans*	[75, 76, 82-85]
	Candida krusei	
	Candida tropicalis	
	Candida dubinensis	
	Pseudomonas aeruginosa	
	Bacillus cereus	
	Escherichia coli	
	Salmonella thypi	
	Yersinia enterocolitica	
	Staphylococcus aureus	
	Listeria monocytogenes	
	Enterococcus faecalis	
Thyme oil	Candida albicans	[68, 69, 75, 83]
	Staphylococcus aureus	
	Enterococcus faecalis	
	Escherichia coli	
	Pseudomonas aeruginosa	
	Salmonella typhi	
	Yersinia enterocolitica	
	Staphylococcus aureus	
	Listeria monocytogenes	
	Enterococcus faecalis	
Lavender oil (linalyl acetate)	*Staphylococcus aureus* ATCC25923	[69, 74, 83]
	Enterococcus faecalis ATC29212	
	Escherichia coli ATCC25922	
	Candida albicans ATCC90028	
	Candida albicans	
	Staphylococcus aureus	
	Enterococcus faecalis	

	Escherichia coli *Pseudomonas aeruginosa* *Salmonella typhi* *Yersinia enterocolitica* *Staphylococcus aureus* *Listeria monocytogenes* *Enterococcus faecalis*	
Tea tree oil	*Staphylococcus aureus* ATCC25923 *Enterococcus faecalis* ATC29212 *Escherichia coli* ATCC25922 *Candida albicans* ATCC90028 *Escherichia coli* *Candida glabrata* *Herpes simplex* virus type 1 (HSV-1) *Methicillin-resistant Staphylococcus aureus* (MRSA) *Pseudomonas aeruginosa*	[77, 86, 87]
Cinnamon	*Escherichia coli* *Staphylococcus aureus*	[88]

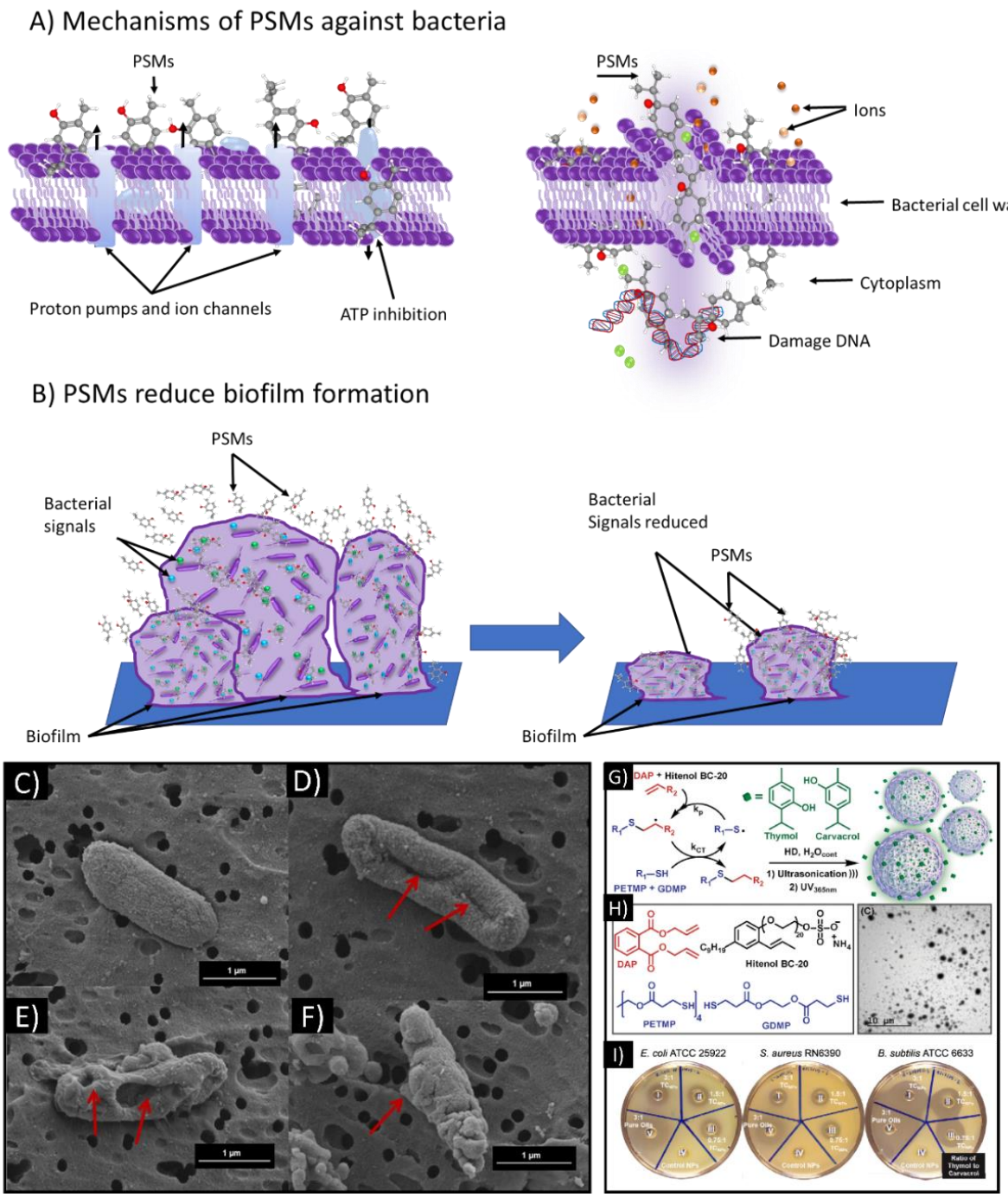

Figure 2. 4. Mechanisms of PSMs against bacteria and biofilms. A) PSMs disturb ions exchange and ATP process, induce membrane permeability, DNA damage, and leakage of ions. B) PSMs reduces biofilms by interrupting bacterial signaling and quorum sensing. C)-F) Field emission scanning electronic microscopy (FESEM) images show the antibacterial properties of commercially available bone regenerator material (Surgibone ®) uncoated C) and coated with different concentrations D)-F) of vanillin essential oil. Reproduced with permission [80]. Copywrite 2018. Elsevier. G) Antimicrobial thymol/carvacrol-loaded polythioether nanoparticles H) various multifunctional monomers used to generate polythioether nanoparticles via thiol alkene photopolymerization in miniemulsion I) Antimicrobial activity of nanoparticles loaded with different ratios of carvacrol and thymol. Reproduced with permission [81]. Copywrite 2016, Wiley.

2.5. Incorporation of PSMs-based polymers in wound dressings

PSMs-based polymers occur by the polymerization of PSMs molecules to form crosslinked PSMs-derived polymers or by the incorporation of PSMs into organic or synthetic polymer matrix. PSMs-based polymers for wound dressing applications include fibers, hydrogels, membranes, films and a variety of nanostructured materials. The advantage of PSMs-based polymers is that the medicinal properties of PSMs can be retained and protect them from oxidation and volatility. PSMs-based polymers can be used as drug delivery agents in wound dressing applications. In this section, we summarize the most relevant polymerization methods to obtain PSMs-based polymers in wound dressings. We also present the wound-healing activity of PSMs-based polymers in *in vitro* and *in vivo* studies. Table 2.3 outlines the polymerization methods used to incorporate PSMs in wound dressings and the wound-healing activity of these polymers.

Table 2. 3. Polymerization methods to incorporate PSMs in wound dressings.

Polymerization method	PSMs	Polymer-based	Dressing type	Wound-healing activity	References
Electrospinning	Thymol	PCL, PVA and hybrid matrix of 50/50%	Nanofibrous mats	Antibacterial against S. aureus, 92.5% wound-closure in *in vivo* rat models in a period of 14 days.	[89]
		PCL	Patch	Anti-inflammatory activity against LPS-activated murine macrophages, downregulation of IL-1β and iNOS.	[90]
	Ajwain	PVA	Core-shell nanofibers	Accelerated wound-healing in infected wounds in rat	[91]

				model, 100% in 14 days (40%).	
	Curcumin	PCL	Nanofibers	Antioxidant activity, viability of human foreskin fibroblasts under oxidative stress and reduced IL-6 in mouse monocyte macrophages. Increasing of wound-closure rate in streptozotocin induced diabetic mice model (17%).	[92]
	Clove	Zein	Films	Antibacterial against *S. aureus* and *E. coli.* Improved wound-closure rate in Kunming mice wound model.	[93]
	Tea tree	Chitosan	Nanofibers mats	Long-term microbicidal capability against *S. aureus, E. coli* and *C. albicans*.	[94]
	Cinnamon	Chitosan/gelatin	Membrane	Antibacterial properties against *E. coli and S. aureus*	[88]
Coprecipitation method	Thyme	Chitosan	Hydrogel	Low cytotoxicity and controlled drug release of	[95]

				thyme oil by diffusion.	
Absorption	Thymol	Bacterial-cellulose		faster wound closure rate when compared to bacterial-cellulose (BC) and control.	[96]
Emulsification	β-caryophyllene	PSM-derived polymer		Anti-inflammatory effect on dorsal wound model on Wistar rats.	[97]
Ion gelation method	*Homalomena pineodora*	Chitosan	Nanoparticles	Inhibition of Gram-positive, Gram-negative bacteria and yeast.	[98]
Emulsification	*Satureja khuzistanica*		Nanoemulsion	Antibacterial against *P. aeruginosa.*	[99]
Hot melt homogenization	*Piper cubeba*		Self nanoemulsifying drug delivery system	Significant wound-healing rate in wound excision rat model.	[100]
	Peppermint	PSM-derived polymer	Nanostructured lipid carriers	Reduction of bacteria and faster wound closure on infected wound model on mice.	[101]
Film hydration method	*Artemisa annua*		Nanoliposomes	Drug release of 80% after 12 h and 90% after 24 h. Effective against *C. krusei* and *C. tropicalis.*	[102]

Film hydration method	*Salvia triloba* and *Rosmarinus officinalis*	Liposomes	Nanovesicles	Effective against *K. pneumonia.* Inhibition of pro-inflammatory enzyme soy bean lipoxygenase	[103]
	Patchouli	Mesoporous silica nanoparticles	Nanoparticles	Antibacterial effect on *S. aureus* for 2 days, no toxicity to L929 cells	[104]
Supercritical impregnation	Thymol	*Cotton gauze*	Gauze	Effective against E. coli, S. aureus, Bacillus subtilis, E. faecalis and C. albicans	[105]
	Libidibia ferrea	N-carboxybutyl chitosan	Polymer matrix	Downregulation of TNF-α and IL-1 in LPS-stimulated macrophages	[106]
	Thymol/Carvacrol	Collagen/cellulose		Antibacterial activity against *E. coli, S. aureus.*	[107]
	1,8-cineole			*S. aureus* and *E. coli*	[108]
Plasma polymerization	Terpinene-4-ol	*PSM-derived polymer*	Films	Effective against *S. aureus*, *P. aeruginosa*	[109-111]
	Oregano			Effective against *S. aureus*, *P. aeruginosa.* Biocompatibility with fibroblasts	[112]

2.5.1 Electrospinning

Electrospinning is a technique used to produce micro or nanofibers from solutions or melts using electrostatic forces. Electrospinning includes synthetic and natural materials along the fibers; in encapsulated form or as nanoparticles [113]. Electrospun collagen hydrolysate nanofibers loaded with thyme or oregano presents antibacterial properties with potential for use in wound dressings or cosmetics [110, 111]. Wound dressing mats from polycaprolactone and polylactic acid (PCL/PLA) fibers are fabricated by electrospinning. Thymol was incorporated in the synthesis process and their anti-inflammatory and antibacterial properties were retained [89]. The antibacterial assays showed inhibition to S*taphylococcus aureus* and *Escherichia coli*. The results in the wound-closure assay (using male Wistar rat model) were significant for the samples containing thymol compared to the control (commercial gauze and Comfeel Plus® samples). Electrospun PCL/PLA with thymol accelerated wound closure by more than 92% in 14 days, whereas gauze and Comfeel Plus® showed 68% and 87% wound closure, respectively. Consequently, enhanced cell growth and fibroblast cell formation occurred in the samples compared to the dry wound environment using gauze. The downregulation of pro-inflammatory cytokines is a key factor to prevent inflammation and stimulate healing progression. One example is the incorporation of thymol to electrospun PCL fibers. This study evaluated the anti-inflammatory properties on LPS-activated macrophages as is represented in (Figure. 2.5). The results show an expression of the pro-inflammatory mediators IL-1β and iNos. In addition, PCL/thymol reduced the size of the inflamed cells suggesting an alleviation of the inflammatory response. These results demonstrate the potential for using anti-inflammatory electrospun mats in wound-healing dressings [114].

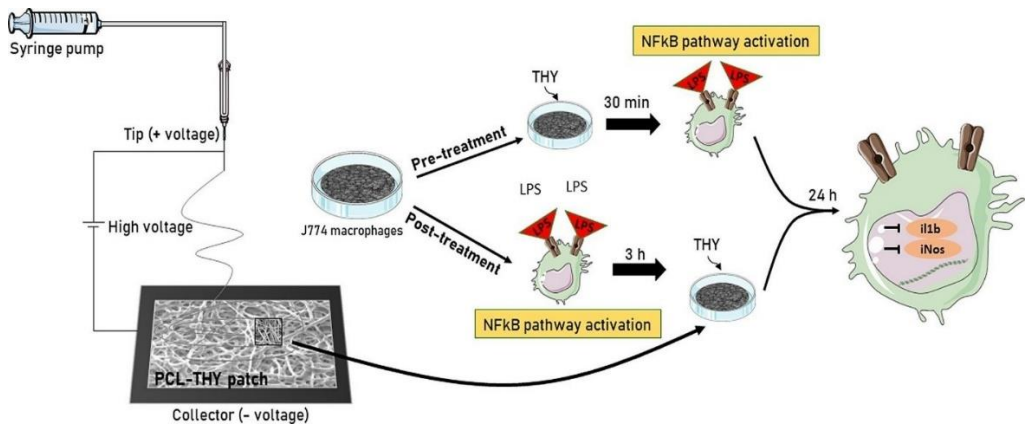

Figure 2. 5. PSMs incorporated to electrospun for anti-inflammatory wound dressings. A) Shows a schematic of the PCL/Thymol electrospun mats that alleviate inflammation of LPS-activated macrophages through activation of NF-κβ pathway. Reproduced with permission [114]. Copyright 2021, Elsevier.

Ajwain essential oil, incorporated in core-shell electrospun nanofibers, shows antibacterial and wound-healing potential. The nanofibers were tested in a rat wound model infected with *S. aureus* bacteria. The results showed the potential to diminish bacterial infection and enhance wound closure. In addition, the histological outcomes showed no inflammation and increasing collagen deposition (Figure. 2.6) [91]. Anti-inflammatory curcumin-loaded nanofibers have been developed. The contribution of this novel material is the reduction of inflammation through partial inhibition of IL-6 in a streptozotocin-induced diabetes mouse model. These results are promising for the future use of nanofibers in chronic wounds in patients with diabetes [92]. Moreover, electrospun zein/clove essential oil membranes were deposited in situ and tested as a potential wound dressing in a Kunming mice model. These membranes exhibited good antibacterial properties and enhanced wound closure when compared to a control [93]. Antibacterial properties of TTO were retained in the chitosan nanofibers after electrospinning. Furthermore, the mechanical properties, permeability and breathability of the TTO-chitosan nanofibers were enhanced with the addition of TTO, positively contributing to the overall performance of the dressing. This combination was also effective against different bacteria (*Staphylococcus aureus, Escherichia coli* and *Candida albicans*) suggesting the potential application of these fibres as nonwoven dressings with prolonged antimicrobial properties [94]. Electrospun chitosan/gelatin membranes loaded with cinnamon have also shown antibacterial properties against *S. aureus and E. coli* [88].

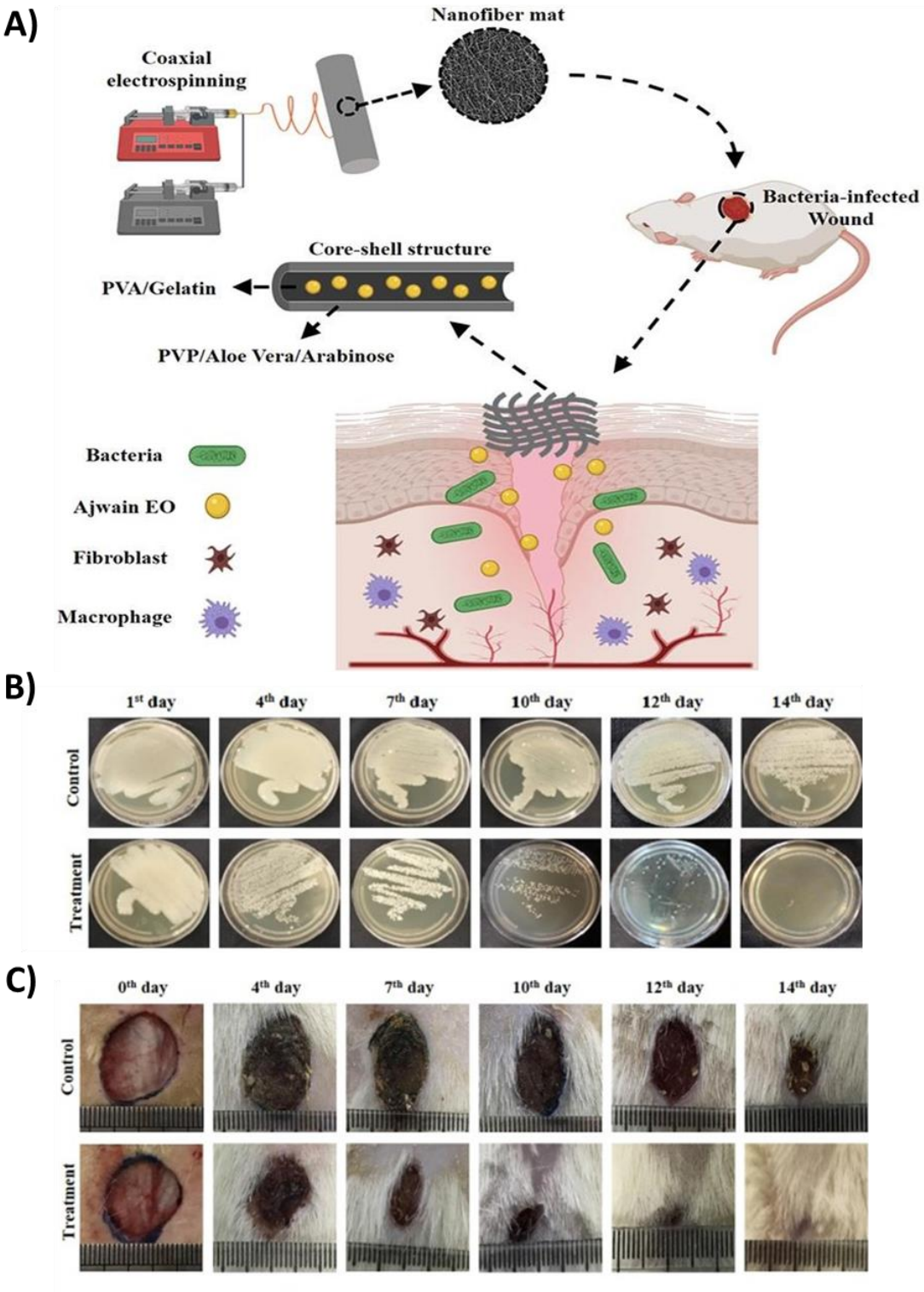

Figure 2. 6. Ajwain essential oils incorporated to nanofibers by electrospinning to accelerate healing in infected wounds in a rat model. A) Shows the scheme graphical abstract of the study. B) shows the antibacterial effect against *S. aureus* after 14 days. C) shows accelerated wound-healing on infected wounds in a rat model. Reproduced with permission [91]. Copyright 2021, Elsevier.

2.5.2 Hydrogels

The main feature of hydrogels in wound dressings is their capability to absorb and retain large amounts of water or biological fluids [115]. Hydrogel technologies can be prepared in two different ways: three-dimensional polymerization and direct cross-linking. In three-dimensional polymerization, a hydrophilic monomer is polymerized in the presence of a polyfunctional cross-linking agent, whereas in direct cross-linking, polymerization occurs with water-soluble polymers. A candidate for hydrogel wound dressings is a chitosan-based hydrogel loaded with γ-cyclodextrin inclusion compounds of thyme oil. This material showed low cytotoxicity and controlled drug release of thyme oil by diffusion. The results suggest that this material is suitable for controlled drug delivery and potentially wound dressings [95]. The wound-healing activity of hydrogel containing nano-emulsified β-caryophyllene was assessed on a dorsal wound model of Wistar rats. On the second day, animals treated with this hydrogel showed a considerable reduction in the wound area compared with the control group, indicating its anti-inflammatory effect. After 7 days, all groups showed a greater reduction in the superficial area of the wound compared to the control group. On day 12, there were no significant differences observed between the groups, this could be due to the end of the inflammatory process and the start of the proliferation process [97]. A thymol-enriched bacterial-cellulose (BCT) hydrogel has been used for third-degree burn wound repair in a burn injury model on Wistar rats. BCT hydrogel showed a faster wound closure rate when compared to bacterial-cellulose (BC) and control, suggesting its potential use as burn wound dressing material [96].

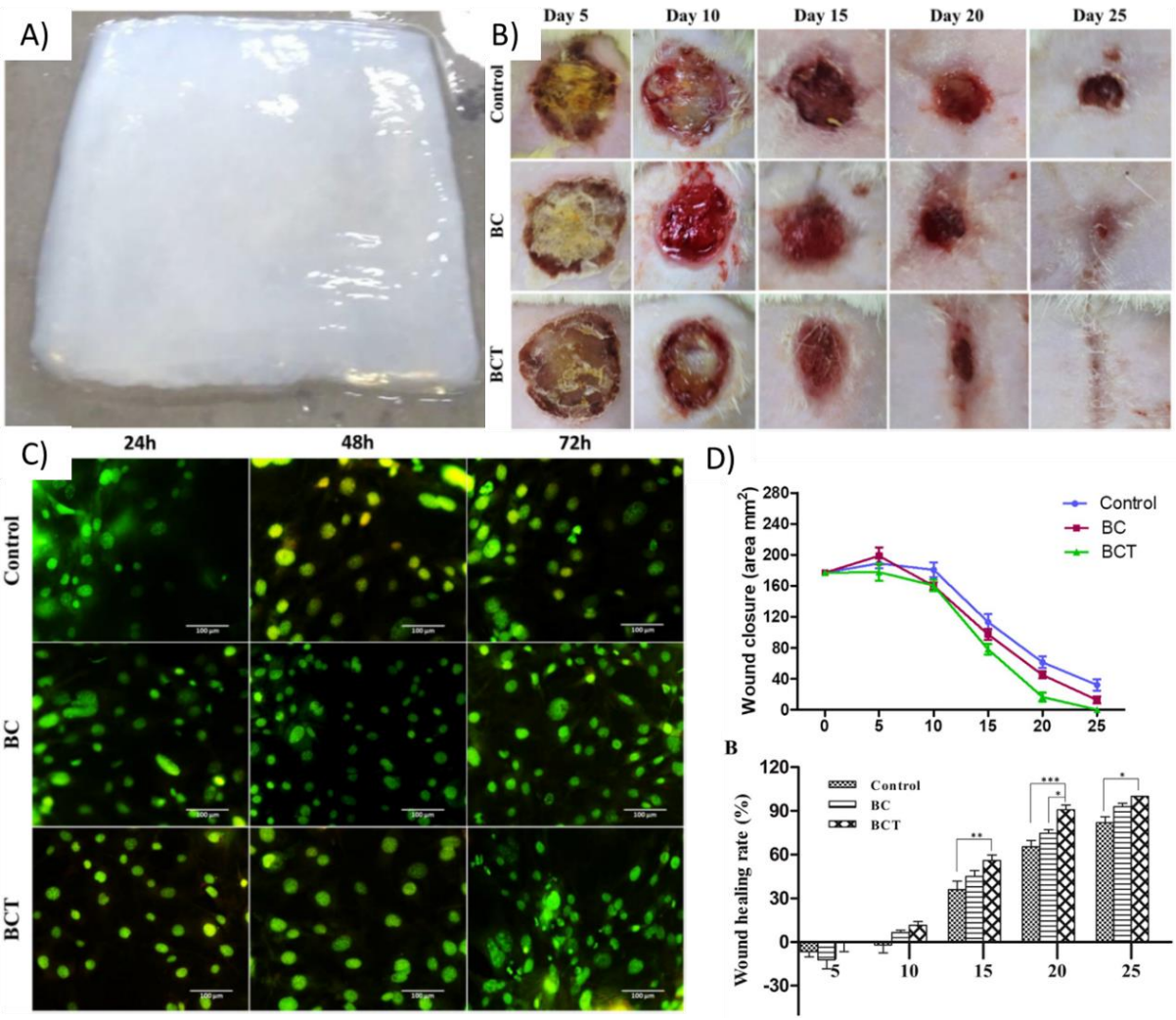

Figure 2. 7. A) thymol enriched bacterial cellulose hydrogel B) Representative images of burn wounds in control, BC and BCT groups at days 5, 10, 5, 20 and 25.C) Fluorescent images of control, BC and BC loaded thymol (1%) in NIH 3T3 fibroblast cells. D) Upper image shows wound closure area in control, BC and BCT groups at days 0, 5, 10, 5, 20 and 25 and bottom image shows wound-healing rate percentage in control, BC and BCT groups at days 5, 10, 5, 20 and 25. Reproduced with permission [96]. Copywrite 2018, Elsevier.

2.5.3 Nanostructured PSMs for controlled drug delivery systems

One effective way to incorporate PSMs in controlled drug delivery systems for wound dressing applications is by fabricating nanostructured PSMs-based materials. This could be achieved by different polymerization methods. For example, antibacterial chitosan nanoparticles containing *Homalomena pineodora* essential oil, a Malaysian plant extract, were synthesized using the ion gelation method. The chitosan matrix encapsulates the essential oil, controlling its diffusion from the core across its matrix. *Homalomena pineodora* oil/chitosan nanoparticles were

efficient against bacteria (both gram-positive and gram-negative) and yeast. The medicinal effect of the *Homalomena pineodora* oil lasted up to 3 days, suggesting a possible prolonged effect of these nanoparticles in antibacterial wound dressings [98].

Nanoemulsion preparation is another way to incorporate PSMs into wound dressings. For example, *satureja khuzistanica* (SK) nanoemulsions were effective against *P. aeruginosa* biofilms [99]. *Piper cubeba* (PO), was prepared as a "self-nanoemulsifying drug delivery system" (SNEDDS) by emulsification. The wound-healing activity of PC-SNEDDS was evaluated using a wound excision rat model. The wound-healing rate was significant when compared to pure PO and to a control. The formulation also showed significant enhancement in collagen production, as well as no signs of inflammatory cells that indicate the safety of this nanoemulsion [100].

Nanostructured lipid carriers (NLC) are also prepared using a hot melt homogenization technique. NLC from peppermint essential oil tested *in-vivo,* on infected wound mice model, showed a significant reduction of bacteria and faster wound closure when compared to a control [101]. The film hydration method allows the encapsulation of PSMs in nanoliposomes. *Artemisa annua* (AA) nanoliposomes were prepared, its drug release profile was studied and it was tested against ten strains of *Candida*. The results showed that after 12h 80% of AA was released, reaching approximately 90% in 24h. AA nanoliposomes were active against *C. krusei* and *C. tropicalis* [102]. Other PSMs such as *Salvia triloba* and *Rosmarinus officinalis* were also prepared using the film hydration method. The anti-inflammatory activity of these nanostructured PSMs results from the inhibition of soybean lipoxygenase, an enzyme involved in the metabolisms of inflammatory mediators. These nanostructures were also effective against *K. pneumonia* [103].

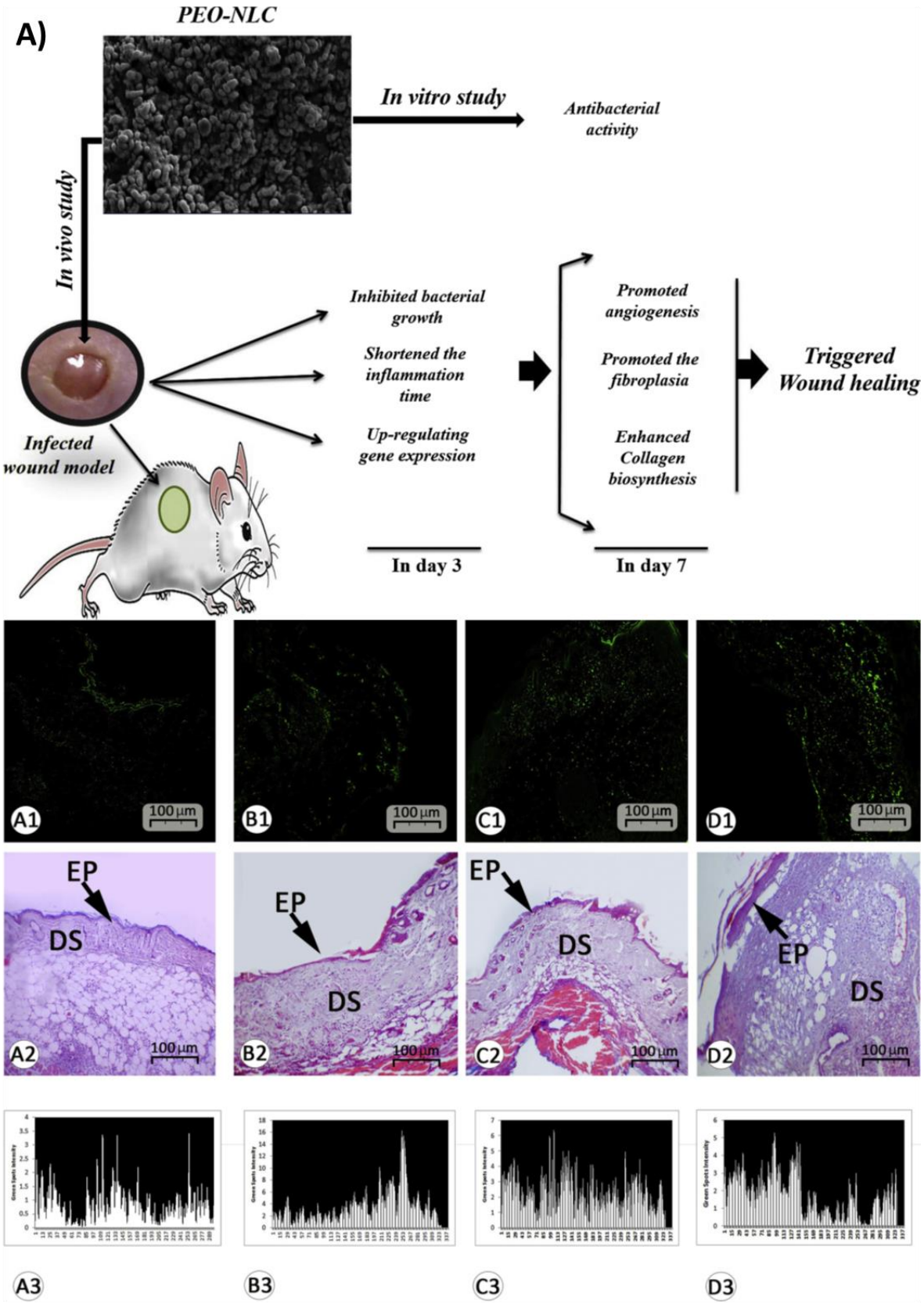

Figure 2. 8. A) shows the encapsulation of peppermint essential oil in nanostructured lipid carriers and significant results of the study. The histological section from the wound area on day 7 after wound induction; A1 to D1 indicate the Immuno-fluorescent staining for fibroblast.

The increase in green spots indicates significantly higher fibroblast cellularity in PEO-NLC. In A2 to D2, the H&E staining is presented for dermal (DS) and epidermal (EP) remodelling. See well-formed epidermis as well as mature dermis in PEO and PEO-NLC-treated groups. A3 to D3 represent software analyses for immune reactions for fibroblast, which are increased in PEO and PEO-NLC-treated groups (A: Control, B: Mupirocin-treated, C: PEO-treated, and D: PEO-NLC-treated). Reproduced with permission [101]. Copywrite 2019, Elsevier.

2.5.4 Supercritical impregnation

Supercritical impregnation is an effective method to incorporate active compounds into polymers [116]. While most of the literature about the use PSMs incorporated by supercritical impregnation is in food packaging technologies [117-120], some literature describes this technique being used to impregnate PSMs into wound dressings. A patchouli essential oil (PEO) nanocomposite, a film nanocomposite (PEO-FNC) and mesoporous silica nanoparticles (PEO-MSNs) were prepared by supercritical CO_2 cyclic impregnation for wound dressings applications. The release of PEO from the film nanocomposite persisted for more than 5 days and exhibited antibacterial effect on *S. aureus* for more than 2 days. Also, the film showed no toxicity to L929 cells [104]. Thymol was impregnated in cotton gauze by supercritical impregnation using carbon dioxide as a solvent, demonstrating 11% and 19.6% impregnation after 2h and 24h respectively. This gauze was effective against *E. coli, S. aureus, Bacillus subtilis, E. faecalis* and *C. albicans* [105]. Other examples are polymeric dressings from N-carboxybutyl chitosan, collagen/cellulose, and hyaluronic acid loaded with Jucá fruit extract.

The combination of Jucá fruit extract into the dressings downregulated pro-inflammatory cytokines TNF-α and IL-1 in LPS-stimulated macrophages [106].

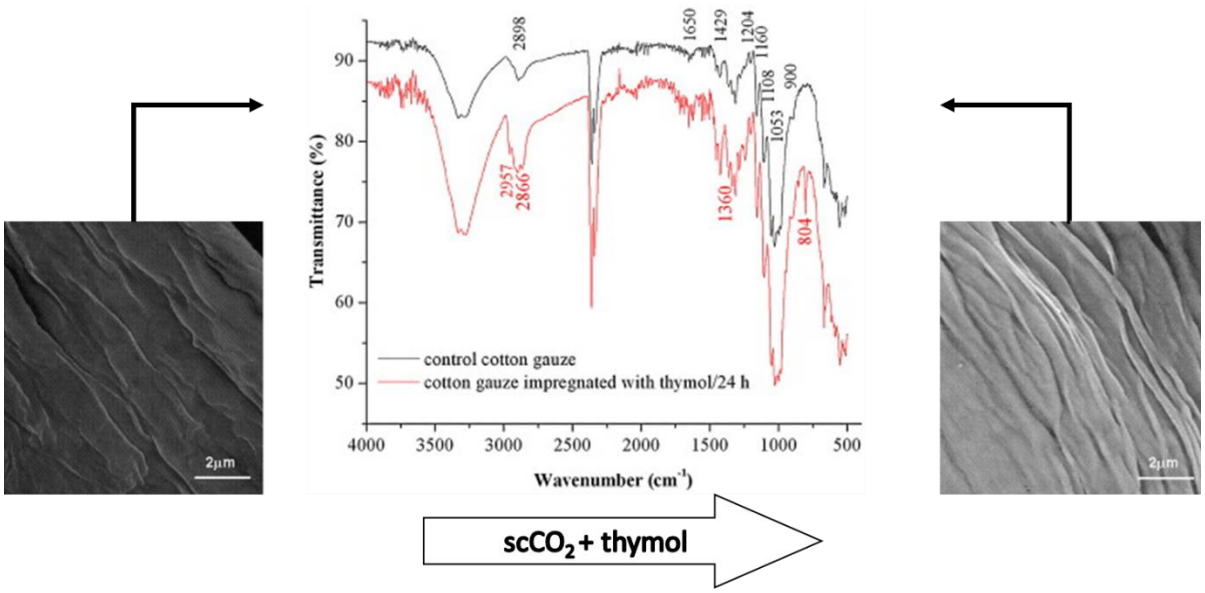

Figure 2. 9. Supercritical impregnation of thymol on cotton gauze Reproduced with permission [105]. Copywrite 2013, Elsevier.

Thymol/Carvacrol and clinoptilolite composites, prepared by supercritical solvent impregnation in supercritical carbon dioxide, demonstrate antibacterial activity [107]. These composites showed antibacterial properties against *E. coli* and *S. aureus* in PBS, spring water and lake water following 24h of contact.

2.5.5 Radiofrequency plasma-enhanced chemical vapour deposition (RF-PECVD)

Radiofrequency plasma-enhanced chemical vapour deposition (RF-PECVD) is a polymerization technique that can easily integrate PSM vapours into wound dressings. The retention of PSM properties along with a low temperature of deposition and its relatively easy control are the main advantages of RF-PECVD polymerization. A previous study utilized the RF-PECVD plasma thin film preparation method from terpinen-4-ol and found that the antibacterial properties of terpinen-4-ol were successfully retained and were effective against *Staphylococcus aureus* [109]. In similar studies, antibacterial terpinen-4-ol thin films were fabricated with pulsed plasma polymerization and the resulting films were effective against

Pseudomonas aeruginosa (ATCC-589), as seen in (Figure. 2.9.) [110, 111]. Like carvacrol, the antibacterial properties of terpinen-4-ol are related to their lipophilicity. Carvacrol works by penetrating the bacteria cell wall and cytoplasmic membrane, causing structural damage and intracellular loss. [121]. The retention of antibacterial activity of pristine 1,8-cineole was achieved by plasma polymerization. 1, 8-cineole thin films were effective against *S. aureus* and *E. coli* [108]. Oregano PSMs were polymerized by plasma polymerization, these non-cytotoxic polymers supported fibroblast growth and proliferation and were antibacterial against *S. aureus* and *P. aeruginosa* [112]. Thus, the above studies suggest that plasma polymerization is a robust method to incorporate PSMs in wound dressings. However, more studies of the wound-healing properties of these polymers are needed.

2.6 Conclusion

Delayed wound-healing is promoted by chronic inflammation (upregulation of pro-inflammatory cytokines), oxidative stress (ROS generation) and bacterial infection (biofilm formation, antibiotic resistance). Downregulation of pro-inflammatory cytokines and ROS, as well as protection against bacterial infection and biofilm formation, are targets to achieve effective wound-healing. It has been demonstrated that the main active compounds of PSMs have antioxidant, anti-inflammatory and antibacterial properties. We reviewed the methods for incorporating PSMs into wound dressings. The variety of polymerization techniques available provides much choice to select the right PSMs-based polymer for a particular wound. The selection procedure of the PSMs-based polymer for wound-healing purposes depends on its bioactivity mechanism, type of wound and the available polymerization technique. Electrospinning is currently the most used technique to incorporate PSMs into wound dressings. The final electrospun product is fibres that can be processed to create wound dressings or to be applied directly on the wound site.

Despite the efforts to successfully integrate PSMs in wound-healing materials, more clinical studies are needed to rigorously test these dressing compounds. There is a need to study the efficacy of PSMs-based polymers after a long storage period as the compounds tend to auto-oxidase and may evaporate. It is also necessary to study the long-term toxicity of such dressings on human cells to know the appropriate duration of use in wound dressings. It also is important to consider the use of multicomponent PSMs in the prevention of resistance in bacteria, as multiple systems in the cell are targeted. On the other hand, the use of pure monomers ensures consistency and addresses seasonal and regional variability. The promising properties of PSMs

together with the available processing techniques to incorporate them into polymers suggest their potential application in wound dressings.

2.7 References

[1] L.G. Ovington, Advances in wound dressings, Clinics in Dermatology 25(1) (2007) 33-8.

[2] H. Yang, Y. Liang, J. Wang, Q. Li, Q. Li, A. Tang, Y. Liu, H.-B. Liu, Multifunctional wound dressing for rapid hemostasis, bacterial infection monitoring and photodynamic antibacterial therapy, Acta biomaterialia 135 (2021) 179-190.

[3] W. Hu, Z. Wang, Y. Zha, X. Gu, W. You, Y. Xiao, X. Wang, S. Zhang, J. Wang, High Flexible and Broad Antibacterial Nanodressing Induces Complete Skin Repair with Angiogenic and Follicle Regeneration, Advanced Healthcare Materials 9(23) (2020) 2000035.

[4] H. Cheng, Z. Shi, K. Yue, X. Huang, Y. Xu, C. Gao, Z. Yao, Y.S. Zhang, J. Wang, Sprayable hydrogel dressing accelerates wound healing with combined reactive oxygen species-scavenging and antibacterial abilities, Acta biomaterialia 124 (2021) 219-232.

[5] L. Mao, L. Wang, M. Zhang, M.W. Ullah, L. Liu, W. Zhao, Y. Li, A.A.Q. Ahmed, H. Cheng, Z. Shi, G. Yang, In Situ Synthesized Selenium Nanoparticles-Decorated Bacterial Cellulose/Gelatin Hydrogel with Enhanced Antibacterial, Antioxidant, and Anti-Inflammatory Capabilities for Facilitating Skin Wound healing, Advanced healthcare materials 10(14) (2021) 2100402-n/a.

[6] R.R. Huerta, E.K. Silva, T. El-Bialy, M.D.A. Saldaña, Clove essential oil emulsion-filled cellulose nanofiber hydrogel produced by high-intensity ultrasound technology for tissue engineering applications, Ultrasonics sonochemistry 64 (2020) 104845.

[7] N. Zandi, B. Dolatyar, R. Lotfi, Y. Shallageh, M.A. Shokrgozar, E. Tamjid, N. Annabi, A. Simchi, Biomimetic nanoengineered scaffold for enhanced full-thickness cutaneous wound healing, Acta biomaterialia 124 (2021) 191-204.

[8] F. Lopresti, S. Campora, G. Tirri, E. Capuana, F. Carfì Pavia, V. Brucato, G. Ghersi, V. La Carrubba, Core-shell PLA/Kef hybrid scaffolds for skin tissue engineering applications prepared by direct kefiran coating on PLA electrospun fibers optimized via air-plasma treatment, Materials Science & Engineering C 127 (2021) 112248-112248.

[9] S. Nour, R. Imani, G.R. Chaudhry, A.M. Sharifi, Skin wound healing assisted by angiogenic targeted tissue engineering: A comprehensive review of bioengineered approaches, Journal of biomedical materials research. Part A 109(4) (2021) 453-478.

[10] F. Reinboldt-Jockenhöfer, Z. Babadagi, H.D. Hoppe, A. Risse, C. Rammos, A. Cyrek, C. Blome, S. Benson, J. Dissemond, Association of wound genesis on varying aspects of health-related quality of life in patients with different types of chronic wounds: Results of a cross-sectional multicentre study, International wound journal 18(4) (2021) 432-439.

[11] Z. Yao, J. Niu, B. Cheng, Prevalence of Chronic Skin Wounds and Their Risk Factors in an Inpatient Hospital Setting in Northern China, Advances in skin & wound care 33(9) (2020) 1-10.

[12] S.R. Nussbaum, M.J. Carter, C.E. Fife, J. DaVanzo, R. Haught, M. Nusgart, D. Cartwright, An Economic Evaluation of the Impact, Cost, and Medicare Policy Implications of Chronic Nonhealing Wounds, Value in health 21(1) (2018) 27-32.

[13] C.J. Phillips, I. Humphreys, J. Fletcher, K. Harding, G. Chamberlain, S. Macey, Estimating the costs associated with the management of patients with chronic wounds using linked routine data, International wound journal 13(6) (2016) 1193-1197.

[14] H. Edwards, K. Finlayson, M. Courtney, N. Graves, M. Gibb, C. Parker, Health service pathways for patients with chronic leg ulcers: identifying effective pathways for facilitation of evidence based wound care, BMC health services research 13(1) (2013) 86-86.

[15] R. Avola, G. Granata, C. Geraci, E. Napoli, A.C.E. Graziano, V. Cardile, Oregano (Origanum vulgare L.) essential oil provides anti-inflammatory activity and facilitates wound healing in a human keratinocytes cell model, Food and chemical toxicology 144 (2020) 111586-111586.

[16] D. Coelho, B. Veleirinho, L. Mazzarino, T. Alberti, E. Buzanello, R.E. Oliveira, R.A. Yunes, M. Moraes, M. Steindel, M. Maraschin, Polyvinyl alcohol-based electrospun matrix as a delivery system for nanoemulsion containing chalcone against Leishmania (Leishmania) amazonensis, Colloids and surfaces, B, Biointerfaces 198 (2021) 111390-111390.

[17] D. Stan, C. Tanase, M. Avram, R. Apetrei, N.B. Mincu, A.L. Mateescu, D. Stan, Wound healing applications of creams and "smart" hydrogels, Exp Dermatol 30(9) (2021) 1218-1232.

[18] B. Jamil, R. Abbasi, S. Abbasi, M. Imran, S.U. Khan, A. Ihsan, S. Javed, H. Bokhari, Encapsulation of Cardamom Essential Oil in Chitosan Nano-composites: In-vitro Efficacy on Antibiotic-Resistant Bacterial Pathogens and Cytotoxicity Studies, Frontiers in microbiology 7 (2016) 1580-1580.

[19] S. Jurić, K. Sopko Stracenski, Ż. Król-Kilińska, I. Žutić, S.F. Uher, E. Đermić, S. Topolovec-Pintarić, M. Vinceković, The enhancement of plant secondary metabolites content in Lactuca sativa L. by encapsulated bioactive agents, Scientific reports 10(1) (2020) 3737-3737.

[20] G.K. Zorzi, E.L.S. Carvalho, G.L. von Poser, H.F. Teixeira, On the use of nanotechnology-based strategies for association of complex matrices from plant extracts, Revista brasileira de farmacognosia 25(4) (2015) 426-436.
[21] P.A. Uwineza, A. Waśkiewicz, Recent Advances in Supercritical Fluid Extraction of Natural Bioactive Compounds from Natural Plant Materials, Molecules (Basel, Switzerland) 25(17) (2020) 3847.
[22] S.A. Eming, P. Martin, M. Tomic-Canic, Wound repair and regeneration: mechanisms, signaling, and translation, Sci Transl Med 6(265) (2014) 265sr6.
[23] J.-O. Jensen, L. Schulz, S. Schleusser, N. Matzkeit, F.H. Stang, P. Mailaender, R. Kraemer, M. Kleemann, H. Deichmann, T. Kisch, The repetitive application of cold atmospheric plasma (CAP) improves microcirculation parameters in chronic wounds, Microvascular research 138 (2021) 104220-104220.
[24] I. Messaoudi Moussii, K. Nayme, M. Timinouni, J. Jamaleddine, H. Filali, F. Hakkou, Synergistic antibacterial effects of Moroccan Artemisia herba alba, Lavandula angustifolia and Rosmarinus officinalis essential oils, Synergy 10 (2020) 100057.
[25] M. Aragona, S. Dekoninck, S. Rulands, S. Lenglez, G. Mascré, B.D. Simons, C. Blanpain, Defining stem cell dynamics and migration during wound healing in mouse skin epidermis, Nature communications 8(1) (2017) 14684.
[26] A.M. Di Re, D. Wright, J.W.T. Toh, T. El-Khoury, N. Pathma-nathan, M.P. Gosselink, S. Khanijaun, S. Raman, G. Ctercteko, Surgical wound infection prevention using topical negative pressure therapy on closed abdominal incisions – the 'SWIPE IT' randomized clinical trial, The Journal of hospital infection 110 (2021) 76-83.
[27] H.J. Forman, H. Zhang, Targeting oxidative stress in disease: promise and limitations of antioxidant therapy, Nature Reviews Drug Discovery 20(9) (2021) 689-709.
[28] E.A. Slade, R.M.S. Thorn, A.E. Young, D.M. Reynolds, Real-time detection of volatile metabolites enabling species-level discrimination of bacterial biofilms associated with wound infection, Journal of applied microbiology (2021).
[29] CDC, Antibiotic resistance threats in United States, U.S. Department of Health and Human Services (2019).
[30] R.C. MacLean, A. San Millan, The evolution of antibiotic resistance, Science 365(6458) (2019) 1082-1083.
[31] Y.-K. Wu, N.-C. Cheng, C.-M. Cheng, Biofilms in Chronic Wounds: Pathogenesis and Diagnosis, Trends in biotechnology (Regular ed.) 37(5) (2019) 505-517.

[32] E.M. Townsend, L. Sherry, R. Kean, D. Hansom, W.G. Mackay, C. Williams, J. Butcher, G. Ramage, Implications of Antimicrobial Combinations in Complex Wound Biofilms Containing Fungi, Antimicrobial agents and chemotherapy 61(9) (2017).
[33] K.T. Hughes, H.C. Berg, The bacterium has landed: Mechanosensing mechanisms for surface recognition by bacteria allow biofilm formation, American Association for the Advancement of Science 358(6362) (2017) 446-447.
[34] I. Hug, S. Deshpande, K.S. Sprecher, T. Pfohl, U. Jenal, Second messenger-mediated tactile response by a bacterial rotary motor, American Association for the Advancement of Science 358(6362) (2017) 531-534.
[35] S. Lencova, V. Svarcova, H. Stiborova, K. Demnerova, V. Jencova, K. Hozdova, K. Zdenkova, Bacterial Biofilms on Polyamide Nanofibers: Factors Influencing Biofilm Formation and Evaluation, ACS applied materials & interfaces 13(2) (2021) 2277-2288.
[36] Y. Su, A. McCarthy, S.L. Wong, R.R. Hollins, G. Wang, J. Xie, Simultaneous Delivery of Multiple Antimicrobial Agents by Biphasic Scaffolds for Effective Treatment of Wound Biofilms, Advanced healthcare materials 10(12) (2021) e2100135-n/a.
[37] H. Wu, C. Moser, H.-Z. Wang, N. Høiby, Z.-J. Song, Strategies for combating bacterial biofilm infections, International journal of oral science 7(1) (2015) 1-7.
[38] D. Stagos, Antioxidant Activity of Polyphenolic Plant Extracts, Antioxidants (Basel) 9(1) (2019).
[39] L. Zhang, X. Liang, B. Wang, Z. Lin, M. Ye, R. Ma, M. Zheng, H. Xiang, P. Xu, Six herbs essential oils suppressing inflammatory responses via inhibiting COX-2/TNF-α/IL-6/NF-κB activation, Microchemical Journal 156 (2020) 104769.
[40] L. Zakaria Nabti, F. Sahli, H. Laouar, A. Olowo-Okere, J.G. Nkuimi Wandjou, F. Maggi, Chemical Composition and Antibacterial Activity of Essential Oils from the Algerian Endemic Origanum glandulosum Desf. against Multidrug-Resistant Uropathogenic E. coli Isolates, Antibiotics (Basel) 9(1) (2020).
[41] M.G. Miguel, Antioxidant and anti-inflammatory activities of essential oils: A short review, Molecules 15(12) (2010) 9252-9287.
[42] N. Gautam, A.K. Mantha, S. Mittal, Essential oils and their constituents as anticancer agents: a mechanistic view, Biomed Res Int 2014 (2014) 154106.
[43] C. Torres-Alvarez, A.N. Gonzalez, J. Rodriguez, S. Castillo, C. Leos-Rivas, J.G. Baez-Gonzalez, Chemical composition, antimicrobial, and antioxidant activities of orange essential oil and its concentrated oils, Cyta-J Food 15(1) (2017) 129-135.

[44] M.D. Rostro-Alanis, J. Baez-Gonzalez, C. Torres-Alvarez, R. Parra-Saldivar, J. Rodriguez-Rodriguez, S. Castillo, Chemical Composition and Biological Activities of Oregano Essential Oil and Its Fractions Obtained by Vacuum Distillation, Molecules 24(10) (2019).
[45] C. Cheng, Y. Zou, J. Peng, Oregano Essential Oil Attenuates RAW264.7 Cells from Lipopolysaccharide-Induced Inflammatory Response through Regulating NADPH Oxidase Activation-Driven Oxidative Stress, Molecules 23(8) (2018).
[46] F. Conforti, M. Marrelli, F. Menichini, R. Tundis, G.A. Statti, U. Solimene, F. Menichini, Chemical composition and protective effect of oregano (Origanum heracleoticum L.) ethanolic extract on oxidative damage and on inhibition of NO in LPS-stimulated RAW 264.7 macrophages, J Enzyme Inhib Med Chem 26(3) (2011) 404-11.
[47] K. Mechergui, J.A. Coelho, M.C. Serra, S.B. Lamine, S. Boukhchina, M.L. Khouja, Essential oils of Origanum vulgare L. subsp. glandulosum (Desf.) Ietswaart from Tunisia: chemical composition and antioxidant activity, Journal of the Science of Food and Agriculture 90(10) (2010) 1745-1749.
[48] N. Leyva-Lopez, V. Nair, W.Y. Bang, L. Cisneros-Zevallos, J.B. Heredia, Protective role of terpenes and polyphenols from three species of Oregano (Lippia graveolens, Lippia palmeri and Hedeoma patens) on the suppression of lipopolysaccharide-induced inflammation in RAW 264.7 macrophage cells, J Ethnopharmacol 187 (2016) 302-12.
[49] M.R. Loizzo, F. Menichini, F. Conforti, R. Tundis, M. Bonesi, A.M. Saab, G.A. Statti, B.d. Cindio, P.J. Houghton, F. Menichini, N.G. Frega, Chemical analysis, antioxidant, antiinflammatory and anticholinesterase activities of Origanum ehrenbergii Boiss and Origanum syriacum L. essential oils, Food chemistry 117(1) (2009) 174-180.
[50] J. Mastelic, I. Jerkovic, I. Blazevic, M. Poljak-Blazi, S. Borovic, I. Ivancic-Bace, V. Smrecki, N. Zarkovic, K. Brcic-Kostic, D. Vikic-Topic, N. Muller, Comparative study on the antioxidant and biological activities of carvacrol, thymol, and eugenol derivatives, J Agric Food Chem 56(11) (2008) 3989-96.
[51] S. Kivrak, Essential oil composition and antioxidant activities of eight cultivars of Lavender and Lavandin from western Anatolia, Industrial Crops and Products 117 (2018) 88-96.
[52] Z.W. Cui, Z.X. Xie, B.F. Wang, Z.H. Zhong, X.Y. Chen, Y.H. Sun, Q.F. Sun, G.Y. Yang, L.G. Bian, Carvacrol protects neuroblastoma SH-SY5Y cells against Fe(2+)-induced apoptosis by suppressing activation of MAPK/JNK-NF-κB signaling pathway, Acta Pharmacol Sin 36(12) (2015) 1426-36.

[53] M.Y. Huang, M.H. Liao, Y.K. Wang, Y.S. Huang, H.C. Wen, Effect of lavender essential oil on LPS-stimulated inflammation, Am J Chin Med 40(4) (2012) 845-59.
[54] G.F.E. Cardia, S.E. Silva-Filho, E.L. Silva, N.S. Uchida, H.A.O. Cavalcante, L.L. Cassarotti, V.E.C. Salvadego, R.A. Spironello, C.A. Bersani-Amado, R.K.N. Cuman, Effect of Lavender (Lavandula angustifolia) Essential Oil on Acute Inflammatory Response, Evid Based Complement Alternat Med 2018 (2018) 1413940.
[55] M.N.M. Nogueira, S.G. Aquino, C. Rossa Junior, D.M.P. Spolidorio, Terpinen-4-ol and alpha-terpineol (tea tree oil components) inhibit the production of IL-1β, IL-6 and IL-10 on human macrophages, Inflammation Research 63(9) (2014) 769-778.
[56] M. Yan, Y. Zhu, H.-J. Zhang, W.-H. Jiao, B.-N. Han, Z.-X. Liu, F. Qiu, W.-S. Chen, H.-W. Lin, Anti-inflammatory secondary metabolites from the leaves of Rosa laevigata, Bioorganic & medicinal chemistry 21(11) (2013) 3290-3297.
[57] J.-X. Zhou, M. Wink, Evidence for Anti-Inflammatory Activity of Isoliquiritigenin, 18β Glycyrrhetinic Acid, Ursolic Acid, and the Traditional Chinese Medicine Plants Glycyrrhiza glabra and Eriobotrya japonica , at the Molecular Level, Medicines (Basel, Switzerland) 6(2) (2019) 55.
[58] B. Bose, H. Choudhury, P. Tandon, S. Kumaria, Studies on secondary metabolite profiling, anti-inflammatory potential, *in vitro* photoprotective and skin-aging related enzyme inhibitory activities of Malaxis acuminata, a threatened orchid of nutraceutical importance, Journal of photochemistry and photobiology. B, Biology 173 (2017) 686-695.
[59] C.-C. Chen, M.-W. Lin, C.-J. Liang, S.-H. Wang, The Anti-Inflammatory Effects and Mechanisms of Eupafolin in Lipopolysaccharide-Induced Inflammatory Responses in RAW264.7 Macrophages, PloS one 11(7) (2016) e0158662-e0158662.
[60] W.M. Ksouri, F. Medini, K. Mkadmini, J. Legault, C. Magné, C. Abdelly, R. Ksouri, LC–ESI-TOF–MS identification of bioactive secondary metabolites involved in the antioxidant, anti-inflammatory and anticancer activities of the edible halophyte Zygophyllum album Desf, Food chemistry 139(1-4) (2013) 1073-1080.
[61] Lipoxygenase inhibitors from natural plant sources. Part 1: Medicinal plants with inhibitory activity on arachidonate 5-lipoxygenase and 5-lipoxygenase[sol]cyclooxygenase, Phytotherapy research. 19(2) (2005) 81-102.
[62] K.-K. Lee, J.-D. Choi, The Effects of Areca Catechu L Extract on Anti-Inflammation and Anti-Melanogenesis, International journal of cosmetic science 21(4) (1999) 275-284.

[63] A. Al-Jumaili, A. Kumar, K. Bazaka, M.V. Jacob, Plant Secondary Metabolite-Derived Polymers: A Potential Approach to Develop Antimicrobial Films, Polymers (Basel) 10(5) (2018).

[64] A. Weseler, H.K. Geiss, R. Saller, J. Reichling, A novel colorimetric broth microdilution method to determine the minimum inhibitory concentration (MIC) of antibiotics and essential oils against Helicobacter pylori, Pharmazie 60(7) (2005) 498-502.

[65] A. Ahmad, M.Y. Wani, A. Khan, N. Manzoor, J. Molepo, Synergistic interactions of eugenol-Tosylate and its congeners with fluconazole against candida albicans, PLoS ONE 10(12) (2015) e0145053.

[66] L. Dhara, A. Tripathi, Antimicrobial activity of eugenol and cinnamaldehyde against extended spectrum beta lactamase producing enterobacteriaceae by *in vitro* and molecular docking analysis, European Journal of Integrative Medicine 5(6) (2013) 527-536.

[67] S. Hemaiswarya, M. Doble, Synergistic interaction of eugenol with antibiotics against Gram negative bacteria, Phytomedicine 16(11) (2009) 997-1005.

[68] G.S. Labib, H. Aldawsari, Innovation of natural essential oil-loaded Orabase for local treatment of oral candidiasis, Drug Design, Development and Therapy 9 (2015) 3349-3359.

[69] N. Thosar, S. Basak, R.N. Bahadure, M. Rajurkar, Antimicrobial efficacy of five essential oils against oral pathogens: An *in vitro* study, European Journal of Dentistry 7(S 01) (2013) S071-S077.

[70] L. Zhou, L. Zhou, H. Zheng, H. Zheng, Y. Tang, Y. Tang, W. Yu, W. Yu, Q. Gong, Q. Gong, Eugenol inhibits quorum sensing at sub-inhibitory concentrations, Biotechnology Letters 35(4) (2013) 631-637.

[71] J. Shin, V.-S. Prabhakaran, K.-s. Kim, The multi-faceted potential of plant-derived metabolites as antimicrobial agents against multidrug-resistant pathogens, Microbial pathogenesis 116 (2018) 209-214.

[72] C.L. Gorlenko, H.Y. Kiselev, E.V. Budanova, A.A. Zamyatnin, Jr., L.N. Ikryannikova, Plant Secondary Metabolites in the Battle of Drugs and Drug-Resistant Bacteria: New Heroes or Worse Clones of Antibiotics?, Antibiotics (Basel) 9(4) (2020).

[73] H.Y. Cui, C.H. Zhang, C.Z. Li, L. Lin, Antibacterial mechanism of oregano essential oil, Industrial Crops and Products 139 (2019).

[74] D. Trombetta, F. Castelli, M.G. Sarpietro, V. Venuti, M. Cristani, C. Daniele, A. Saija, G. Mazzanti, G. Bisignano, Mechanisms of Antibacterial Action of Three Monoterpenes, Antimicrobial Agents and Chemotherapy 49(6) (2005) 2474-2478.

[75] R.J.W. Lambert, P.N. Skandamis, P.J. Coote, G.J.E. Nychas, A study of the minimum inhibitory concentration and mode of action of oregano essential oil, thymol and carvacrol, Journal of applied microbiology 91(3) (2001) 453-462.
[76] A. Ultee, M.H.J. Bennik, R. Moezelaar, The Phenolic Hydroxyl Group of Carvacrol Is Essential for Action against the Food-Borne Pathogen Bacillus cereus, Applied and Environmental Microbiology 68(4) (2002) 1561-1568.
[77] Cox, Gustafson, Mann, Markham, Liew, Hartland, Bell, Warmington, Wyllie, Tea tree oil causes K+ leakage and inhibits respiration in Escherichia coli, Letters in Applied Microbiology 26(5) (1998) 355-358.
[78] K.P. Devi, S.A. Nisha, R. Sakthivel, S.K. Pandian, Eugenol (an essential oil of clove) acts as an antibacterial agent against Salmonella typhi by disrupting the cellular membrane, Journal of Ethnopharmacology 130(1) (2010) 107-115.
[79] R. Iseppi, A. Di Cerbo, P. Aloisi, M. Manelli, V. Pellesi, C. Provenzano, S. Camellini, P. Messi, C. Sabia, *In Vitro* Activity of Essential Oils Against Planktonic and Biofilm Cells of Extended-Spectrum β-Lactamase (ESBL)/Carbapenamase-Producing Gram-Negative Bacteria Involved in Human Nosocomial Infections, Antibiotics (Basel) 9(5) (2020).
[80] L. Polo, B. Díaz de Greñu, E. Della Bella, S. Pagani, P. Torricelli, J.L. Vivancos, M. Ruiz-Rico, J.M. Barat, E. Aznar, R. Martínez-Máñez, M. Fini, F. Sancenón, Antimicrobial activity of commercial calcium phosphate based materials functionalized with vanillin, Acta biomaterialia 81 (2018) 293-303.
[81] D.N. Amato, D.V. Amato, O.V. Mavrodi, D.A. Braasch, S.E. Walley, J.R. Douglas, D.V. Mavrodi, D.L. Patton, Destruction of Opportunistic Pathogens via Polymer Nanoparticle-Mediated Release of Plant-Based Antimicrobial Payloads, Advanced healthcare materials 5(9) (2016) 1094-1103.
[82] M.N. Gallucci, M.E. Carezzano, M.M. Oliva, M.S. Demo, R.P. Pizzolitto, M.P. Zunino, J.A. Zygadlo, J.S. Dambolena, *In vitro* activity of natural phenolic compounds against fluconazole-resistant Candida species: a quantitative structure–activity relationship analysis, Journal of Applied Microbiology 116(4) (2014) 795-804.
[83] A. Puskarova, M. Buckova, L. Krakova, D. Pangallo, K. Kozics, The antibacterial and antifungal activity of six essential oils and their cyto/genotoxicity to human HEL 12469 cells, Scientific Reports 7 (2017).
[84] R. Scaffaro, F. Lopresti, M. D'Arrigo, A. Marino, A. Nostro, Efficacy of poly(lactic acid)/carvacrol electrospun membranes against Staphylococcus aureus and Candida albicans

in single and mixed cultures, Applied microbiology and biotechnology 102(9) (2018) 4171-4181.
[85] Y. Yue, X. Gong, W. Jiao, Y. Li, X. Yin, Y. Si, J. Yu, B. Ding, In-situ electrospinning of thymol-loaded polyurethane fibrous membranes for waterproof, breathable, and antibacterial wound dressing application, Journal of colloid and interface science 592 (2021) 310-318.
[86] P. Brun, G. Bernabè, R. Filippini, A. Piovan, *In Vitro* Antimicrobial Activities of Commercially Available Tea Tree (Melaleuca alternifolia) Essential Oils, Curr Microbiol 76(1) (2019) 108-116.
[87] Y. Li, Z. Fang, H. Zhu, L. Yang, H. Liu, *In Vitro* Antibacterial Effect and Sensitization Evaluation of Tea-Tree Oil Preparation, IOP Conf. Ser.: Mater. Sci. Eng, IOP Publishing, 2019, p. 22128.
[88] S. Ahmadi, A. Hivechi, S.H. Bahrami, P.B. Milan, S.S. Ashraf, Cinnamon extract loaded electrospun chitosan/gelatin membrane with antibacterial activity, International journal of biological macromolecules 173 (2021) 580-590.
[89] Z. Karami, I. Rezaeian, P. Zahedi, M. Abdollahi, Preparation and performance evaluations of electrospun poly(ε-caprolactone), poly(lactic acid), and their hybrid (50/50) nanofibrous mats containing thymol as an herbal drug for effective wound healing, Journal of Applied Polymer Science 129(2) (2013) 756-766.
[90] S. García-Salinas, M. Evangelopoulos, E. Gámez-Herrera, M. Arruebo, S. Irusta, F. Taraballi, G. Mendoza, E. Tasciotti, Electrospun anti-inflammatory patch loaded with essential oils for wound healing, International journal of pharmaceutics 577 (2020) 119067-119067.
[91] M.R. Zare, M. Khorram, S. Barzegar, F. Asadian, Z. Zareshahrabadi, M.J. Saharkhiz, S. Ahadian, K. Zomorodian, Antimicrobial core–shell electrospun nanofibers containing Ajwain essential oil for accelerating infected wound healing, International journal of pharmaceutics 603 (2021) 120698-120698.
[92] J.G. Merrell, S.W. McLaughlin, L. Tie, C.T. Laurencin, A.F. Chen, L.S. Nair, Curcumin Loaded Poly(ε-Caprolactone) Nanofibers: Diabetic Wound Dressing with Antioxidant and Anti-inflammatory Properties, Clinical and experimental pharmacology and physiology 36(12) (2009) 1149-1156.
[93] M. Qin, X.J. Mou, W.H. Dong, J.X. Liu, H. Liu, Z. Dai, X.W. Huang, N. Wang, X. Yan, In Situ Electrospinning Wound healing Films Composed of Zein and Clove Essential Oil, Macromolecular Materials and Engineering 305(3) (2020).

[94] Y. Ge, J. Tang, H. Fu, Y. Fu, Y. Wu, Characteristics, Controlled-release and Antimicrobial Properties of Tea Tree Oil Liposomes-incorporated Chitosan-based Electrospun Nanofiber Mats, Fibers and polymers 20(4) (2019) 698-708.
[95] S. Moradi, A. Barati, A.E. Tonelli, H. Hamedi, Effect of clinoptilolite on structure and drug release behavior of chitosan/thyme oil γ-Cyclodextrin inclusion compound hydrogels, Journal of applied polymer science 138(6) (2021) 49822-n/a.
[96] S. Jiji, S. Udhayakumar, C. Rose, C. Muralidharan, K. Kadirvelu, Thymol enriched bacterial cellulose hydrogel as effective material for third degree burn wound repair, International journal of biological macromolecules 122 (2019) 452-460.
[97] J. Parisotto-Peterle, J. Bidone, L.G. Lucca, G.d.M.S. Araújo, M.C. Falkembach, M. da Silva Marques, A.P. Horn, M.K. dos Santos, V.F. da Veiga, R.P. Limberger, H.F. Teixeira, C.L. Dora, L.S. Koester, Healing activity of hydrogel containing nanoemulsified β-caryophyllene, European journal of pharmaceutical sciences 148 (2020) 105318.
[98] N.A.S. Rozman, W.Y. Tong, C.R. Leong, M.R. Anuar, S. Karim, S.K. Ong, F.A.M. Yusof, W.N. Tan, B. Sulaiman, M.L. Ooi, K.C. Lee, Homalomena pineodora essential oil nanoparticle inhibits diabetic wound pathogens, Sci Rep 10(1) (2020) 3307.
[99] L. Ghaderi, A. Aliahmadi, S.N. Ebrahimi, H. Rafati, Effective Inhibition and eradication of Pseudomonas aeruginosa biofilms by Satureja khuzistanica essential oil nanoemulsion, Journal of drug delivery science and technology 61 (2021) 102260.
[100] F. Shakeel, P. Alam, M.K. Anwer, S. Alanazi, I.A. Alsarra, M.H. Alqarni, Wound healing evaluation of self-nanoemulsifying drug delivery system containing Piper cubeba essential oil, 3 Biotech 9(3) (2019).
[101] M. Ghodrati, M.R. Farahpour, H. Hamishehkar, Encapsulation of Peppermint essential oil in nanostructured lipid carriers: In-vitro antibacterial activity and accelerative effect on infected wound healing, Colloids and Surfaces A: Physicochemical and Engineering Aspects 564 (2019) 161-169.
[102] L. Risaliti, G. Pini, R. Ascrizzi, R. Donato, C. Sacco, M.C. Bergonzi, M.C. Salvatici, A.R. Bilia, Artemisia annua essential oil extraction, characterization, and incorporation in nanoliposomes, smart drug delivery systems against Candida species, Journal of drug delivery science and technology 59 (2020) 101849.
[103] L. Risaliti, A. Kehagia, E. Daoultzi, D. Lazari, M.C. Bergonzi, S. Vergkizi-Nikolakaki, D. Hadjipavlou-Litina, A.R. Bilia, Liposomes loaded with Salvia triloba and Rosmarinus officinalis essential oils: *In vitro* assessment of antioxidant, antiinflammatory and antibacterial activities, Journal of drug delivery science and technology 51 (2019) 493-498.

[104] J. Jia, S. Duan, X. Zhou, L. Sun, C. Qin, M. Li, F. Ge, Long-Term Antibacterial Film Nanocomposite Incorporated with Patchouli Essential Oil Prepared by Supercritical CO2 Cyclic Impregnation for Wound Dressing, Molecules (Basel, Switzerland) 26(16) (2021) 5005.
[105] S. Milovanovic, M. Stamenic, D. Markovic, M. Radetic, I. Zizovic, Solubility of thymol in supercritical carbon dioxide and its impregnation on cotton gauze, The Journal of supercritical fluids 84 (2013) 173-181.
[106] A.M.A. Dias, A. Rey-Rico, R.A. Oliveira, S. Marceneiro, C. Alvarez-Lorenzo, A. Concheiro, R.N.C. Júnior, M.E.M. Braga, H.C. de Sousa, Wound dressings loaded with an anti-inflammatory jucá (Libidibia ferrea) extract using supercritical carbon dioxide technology, The Journal of supercritical fluids 74 (2013) 34-45.
[107] J. Dikić, I. Lukić, J. Pajnik, J. Pavlović, J. Hrenović, N. Rajić, Antibacterial activity of thymol/carvacrol and clinoptilolite composites prepared by supercritical solvent impregnation, Journal of porous materials 28(5) (2021) 1577-1584.
[108] A. Pegalajar-Jurado, C.D. Easton, K.E. Styan, S.L. McArthur, Antibacterial activity studies of plasma polymerised cineole films, Journal of Materials Chemistry B 2(31) (2014) 4993-5002.
[109] K. Bazaka, M. Jacob, V.K. Truong, R.J. Crawford, E.P. Ivanova, The Effect of Polyterpenol Thin Film Surfaces on Bacterial Viability and Adhesion, Polymers 3(1) (2011) 388-404.
[110] A. Kumar, A. Al-Jumaili, K. Prasad, K. Bazaka, P. Mulvey, J. Warner, M.V. Jacob, Pulse Plasma Deposition of Terpinen-4-ol: An Insight into Polymerization Mechanism and Enhanced Antibacterial Response of Developed Thin Films, Plasma Chemistry and Plasma Processing 40(1) (2019) 339-355.
[111] A. Kumar, A. Al-Jumaili, K. Bazaka, P. Mulvey, J. Warner, M.V. Jacob, In-Situ Surface Modification of Terpinen-4-ol Plasma Polymers for Increased Antibacterial Activity, Materials 13(3) (2020) 586.
[112] S.M.K. Jesus Romo-Rico, Jonathan Golledge, Andrew Hayles, Krasimir Vasilev, Mohan Jacob, Plasma polymers from oregano secondary metabolites: An antibacterial and biocompatible plant-based polymers, Plasma Process Polym (2022).
[113] J. Wang, M. Windbergs, Functional electrospun fibers for the treatment of human skin wounds, European Journal of Pharmaceutics and Biopharmaceutics 119 (2017) 283-299.
[114] S. García-Salinas, M. Evangelopoulos, E. Gámez-Herrera, M. Arruebo, S. Irusta, F. Taraballi, G. Mendoza, E. Tasciotti, Electrospun anti-inflammatory patch loaded with essential oils for wound healing, International Journal of Pharmaceutics 577 (2020) 119067.

[115] E. Caló, V.V. Khutoryanskiy, Biomedical applications of hydrogels: A review of patents and commercial products, European polymer journal 65 (2015) 252-267.
[116] A. Rojas, A. Torres, M. José Galotto, A. Guarda, R. Julio, Supercritical impregnation for food applications: a review of the effect of the operational variables on the active compound loading, Critical reviews in food science and nutrition 60(8) (2022) 1290-1301.
[117] J. Sepulveda, C. Villegas, A. Torres, E. Vargas, F. Rodriguez, S. Baltazar, A. Prada, A. Rojas, J. Romero, S. Faba, M.J. Galotto, Effect of functionalized silica nanoparticles on the mass transfer process in active PLA nanocomposite films obtained by supercritical impregnation for sustainable food packaging, The Journal of supercritical fluids 161 (2020) 104844.
[118] C. Cejudo Bastante, L. Casas Cardoso, M.T. Fernández Ponce, C. Mantell Serrano, E.J. Martínez de la Ossa-Fernández, Characterization of olive leaf extract polyphenols loaded by supercritical solvent impregnation into PET/PP food packaging films, The Journal of supercritical fluids 140 (2018) 196-206.
[119] A. Torres, J. Romero, A. Macan, A. Guarda, M.J. Galotto, Near critical and supercritical impregnation and kinetic release of thymol in LLDPE films used for food packaging, The Journal of supercritical fluids 85 (2014) 41-48.
[120] G.A. Albuquerque, F.W.F. Bezerra, M.S. de Oliveira, W.A. da Costa, R.N. de Carvalho Junior, M.R.S.P. Joele, Supercritical CO2 Impregnation of Piper divaricatum Essential Oil in Fish (Cynoscion acoupa) Skin Gelatin Films, Food and bioprocess technology 13(10) (2020) 1765-1777.
[121] F.C. Christine, J.M. Brian, V.R. Thomas, Mechanism of Action of Melaleuca alternifolia (Tea Tree) Oil on Staphylococcus aureus Determined by Time-Kill, Lysis, Leakage, and Salt Tolerance Assays and Electron Microscopy, Antimicrobial Agents and Chemotherapy 46(6) (2002) 1914-1920.

Chapter 3

Plasma polymers from oregano secondary metabolites: An antibacterial and biocompatible plant-based polymers

In this chapter, a plasma polymer (PP) from Oregano Secondary Metabolites (OSM) fabricated by RF-PECVD as a potential wound-healing agent is presented. The surface, antibacterial properties and biocompatibility of the PP-OSMs were investigated. PP-OSMs preserved the medicinal functional groups of Oregano and shown smooth roughness and superhydrophilic properties. Moreover, PP-OSMs shown bactericidal properties against *P. aeruginosa* and *S. aureus*. PP-OSMs were biocompatible with human dermal fibroblasts, promoting its adhesion and spreading.

This chapter was published as: *Jesus Romo-Rico, Smriti Murali Krishna, Jonathan Golledge, Andrew Hayles, Krasimir Vasilev, and Mohan Jacob*. Plasma polymers from oregano secondary metabolites: An antibacterial and biocompatible plant-based polymers. Plasma Processes and Polymers, 2022. Volume 19, 2022, ISSN 1612-8850, https://doi.org/10.1002/ppap.202100220.

Plasma polymers from oregano secondary metabolites: An antibacterial and biocompatible plant-based polymers

Graphical abstract

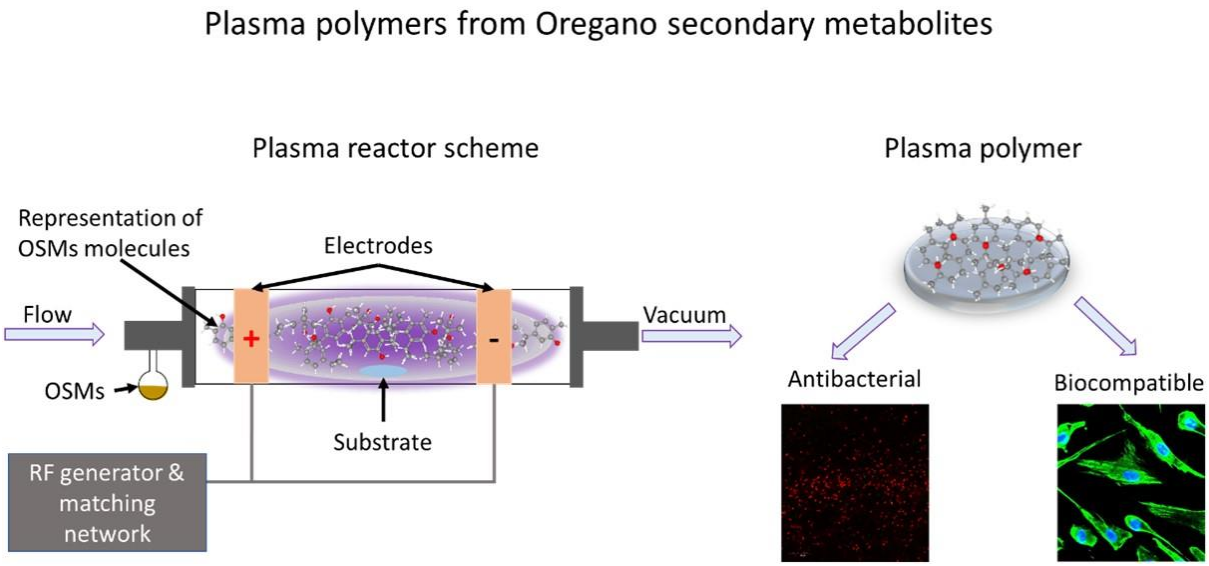

Abstract

Bacterial infection of chronic wounds is a major healthcare problem which affects the quality of life of millions of patients worldwide and causes a substantial healthcare cost burden. This project focused on the manufacture of a potential wound-healing agent. Plasma polymers from oregano secondary metabolites (PP-OSMs) were fabricated by Radiofrequency Plasma Enhanced Chemical Vapor Deposition (RF-PECVD) in continuous and pulse plasma mode at room temperature. The surface, biocompatibility, and antibacterial properties of the PP-OSMs were investigated. Polymers fabricated by RF-PECVD retained the functional groups of OSMs, promoted human dermal fibroblast adhesion, inhibited *Staphylococcus aureus* attachment, and eliminated *Pseudomonas aeruginosa*. The PP-OSM coatings are potential candidates to be used in medical applications where cell biocompatibility and antibacterial properties are required.

3.1. Introduction

Chronic wounds are a major issue impacting the quality of life of 2% of the world population[1] and causing a substantial burden to healthcare systems.[2-4] In Australia alone, chronic wound care costs more than AUD 3 billion per year and wound affects nearly half a million people.[5] Approximately, 50,000 Australians suffer from diabetic foot ulcers whereas 300,000 are at risk of developing it.[6] Diabetes-related chronic wounds frequently become infected that impairs healing and can lead to major amputation and death.[7]

Plasma technology is being investigated as a novel method to fabricate wound-healing materials such as plant secondary metabolites (PSMs), which have been reported to have anti-bacterial properties.[8-14] The anti-bacterial properties of PSMs are believed to result from incorporated monoterpenes inhibiting ATP generation, blocking ion transport and disrupting cytoplasmic membranes of bacteria.[15-18]

One approach to coating PSMs on wound dressings is the use of RF-PECVD.[19] Plasma polymers from PSMs are formed by atoms, positive and negative ions, free and non-free radicals and metastables, colliding in the plasma phase amongst themselves, intact precursor (PSMs) and the depositing coating. During this process, PSMs molecules are partially or fully fragmented, reconstituted and deposited on surfaces as highly crosslinked polymeric coatings.[20] The advantage of this technique is the capability to adjust the polymerization parameters to tune the final properties of the resulting polymeric surface. The RF-PECVD can be optimised to retain PSMs functional groups in coatings deposited on different substrates to provide flexibility of application.

Previous studies have reported the use of terpinen-4-ol (T4), a major constituent of tea tree oil, as a PSM precursor to fabricate plasma polymer coatings.[21] Further, the antibacterial properties of T4 plasma-films have been explored. Bazaka *et al.* have fabricated antibacterial plasma-films from T4 using continuous plasma (CP) power of 10W and 25W. [22] The main difference between both polymers was the antibacterial response against *Staphylococcus aureus* and *Pseudomonas aeruginosa*. In the case of the polyterpenol films fabricated at 10W, inhibition of bacterial adhesion was achieved by the preservation of functionalities of T4 during fabrication at low deposition power. Films fabricated at 25W showed higher bacterial adhesion when compared to control and films fabricated at 10W. This could be associated with the modification and recombination of T4 functional groups that promote bacterial adhesion instead of inhibition. [22]

In another study, Kumar et *al.* developed coatings from T4 using pulse plasma (PP) polymerization. [23] The polymerization conditions were 10W, duty cycle (DC) 40 at 500Hz. The antibacterial properties of these polymers were tested against *P. aeruginosa.* The polymers fabricated in this study were hydrophobic and promoted *P. aeruginosa* attachment, however, this pathogen was unable to survive after 24h of contact with the T4 surface due to the retention of bactericidal molecules of the monomer. [23]

T4 polymers were fabricated and doped with ZnO nanoparticles using CP at 10 W, with and without oxygen ($T4_{oxy}$) and argon carriers ($T4_{arg}$). $T4_{oxy}$ and T4 + ZnO inhibited *Escherichia coli* adhesion. However, the antibacterial properties of the films did not change much with the addition of ZnO nanoparticles when compared to $T4_{oxy}$. [24] These results suggest that the contribution to bacterial inhibition is associated with the nature of T4 and retention of its functional groups.

Pegalajar-Jurado *et al* fabricated films using a minor component of tea tree oil, 1,8-cineole, using plasma polymerization at 20W. The obtained film was a moderate hydrophilic surface with roughness <1 nm. The antibacterial properties of the 1, 8 cineole were retained in the plasma polymers showing inhibition of 64% against *S. aureus* and 98% against *E. coli* when compared to the control sample. A preliminary study on the biocompatibility of these films was also carried out. 1, 8 cineole films did not have cytotoxicity to fibroblasts and inhibited their adhesion to the polymeric matrix surface. [25]

Monomers of geranium essential oil were fabricated as continuous plasma films at a range of deposition powers from 10 to 100 W. [26] The antibacterial properties of the created films reduced as the deposition powers used increased, as a result of monomer fragmentation. At high deposition powers, the functional groups defragment to a greater degree than at low power levels, thus, the retention of the inherent properties of the monomer is difficult to retain.

Oregano (*Origanum Vulgaris*) is a popular herb widely used in Mediterranean and Latin American cuisines. Ancient civilizations not only used this herb to spice up their foods but also used it in treatments against respiratory infections, skin conditions and digestive disorders. Oregano secondary metabolites (OSMs) are volatile molecules expelled by *Origanum Vulgaris* which are believed to be responsible for Oregano's health benefits. [27-31] Antimicrobial activity of oregano has been attributed to its content of phenolic monoterpene carvacrol (CR). The different constituents of oregano oil can vary significantly. However, depending on the origin of the oregano species, the content of CR could be up to approximately 90% [32, 33]. CR affects bacterial membrane permeability, causing leakage of Na^+ and K^+, inhibiting intracellular enzyme activity and irreparably damaging bacteria. [15]

Previous studies have examined the wound-healing properties of oregano but there has been no previous report of using RF-PECVD to fabricate OSMs.[34] The aim of this study was to fabricate plasma polymers (PP) from OSMs with potential applications as antibacterial surfaces for wound-healing applications. We fabricated PP-OSMs using RF-PECVD in continuous and pulse mode. The retention of the functional groups of oregano in PP-OSMs was corroborated using Fourier Transformed Infrared Spectroscopy (FTIR). Thickness, homogeneity and hydrophilic properties were determined by ellipsometry, atomic force microscopy (AFM) and sessile drop water contact angle measurements, respectively. Leaching of PP-OSMs surface was determined as well as the changes in the pH after submerging in water for 24 hrs. The antibacterial properties of the PP-OSMs were evaluated against *P. aeruginosa* and *S. aureus*. These bacteria were selected due to their high prevalence in diabetes-related wound infection. [35, 36] Cell viability, cytotoxicity, and adhesion were evaluated *in vitro* using human dermal fibroblasts (HDF).

3.2. Experimental Section

3.2.1. Fabrication of plasma films and chemical composition

PP-OSMs were fabricated on glass (76 mm x 26 mm) and borosilicate (diameter 6 mm) substrates. The substrates were sonicated for five minutes in propan-2-ol. Then rinsed and sonicated with distilled water for 5 minutes, after, the samples were air-dried. The substrates were introduced into the RF-PECVD plasma reactor that consisted of a horizontally positioned tube chamber (l: 90 cm, d: 5 cm) with a rotary vacuum pump and a monomer inlet at each end. The rotary vacuum pump maintained the chamber at a pressure of 300 mTorr. Two copper electrodes were positioned in the middle of the tube chamber separated by 7 cm. During each experiment, the substrates were placed at the centre between the electrodes. Both electrodes were coupled to a Radio Frequency (RF) generator (ACG-3B, MKS Instrument, Andover, MA, USA). Two hundred µl of Oregano essential oil (OEO) were placed in a Florence flask to feed the plasma reactor, and the flow rate of the monomer was controlled with a vacuum stopcock. The deposition of the film was performed using CP and PP (duty cycle of 50% and 500Hz) modes at 50 W for 10 minutes.

3.2.2. Chemical characterization

FTIR (Perkinelmer Inc., Boston, MA, USA) was used to confirm the retention of Oregano functional groups in the PP-OSMs. For this purpose, FTIR was used in attenuated total reflection (ATR) mode.

3.2.3. Thickness and roughness

The thickness and topography of CP50W and PP50W were estimated using Variable Angle Spectroscopic Ellipsometry (JA Woollam-M200 D, Lincoln, NE, USA) at 55°, 60° and 65°. Data acquisition parameters were standard and high-accuracy modes. The 25 points of measurement were situated in a polar grid mesh starting from the center and forming the circle every 30°. A graded layer model (#slices = 5) consisting of a glass substrate layer and a B-spline was applied to the data within the 400 – 1000 nm region where the film is optically transparent. Mean squared error (MSE) lower than 1 was used in these analyses. The surface roughness of PP-OSMs was obtained using an Atomic Force Microscope (AFM) (NT-MDT, Russian Federation) in semi-contact mode. The examination was carried out at room temperature and the scanned area of 3D images was 9 μm^2. Three samples of each condition were measured, and a minimum of 3 spots of 3x3 μm were analyzed.

3.2.4. Wettability

Hydrophobic or hydrophilic properties in CP50W and PP50W could be elucidated from a contact angle test using a KSV CAM 101 optical apparatus. It has been reported that the wettability properties are related to the chemical composition and surface roughness of films. [37] Wettability represents the affinity of a liquid to spread on a surface, which is measured using contact angle analysis of PP-OSMs performed by the sessile drop method, where a drop of liquid (polar or dispersed) is placed into the film surface and observed with a camera. The angle is measured using a reference baseline of the drop and the tangent of the drop boundary, the droplet volume, surface and height and the basal diameter.

3.2.5. Bacterial studies

*S. aureus (*ATCC 25923) and *P. aeruginosa* (clinical isolate, PAO1 type, SA Pathology) were both retrieved from glycerol stocks stored at -80°C, plated onto tryptone soy agar plates, and

cultured overnight at 37°C. For each strain, a single colony was aseptically transferred to 2 ml of tryptone soy broth and incubated for 18h. Triplicate samples of various essential oils plasma coated onto fragmented glass slides were individually placed in 6-well tissue culture plates and UV sterilized for 20 minutes. Bare glass slides were UV sterilized and used as the no-treatment control. Cell densities of the overnight cultures were measured using absorbance (600 nm, OD600) in a cuvette reader. The OD600 was set to 1, which is approximately 10^9 CFU/ml as previously determined by colony enumeration calibration. The cell density of the overnight cultures was then further diluted down to an approximately 10^6 CFU/ml. The glass slide samples were then immersed in 2 ml of the diluted cell cultures and incubated at 37°C for 18h.

3.2.6. LIVE/DEAD analyses

After incubation, the culture media was aspirated out of the well plates and replaced with 2 ml phosphate-buffered saline (PBS) for 1 minute to gently rinse away planktonic cells. The PBS was replaced, and the sample surfaces were coated with BacLight LIVE/DEAD (Invitrogen, Thermofisher, MA, USA) reagent, using equal proportions of Syto9 and propidium iodide at 1.5 µl/ml PBS. The samples were incubated for 15 minutes in the dark and immediately imaged with an Olympus FV3000 confocal laser scanning microscope. Three micrographs were taken at 40x magnification at random locations on each replicate sample. Green and red-stained cells were quantified using ImageJ software (V1.53, NIH, USA).

3.2.7. Fibroblast studies

HDF cells were cultured using Fibroblast Growth Medium -2 Bullet kit -from Lonza ™. Each experiment was done using cultured fibroblasts in passages 7 or 8. HDF was seeded (~50,000 cells/ml) in 6 mm round borosilicate coverslips containing CP50W and PP50W using 100 µl of cell culture in 96 well plates. Lysed cells were used as the negative control and healthy cells seeded on bare coverslips were used as a positive control.

3.2.8. Cell viability and cytotoxicity

ViaLight™ plus kit was used to estimate HDF viability by determination of their ATP levels using the assay protocol for a 96 well plate published by Lonza. Toxilight™ 100% lysis reagent set was used for determining cytotoxicity. This assay measures the release of adenylate kinase

(AK) from damaged cells. AK actively phosphorylates ADP to form ATP, which is then measured in a luminometer POLAR STAR OMEGA Model 415-0530.

3.2.9. Cell adhesion and spreading

HDF with a density of 50,000 cells/mL were seeded on 16 mm round borosilicate substrates. After being cultured for 24h, the cells were rinsed with PBS 3 times for 5 minutes and fixed with methanol at -20°C and rinsed again 3 times for 5 minutes with PBS. Subsequently, the primary antibody, vimentin (ab92547, Abcam, Cambridge, UK) was added at concentration 1/200 for 1h. or overnight at 4°C. A secondary antibody was then added, at a dilution factor 1/500 or 1/1000 1h. at room temperature. Finally, cell nuclei were counterstained with a drop of DAPI antifade gold (Thermofisher). Fluorescence images of cell nuclei and Vimentin were observed via fluorescence microscope Axio Imager Z1.

3.2.10. Statistical analyses

In bacterial experiments, 3 biological replicates and 3 technical replicate images were performed. Technical replicates were averaged, and the values were used to calculate the overall mean and standard deviation of cell viability across the 3 biological replicates. Data was plotted in GraphPad Prism (v8.3.0). Significance was obtained with Prism, using a 2-way ANOVA with Dunnett's multiple comparisons test. In cell viability and cytotoxicity experiments, 5 replicates were performed. Mean and standard deviation were reported for each sample. Data was plotted using the same software. Significance was calculated using ANOVA multi analyses comparison test.

3.3. Results and Discussion

3.3.1. Surface leachate as pH modifier

The thickness of PP-OSMs, CP50W and PP50W coatings were measured by Ellipsometry immediately after fabrication and after 24h immersion in MiliQ water (pH of 6.75). The average thickness of CP50W and PP50W films after fabrication were 90 nm and 123 nm, respectively. After immersion in water CP50W lost 59.2% of the film thickness whereas PP50W lost 35.3% of the film thickness as shown in **Figure 3.1**.

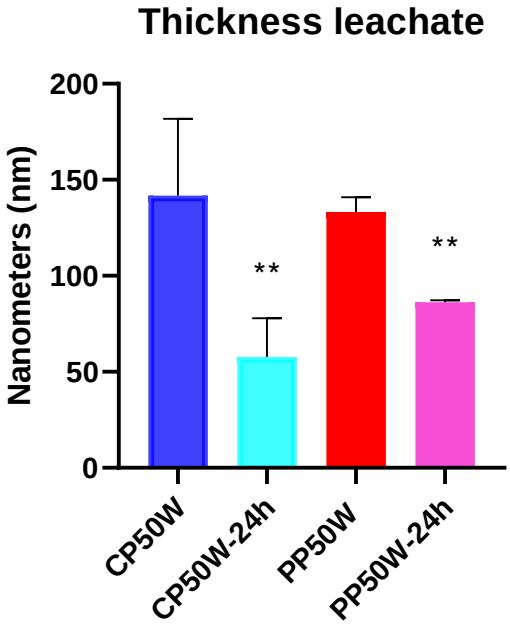

Figure 3. 1. The thickness of PP-OSMs before and after being submerged in distilled water for 24h.

Distilled water pH changed after 24h due to the PP-OSMs leachate from a near-neutral of 6.75 to an acidic of 4.6 and 5 for CP50W and PP50W, respectively. This result is interesting for wound dressing applications. In chronic wounds, elevated protease levels have been implicated in the degradation of new extracellular matrix (ECM). Protease activity is dependent on the pH of the surroundings. [38] One strategy for healing chronic wounds is to lower protease levels by using a pH modulator. Chronic wounds' pH values are in the range of 6.5-8.5, however, if it is reduced to 5, protease activity is expected to be reduced. Therefore, degradation of the new ECM would potentially not occur and wound-healing might be promoted. [39]

Figure 3.2 shows AFM images of CP50W and PP50W. Super smooth roughness, less than 1 nm was obtained in both samples (n=3) (CP50W = 0.2 nm and PP50W = 0.62 nm). The AFM image of PP50W showed random rough peaks (height 1 nm) along the scanned area whereas the image of CP50W showed a smooth surface. The observed 1 nm peaks along the PP50W image could be related to the accumulation of large OSM molecules bound to its surface. **Figure S.2** shows the topography of both samples. The roughness of the PP-OSMs increased to around 10 nm in peaks and valleys after 24h of submersion in MiliQ, this was associated with the leaching of thickness illustrated in **Figure 3.1.**

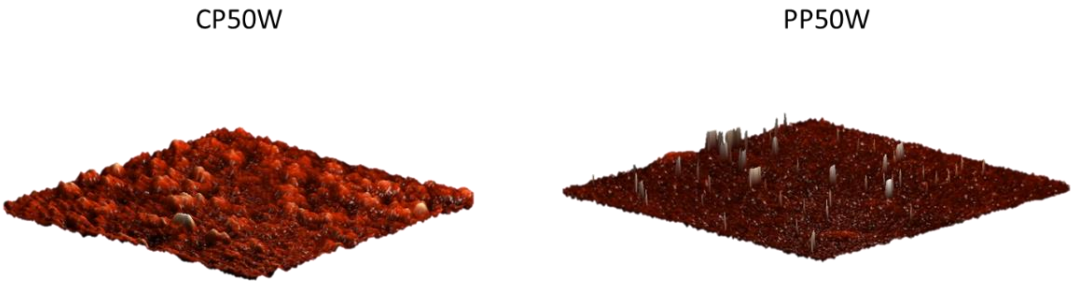

Figure 3. 2. Surface images of CP50W and PP50W obtained by AFM. Dimension of images are 3 µm x 3 µm x 3 nm.

3.3.2. Chemistry, wettability and smoothness of PP-OSMs surfaces

The chemical properties of PP-OSMs were investigated by FTIR. **Figure 3.3** shows the IR spectra of the PP-OSMs before and after submerged in MiliQ water. The functional groups of the OSMs were retained during PP-OSMs fabrication and after 24h of water submersion. The peaks between 2960 cm^{-1} and 2866 cm^{-1} appear due the vibration of the CH alkane strength and the CH_2 symmetric stretch. These peaks could be associated with the presence of CR [40]. At 1700 cm^{-1} a peak in the spectra of both CP50W and PP50W images can be seen. This was likely due to the carboxyl COOH bonds formed by the recombination of monomer molecules. Peaks between 1457 and 1380 cm^{-1} correspond to the symmetrical vibration of CH_3. [41-43] During continuous wave plasma deposition, the constant power leads to increasing fragmentation of the monomer and loss of some monomer functional groups, whereas, pulsed-wave plasma deposition results in less fragmentation and retention of the monomer functional groups. [23] Therefore, the thickness difference between CP50W and PP50W could be related to the deposition time as well as to the fragmentation effect of a plasma wave in the monomer and its polymerization.

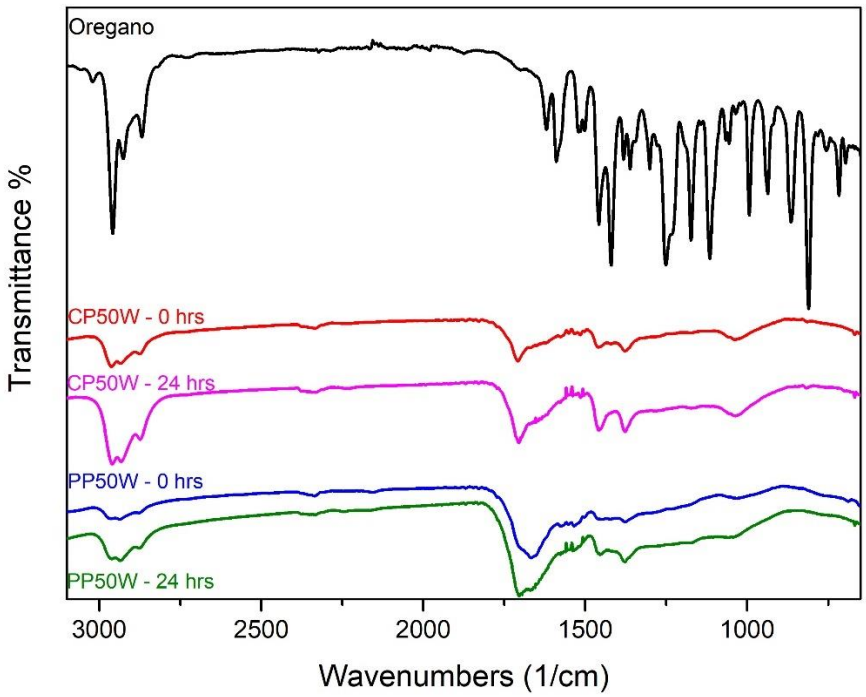

Figure 3. 3. FTIR spectrum of oregano essential oil, and PP-OSMs fabricated at different plasma conditions CP50W and PP50W.

The wettability of CP50W and PP50W was determined by water contact angle (WCA) measurements. The wettability of a material surface is related to its chemical composition and surface roughness. [37] **Figure 3.4** shows WCA for control, CP50W and PP50W. WCA for control and CP50W were similar at around 45°. WCA below 90° is considered hydrophilic, whereas a contact angle above 90° is hydrophobic. WCA of PP50W was below 7° which is considered superhydrophilic. [44] The low contact angle is likely associated with the high oxygen content observed in the FTIR measurements described above. COOH groups are polar groups that promote the absorption of water molecules on the surface.

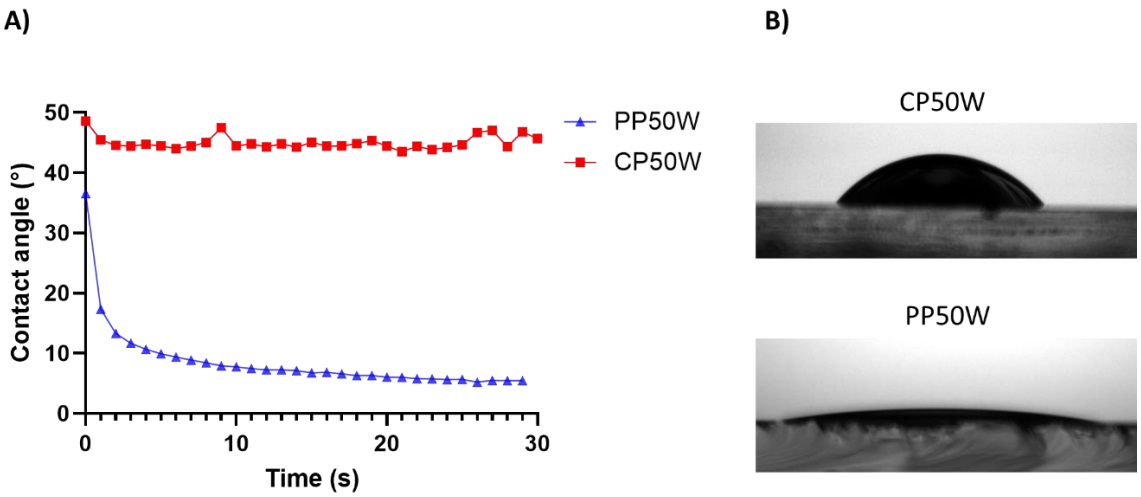

Figure 3. 4. A) Dynamic wetting properties of CP50W and PP50W in time (30 s) evaluated by sessile drop water contact angle measurements. B) Photographs of water droplets on CP50W and PP50W.

3.3.3. Antibacterial Performance of Oregano Polymers

The antibacterial properties of CP50W and PP50W were evaluated by fluorescence imaging using a LIVE/DEAD bacterial viability kit. Using this kit, bacterial cells with an intact cell membrane are fluoresce green, and cells with a perforated or ruptured cell membrane fluoresce red. Survival and attachment of *P. aeruginosa* and *S. aureus* were evaluated by the quantification of fluorescent cells. **Figure 3.5 A** shows fluorescence images, **figure 3.5 B** shows viability and attachment plots of both microorganisms seeded in PP-OSMs and in glass substrate used as a control.

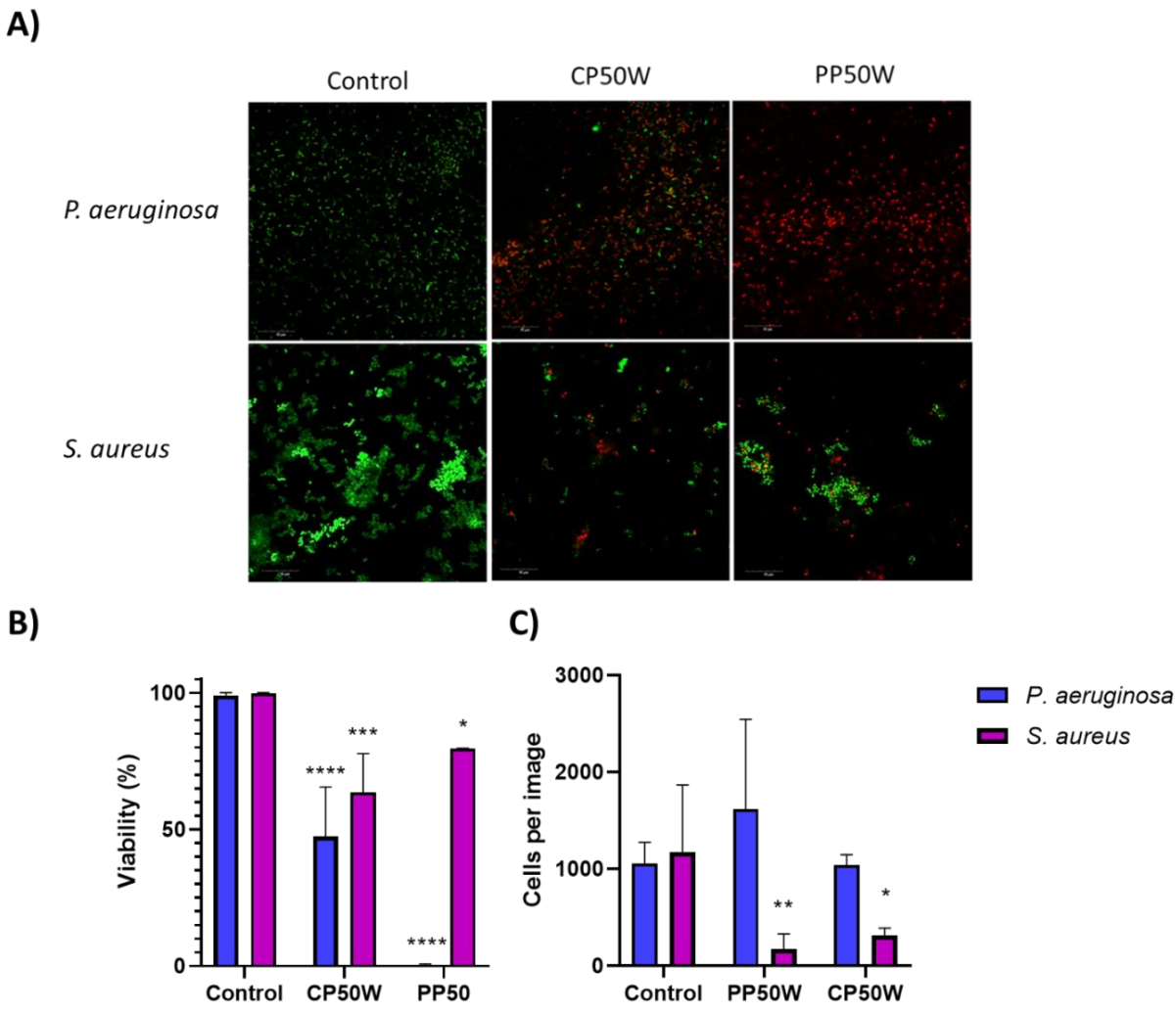

Figure 3. 5. Shows the antibacterial effect of PP-OSMs A) shows LIVE/DEAD images of *P. aeruginosa* and *S. aureus*. The green dye represents live bacteria whereas red stain represents dead bacteria, B) shows viability and C), shows cells per image. Dimensions of fluorescence images are approximately 100 x 100 µm.

Bactericidal activity of CP50W and PP50W are statistically significant ($P < 0.0001$ = ****) against *P. aeruginosa* with viabilities ranging from <1% (PP50W) up to 47% (CP50W), when compared to the glass slide control. However, as shown in **Figure 3.5** C, the rate of attachment of *P. aeruginosa* to CP50W and PP50W was not significantly different from the control. CP50W and PP50W were effective against *S. aureus* viability, $P < 0.0005$ = *** and $P < 0.05$ = *, respectively. Interestingly, *S. aureus* attachment was inhibited by both polymers, $P < 0.005$ = ** for PP50W and $P < 0.05$ = * for CP50W. This suggests that the CP50W and PP50W plasma films possess selective antifouling properties against *S. aureus*. The mechanisms of action of OEO, CR and thymol (TH) against different pathogens have been elucidated. OEO,

CR and TH can kill *P. aeruginosa* and *S. aureus* by penetrating their cytoplasmic membrane causing K^+ and PO_4^- leakage from both pathogens. [17] Recent studies of OEO against methicillin-resistant *Staphylococcus aureus* reported that OEO destroys its cell membrane, causing irreversible damage and producing the leakage of Na^+, and K^+, thereby affecting its physiological function. Additionally, CR can form a chimera with bacterial DNA affecting its replication, transcription and translation. [15]

3.3.4. Biocompatibility assessment: cell adhesion, viability and cytotoxicity

Cell viability and cytotoxicity of fibroblasts were measured 24h after seeding 0.1 ml of healthy cell medium (density 50,000 cells/mL) in glass substrate (control), CP50W and PP50W. After 24h, cell viability in control, CP50W and PP50W were similar. However, CP50W and PP50W were less cytotoxic than control, $P < 0.05$ = * and $P < 0.005$ = **, respectively (**Figure 3.6 A**). After 24h of seeding, the adhesion of cells was corroborated by immunofluorescence staining using Vimentin (Green) and DAPI (Blue) (see **Figure 3.6 B)**. Vimentin is an intermediate filament that acts as a signalling mediator between cells by regulating cellular processes of relevance in wound-healing, like adhesion, migration, differentiation and morphological arrangements [45, 46]. **Figure 3.6 B** shows that fibroblasts adhered and spread well in all samples. Corrected total fluorescence (CTFC) was calculated using ImageJ software (**Figure 3.6 A, right panel**). CP50W and PP50W were not cytotoxic and biocompatible with human dermal fibroblasts, which suggests their potential for use in devices that are in contact with dermal tissue.

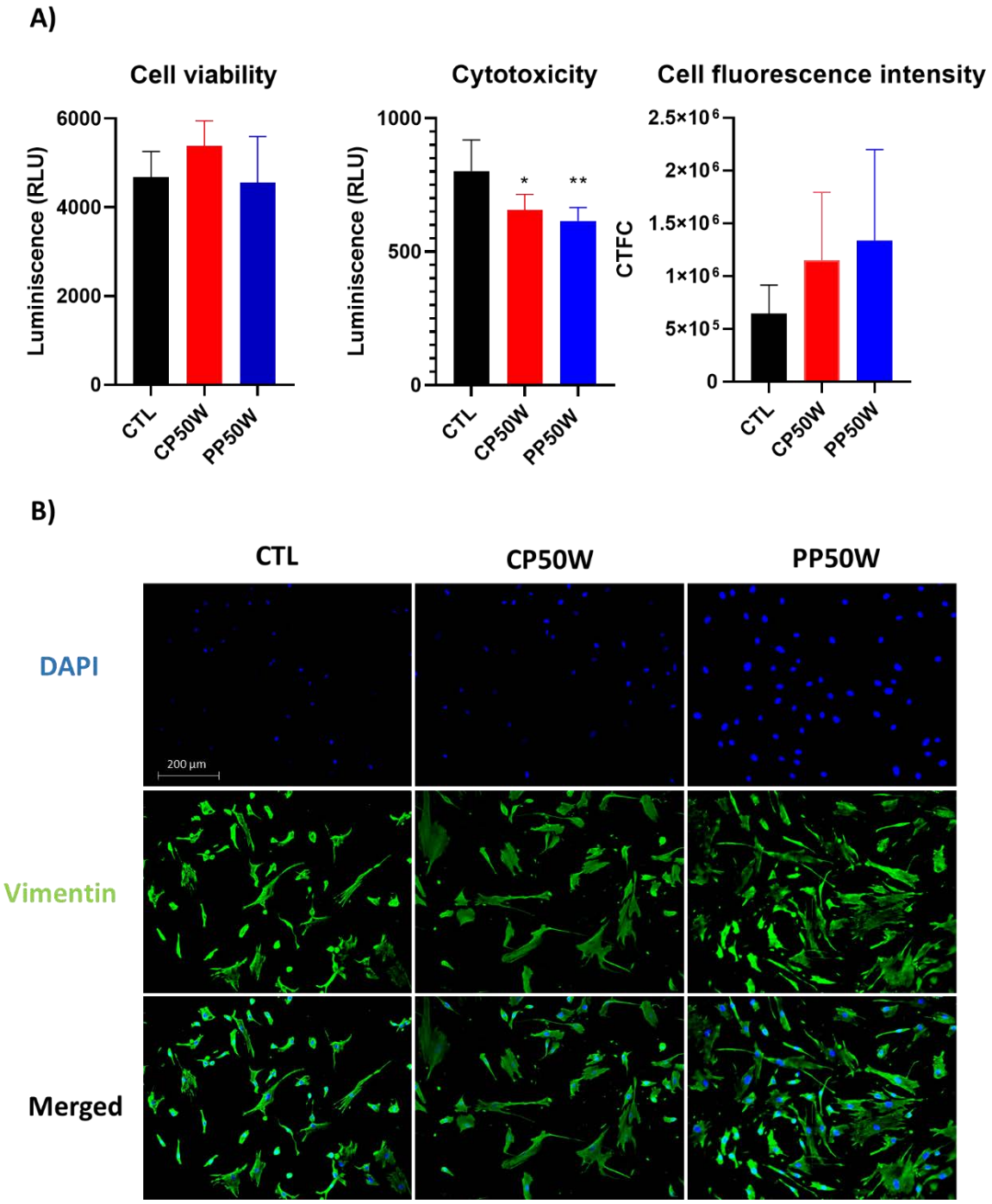

Figure 3. 6. A) Shows the plots for viability, cytotoxicity and fluorescence intensity of HDF after being seeded in PP-OSMs for 24h. B) shows the fluorescence images using DAPI as a nucleus staining (blue) and Vimentin as a cytoskeleton filament staining (green).

One of the main features of the presented polymers were their antibacterial and antifouling properties, which are similar to the antibacterial behaviour exhibited by PP from T4 and geranium monomers fabricated at low plasma power levels. [19, 24, 26] In addition to the antibacterial and antifouling study of oregano, this is the first study where fibroblasts viability,

cytotoxicity and cell adhesion were evaluated for PP-OSMs. Considering these data, our results suggest that PP-OSMs have potential use as coatings for different medical devices, for example, as a coating for dermal wound dressings, catheters and implants. Nevertheless, *in vivo* assessments would be interesting to determine the optimal performance of PP-OSMs, especially, when they are in contact with living tissue in a wound environment.

3.4. Conclusion

Plasma polymer films from OSMs were successfully developed at different RF power levels using RF-PECVD. The functional groups of the oregano monomer were retained in the PP-OPTF resulting in a smooth and hydrophilic polymer. The surface roughness of CP50W resulted in a hydrophilic surface, whereas, PP50W had a contact angle of 5° and is therefore considered super hydrophilic. The results suggest that coating leachate of the PP-OSMs modifies the pH of the media used. PP-OSMs was shown to have bactericidal properties against Gram-negative *P. aeruginosa* and antifouling properties against Gram-positive *S. aureus.* Moreover, PP-OSMs supported fibroblasts' growth and proliferation without producing significant cytotoxicity. Adhesion and spread of fibroblasts on PP-OSMs were also confirmed. The overall results suggest the potential application of these polymers into medical applications, such as wound dressings where antibacterial and biocompatibility are required.

3.5. Acknowledgments

James Cook University Postgraduate Research Scholarship, Strategic Research Investment Fund grant and a Cooperative Research Centre for Developing Northern Australia top-up scholarship funded this project. Jonathan Golledge holds a Practitioner Fellowship from the National Health and Medical Research Council (1117061) and a Senior Clinical Research Fellowship from the Queensland Government. KV thanks NHMRC for Fellowship GNT1194466.

3.6. Conflict of interest

The authors declare no financial or commercial conflict of interest.

3.7. Data availability statement

The data that support the findings of this study are available from the corresponding author upon reasonable request.

3.8. Supporting information

Plasma polymers from oregano secondary metabolites: An antibacterial and biocompatible plant-based polymers.

*Jesus Romo-Rico[1, 2], Smriti Murali Krishna[2, 4], Jonathan Golledge[2, 3], Andrew Hayles[6], Krasimir Vasilev[5, 6], Mohan V. Jacob[1]**

[1]Electronics Materials Lab, College of Science and Engineering, James Cook University, Townsville, QLD 4811, Australia.

[2]College of Medicine and Dentistry, James Cook University, Townsville, QLD 4811, Australia.

[3]Queensland Research Centre for Peripheral Vascular Disease, James Cook University and Department of Vascular and Endovascular Surgery, Townsville University Hospital, Townsville, QLD 4811, Australia.

[4]Atherothrombosis and Vascular Biology, Baker Heart and Diabetes Institute, Melbourne 3004, Australia.

[5]College of Medicine and Public Health, Flinders University, Sturt Road, Bedford Park, South Australia 5042, Australia.

[6]UNISA STEM, Mawson Lakes, South Australia 5095, Australia.

*Correspondence: Mohan Jacob, Electronics Materials Lab, College of Science and Engineering, James Cook University, Townsville, QLD 4811, Australia Email: mohan.jacob@jcu.edu.au

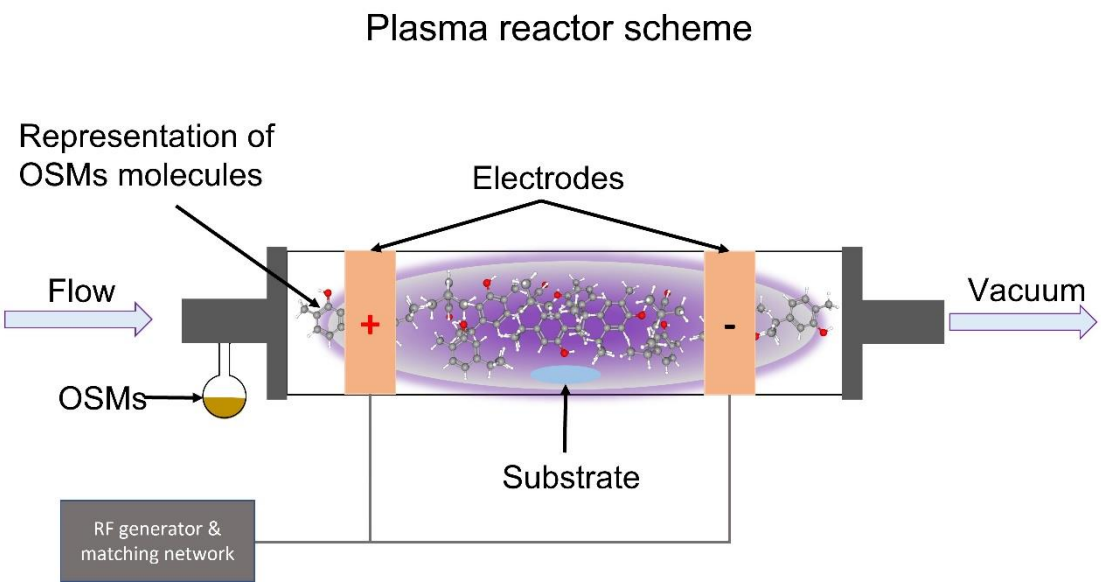

Figure S. 1. Scheme of the plasma reactor.

Figure S. 2. AFM scans of 3x3 µm of PP-OSMs samples after submerged in MiliQ water.

Keywords: antibacterial, biocompatible, oregano, plant secondary metabolites, plasma-polymers.

3.9. References

[1] Z. Yao, J. Niu, B. Cheng *Advances in skin & wound care*. **2020**, *33*, 1-10.

[2] S. R. Nussbaum, M. J. Carter, C. E. Fife, J. DaVanzo, R. Haught, M. Nusgart, D. Cartwright *Value in health*. **2018**, *21*, 27-32.

[3] C. J. Phillips, I. Humphreys, J. Fletcher, K. Harding, G. Chamberlain, S. Macey *International wound journal*. **2016**, *13*, 1193-1197.

[4] H. Edwards, K. Finlayson, M. Courtney, N. Graves, M. Gibb, C. Parker *BMC health services research*. **2013**, *13*, 86-86.

[5] L. McCosker, R. Tulleners, Q. Cheng, S. Rohmer, T. Pacella, N. Graves, R. Pacella *International wound journal*. **2019**, *16*, 84-95.

[6] P. L. Jaap Van Netten, Robert Fitridge, Ewan Kinnear, Ian Griffiths, Matthew Malone, Byron Perrin, Jennifer Prentice, Sharif Sethi and Paul Wraight *Diabetic Feet Australia*. **2017**.

[7] S. Verbanic, Y. Shen, J. Lee, J. M. Deacon, I. A. Chen *NPJ biofilms and microbiomes*. **2020**, *6*, 21-21.

[8] N. Misra, S. Bhatt, F. Arefi-Khonsari, V. Kumar *Plasma Process Polym*. **2021**, *18*, e2000215.

[9] Y. Ferreira da Silva, V. d. M. Queiroz, I. C. S. Kling, B. S. Archanjo, R. N. Oliveira, R. A. Simao *Plasma Processes and Polymers*. **2020**, *17*.

[10] M. Y. Huang, M. H. Liao, Y. K. Wang, Y. S. Huang, H. C. Wen *Am J Chin Med*. **2012**, *40*, 845-859.

[11] C. Cheng, Y. Zou, J. Peng *Molecules*. **2018**, *23*.

[12] Z. W. Cui, Z. X. Xie, B. F. Wang, Z. H. Zhong, X. Y. Chen, Y. H. Sun, Q. F. Sun, G. Y. Yang, L. G. Bian *Acta Pharmacol Sin*. **2015**, *36*, 1426-1436.

[13] M. N. Gallucci, M. E. Carezzano, M. M. Oliva, M. S. Demo, R. P. Pizzolitto, M. P. Zunino, J. A. Zygadlo, J. S. Dambolena *Journal of Applied Microbiology*. **2014**, *116*, 795-804.

[14] A. Puskarova, M. Buckova, L. Krakova, D. Pangallo, K. Kozics *Scientific Reports*. **2017**, *7*.

[15] H. Y. Cui, C. H. Zhang, C. Z. Li, L. Lin *Industrial Crops and Products*. **2019**, *139*.

[16] D. Trombetta, F. Castelli, M. G. Sarpietro, V. Venuti, M. Cristani, C. Daniele, A. Saija, G. Mazzanti, G. Bisignano *Antimicrobial Agents and Chemotherapy*. **2005**, *49*, 2474-2478.

[17] R. J. W. Lambert, P. N. Skandamis, P. J. Coote, G. J. E. Nychas *Journal of applied microbiology*. **2001**, *91*, 453-462.

[18] A. Ultee, M. H. J. Bennik, R. Moezelaar *Applied and Environmental Microbiology*. **2002**, *68*, 1561-1568.

[19] O. Bazaka, K. Bazaka, V. K. Truong, I. Levchenko, M. V. Jacob, Y. Estrin, R. Lapovok, B. Chichkov, E. Fadeeva, P. Kingshott, R. J. Crawford, E. P. Ivanova *Appl Surf Sci*. **2020**, *521*, 146375.

[20] K. Bazaka, M. V. Jacob, R. J. Crawford, E. P. Ivanova *Acta biomaterialia*. **2011**, *7*, 2015-2028.

[21] K. Bazaka, M. V. Jacob *Materials letters*. **2009**, *63*, 1594-1597.

[22] K. Bazaka, M. Jacob, V. K. Truong, R. J. Crawford, E. P. Ivanova *Polymers*. **2011**, *3*, 388-404.

[23] A. Kumar, A. Al-Jumaili, K. Prasad, K. Bazaka, P. Mulvey, J. Warner, M. V. Jacob *Plasma Chemistry and Plasma Processing*. **2019**, *40*, 339-355.

[24] A. Kumar, A. Al-Jumaili, K. Bazaka, P. Mulvey, J. Warner, M. V. Jacob *Materials*. **2020**, *13*, 586.

[25] A. Pegalajar-Jurado, C. D. Easton, K. E. Styan, S. L. McArthur *Journal of Materials Chemistry B*. **2014**, *2*, 4993-5002.

[26] A. Al-Jumaili, K. Bazaka, M. V. Jacob *Nanomaterials (Basel)*. **2017**, *7*, 270.

[27] R. Polat, F. Satil *J Ethnopharmacol*. **2012**, *139*, 626-641.

[28] J. Coccimiglio, M. Alipour, Z. H. Jiang, C. Gottardo, Z. Suntres *Oxid Med Cell Longev*. **2016**, *2016*, 1404505.

[29] K. Malik, M. Ahmad, M. Zafar, R. Ullah, H. M. Mahmood, B. Parveen, N. Rashid, S. Sultana, S. N. Shah, Lubna *BMC Complement Altern Med*. **2019**, *19*, 210.

[30] K. Singletary *Nutrition today (Annapolis)*. **2010**, *45*, 129-138.

[31] H. Yin, X. C. Frettḗ, L. P. Christensen, K. Grevsen *Journal of agricultural and food chemistry*. **2012**, *60*, 136-143.

[32] M. Bertuola, N. Fagali, M. Fernández Lorenzo de Mele *Heliyon*. **2020**, *6*, e03714.

[33] S. Mediouni, J. A. Jablonski, S. Tsuda, A. Barsamian, C. Kessing, A. Richard, A. Biswas, F. Toledo, V. M. Andrade, Y. Even, M. Stevenson, T. Tellinghuisen, H. Choe, M. Cameron, T. D. Bannister, S. T. Valente *J Virol*. **2020**, *94*.

[34] P.-Q. Gloria María, P.-Q. Gloria María, P.-Q. Gloria María, E.-R. Susana, C. Juan Pérez, A. María Rosa, A. María Rosa, V.-L. Blanca, V.-L. Blanca *Frontiers in bioengineering and biotechnology*. **2021**, *9*, 703684-703684.

[35] C. Watters, K. DeLeon, U. Trivedi, J. A. Griswold, M. Lyte, K. J. Hampel, M. J. Wargo, K. P. Rumbaugh *Medical microbiology and immunology*. **2012**, *202*, 131-141.

[36] X. Xie, R. Zhong, L. Luo, X. Lin, L. Huang, S. Huang, L. Ni, B. Chen, R. Shen, L. Yan, C. Duan *Immunity, Inflammation and Disease*. **2021**, *9*, 1428-1438.

[37] E. E. Johnston, B. D. Ratner *Journal of Electron Spectroscopy and Related Phenomena*. **1996**, *81*, 303-317.

[38] G. Schultz, D. Mozingo, M. Romanelli, K. Claxton *Wound repair and regeneration*. **2005**, *13*, S1-S11.

[39] L. Watret, A. Rodgers *The diabetic foot*. **2005**, *8*, 154.

[40] M. M. Gutiérrez-Pacheco, L. A. Ortega-Ramírez, B. A. Silva-Espinoza, M. R. Cruz-Valenzuela, G. A. González-Aguilar, J. Lizardi-Mendoza, R. Miranda, J. F. Ayala-Zavala *Coatings (Basel)*. **2020**, *10*, 614.

[41] S. Beirão da Costa, C. Duarte, A. I. Bourbon, A. C. Pinheiro, A. T. Serra, M. Moldão Martins, M. I. Nunes Januário, A. A. Vicente, I. Delgadillo, C. Duarte, M. L. Beirão da Costa *Journal of food engineering*. **2012**, *110*, 190-199.

[42] X. Hui, G. Yan, F.-L. Tian, H. Li, W.-Y. Gao *Medicinal chemistry research*. **2017**, *26*, 442-449.

[43] S. Kumari, R. V. Kumaraswamy, R. C. Choudhary, S. S. Sharma, A. Pal, R. Raliya, P. Biswas, V. Saharan *Sci Rep*. **2018**, *8*, 6650.

[44] K.-Y. Law *The journal of physical chemistry letters*. **2014**, *5*, 686-688.

[45] C. De Pascalis, C. Pérez-González, S. Seetharaman, B. Boëda, B. Vianay, M. Burute, C. Leduc, N. Borghi, X. Trepat, S. Etienne-Manneville *The Journal of cell biology*. **2018**, *217*, 3031-3044.

[46] F. Cheng, Y. Shen, P. Mohanasundaram, M. Lindström, J. Ivaska, T. Ny, J. E. Eriksson *Proceedings of the National Academy of Sciences - PNAS*. **2016**, *113*, E4320-E4327.

Chapter 4

In Vitro Study of the Wound-healing Properties of an Oregano Based Plasma Polymer

In this chapter the *in vitro* wound-healing properties of oregano-based plasma polymer (OPP) were investigated. OPP did not activate pro-inflammatory responses of RAW macrophages and showed potential anti-inflammatory activity reducing pro-inflammatory cytokines. OPP prevented ROS activation on inflamed macrophages. OPP promoted wound closure faster than the control samples. Overall, these findings suggest that OPP has potential as a wound-healing interface for dressings and bandages, providing mammalian cell support, anti-inflammatory activity, antioxidant properties and enhanced cell proliferation.

This chapter has been submitted for publication as: *Jesus Romo-Rico, Richard Bright, Neethu Ninan, Smriti Murali Krishna, Krasimir Vasilev, Jonathan Golledge, and Mohan Jacob*. *In Vitro* Study of the Wound-healing Properties of an Oregano Based Plasma Polymer, ACS Biomaterials Science & Engineering, 2023.

***In Vitro* Study of the Wound-healing Properties of an Oregano Based Plasma Polymer**

Graphical Abstract

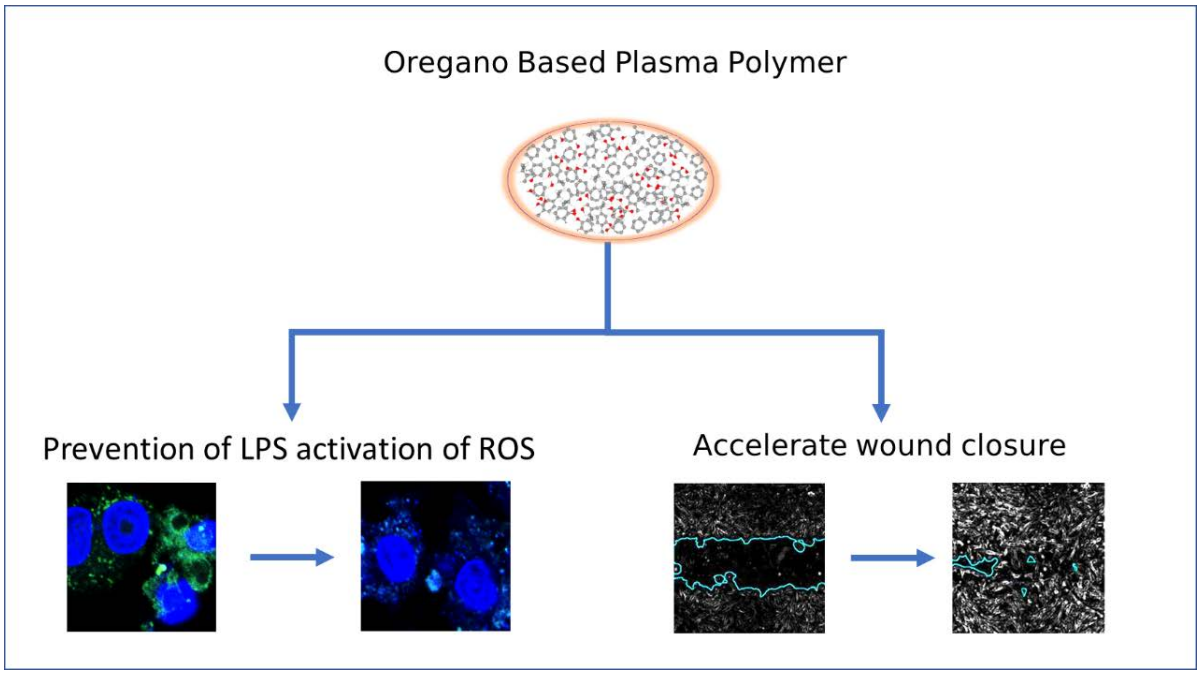

Abstract

Chronic wounds are characterized as wounds that fail to progress through the normal stages of wound-healing. Wound-healing can be delayed by factors such as infection, age, stress, diabetes, obesity, medications, smoking, and nutrition. In this study, the anti-inflammatory, antioxidant and wound-healing properties of oregano-based plasma polymers (OPP) are investigated. An *in vitro* wound closure study performed with human foreskin fibroblasts and OPP, was found that OPP accelerated *in vitro* wound closure ($p<0.05$) when compared to sample control. Furthermore, OPP did not induce any adverse inflammatory response when incubated on RAW macrophages. OPP prevented LPS-activation of ROS on RAW macrophages when compared to LPS-treated control surfaces ($p < 0.0001$). Overall, the results suggest the potential application of OPP as a wound healer interface in wound dressings and medical device coatings.

4. 1. Introduction

The increase in systemic diseases, an ageing population and trauma have resulted in an exponential increase in chronic wounds.[1] Wound dressings have been continuously developed to alleviate chronic wounds. However, chronic wound management is a major ongoing issue. When a wound dressing is in contact with tissue, the host immune system identifies it as a foreign material and triggers an acute inflammatory immune response.[2] If inflammation persists, it can develop into a chronic wound that could lead to long-term pain, decreased mobility and reduced physical well-being, and increased risk of infection[3],[4], accompanied by a representative healthcare cost.[5],[6]

There is an increasing demand for wound dressing materials that can be used as chronic wound healers.[7],[8, 9] The ideal wound-healing materials would not activate the host immune response, prevent oxidation, inflammation, bacterial infection, and support the promotion of cell proliferation and tissue remodelling.[10],[11, 12] [13]

Oregano is an aromatic plant with ancient history as a wound healer, and it has been shown to possess antibacterial, antioxidant, anti-inflammatory and a variety of wound-healing properties in several scientific studies.[14], [15-19], [20], [21] Ointments,[22] hydrogels, nanofibers, nanoparticles, and films are examples of engineered materials that include oregano extracts as wound-healing agents.[23] For example, collagen hydrolysate-based nanofibers loaded with oregano essential oil (OEO) demonstrated *in vitro* biocompatibility with fibroblast and exhibited antioxidant and antibacterial properties along with the capacity to eradicate a variety of biofilms.[24] OEO encapsulated within chitosan-alginate nanoparticles (NP) did not show any sign of skin irritation or edema in rabbits.[25] OEO was encapsulated into poly (L-lactide-co-caprolactone) (PLCL) and silk fibroin (SF) nanofibers membranes (NF). NF-OEO accelerated *in vivo* wound-healing by inducing angiogenesis granulation tissue formation, neo-epithelialization, and collagen deposition. These NF-OEO also presented antibacterial activity against Gram-positive *S. aureus* and Gram-negative *E. coli*.[26]

An oregano-based plasma polymer (OPP), which was fabricated using radiofrequency plasma-enhanced chemical vapour deposition (RF-PECVD), has shown biocompatibility with human dermal fibroblasts (HDF). OPP supported HDF growth, adhesion and spreading. OPP also had selective antibacterial and anti-biofouling properties against *P. aeruginosa* and *S. aureus*.[27] One of the advantages of OPP is that the properties of oregano oil are preserved as a polymer that can be applied to a variety of surfaces. However, the wound-healing properties of these polymers have never been investigated. Therefore, we performed an *in vitro* evaluation of the

biocompatibility and immune responses to OPP using RAW 264.7 macrophage-like cells. We also investigated the antioxidant activity of OPP when macrophages were activated with lipopolysaccharide (LPS) to induce an acute inflammatory response. The *in vitro* wound closure evaluation was performed using human foreskin fibroblasts (HFF-1).

4. 2. Materials and methods

4. 2. 1. Deposition of oregano-based plasma polymers

OPP was deposited on round glass coverslips (Proscitech, diameter 15 mm). Before coating deposition, all substrates were sonicated for 5 min in isopropyl alcohol, then rinsed and sonicated again in distilled water for 5 minutes and subsequently air-dried. The substrates were coated using an RF-PECVD plasma reactor described elsewhere.[28] The deposition conditions of OPP were performed using pulsed plasma of a duty cycle of 50% and 500 Hz mode at 50 W for 10 min.

4. 2. 2. Chemical analyses using X-ray photoelectron spectroscopy

The chemical composition of the OPP was analyzed using X-ray photoelectron spectroscopy (XPS). The respective survey spectra were collected using a Kratos AXIS Ultra DLD spectrometer (Kratos Analytical Ltd., Manchester, UK) coupled with a magnetic charge compensation system, with monochromatic AlKα radiation (hν = 1486.7 eV). Data analysis was carried out with CasaXPS software (Casa Software Ltd., Teignmouth, UK). The C1s peak was recalibrated by setting the carbon binding energies (BE) at 285 eV and the deconvoluted peaks were fitted using the same software.

4. 2. 3. Contact angle analysis

The wettability of the OPP was evaluated using contact angle by a sessile drop method using a KSV CAM 101 optical apparatus (KSV Instruments Ltd., Helsinki, Finland). The contact angle of a drop of MiliQ water (8 µl) was measured using a baseline as a reference of the drop and the tangent of the drop boundary, considering the droplet volume, height and basal diameter.

4. 2. 4. Cell culture, viability, and immunofluorescence

RAW 264.7 macrophage-like cells (Abelson leukaemia virus-transformed cell line derived from BALB/c mice, ATCC TIB-71) were cultured in Dulbecco's modified Eagle's medium (DMEM; ThermoFisher, CA, USA) supplemented with 10% Fetal Bovine Serum (FBS, Life Technologies, CA, USA) plus 1% Pen/Strep (100 U/mL Penicillin and 100 µg/mL Streptomycin, Life Technologies, CA, USA) and incubated at 37°C in 5% CO_2.

4. 2. 4. 1. Cell viability and MTT assay

To perform cell viability assay, OPP-coated coverslips and uncoated coverslips (16 mm diameter) were placed in a 24-well plate and UV sterilized for 20 min. RAW 264.7 were seeded at a density of 2×10^5 cells per well and incubated for 48 h. After incubation, the cell viability of three samples for each plasma polymer and control coverslips were analyzed using an MTT assay 3-(4,5-Dimethylthiazol-2-yl)-2,5-diphenyltetrazolium bromide, Sigma-Aldrich, MO, USA). The MTT assay is a colorimetric test used to measure cellular metabolic activity as an indicator of cell viability and proliferation. MTT was prepared at 0.5 mg/ml concentration in PBS. For 100 µl medium per well, 10µl of 5 mg/mL MTT is added into each well. Following by a 4 h incubation at 37°C in 5% CO_2. Subsequently, the solution was removed and replaced with 200 µl of dimethyl sulfoxide (DMSO) and incubated at room temperature in the dark for 15 min before measuring the absorbance at 570 nm.

4. 2. 4. 2. Cell adhesion and spreading

Cells seeded on OPP-coated and control coverslips were initially incubated for 48 h at 37 °C and 5% CO_2, then processed for immunofluorescence staining. Cells were then rinsed with phosphate buffering saline (PBS, ThermoFisher, MA, USA) and fixed with 4% paraformaldehyde (Sigma-Aldrich, MI, USA) for 20 min at room temperature. Next, cells were washed twice with PBS and permeabilized with 0.1% Triton X-100 (Sigma-Aldrich, MI, USA) in 1x PBS for 5 minutes, then a blocking solution (1% BSA, obtained from Sigma-Aldrich, MI, USA in 1x PBS) was added for 30 minutes. Cells were then washed twice and 1:1000 dilution of TRITC-conjugated Phalloidin (Ex/Em 540/565, FAK100 kit, Sigma-Aldrich, MO, USA) in PBS was added to the samples and incubated in the dark for 60 min at room temperature. Afterwards, nuclei counterstaining was performed by incubating the cells with 4',6-diamidino-

2-phenylindole (DAPI, Sigma-Aldrich, MI, USA; Ex/Em 359/461, FAK100 kit, Sigma-Aldrich, MO, USA) were incubated in the dark for 5 minutes at room temperature followed by washing cells three times with PBS for 10 min. The coverslips were inverted onto microscope slides for imaging. Fluorescent images were acquired using an Olympus FV3000 confocal microscope (CLSM; Olympus, Tokyo, Japan).

4.2.5. Immune response evaluation

Macrophages play important roles in wound-healing since they are one of the first mediators of inflammation; cytokines and growth factors secretion and phagocytosis.[29] Raw 264.7 macrophage-like cells were used as a cell model to investigate the immune responses to OPP surfaces. To determine the level of protein expression of IL-6 and IL-4 pro-inflammatory markers, macrophages were seeded and incubated OPP and control coverslips for 48h at 37 °C and 5% CO_2. The supernatant from samples was collected at 48 h and prepared for ELISA assay of IL-6 and IL-4 pro-inflammatory cytokines. ELISA assay was performed according to the manufacturer's protocol (ThermoFisher, MA, USA).

4. 2. 6. Antioxidant evaluation of Oregano-based plasma polymers

RAW 264.7 macrophage-like cells were grown in DMEM supplemented with 10% fetal calf serum and seeded at $2x10^5$ cells/well in a 24-well plate and incubated overnight at 37°C in 5% CO_2. One group was treated with fresh media containing 100 ng/mL of bacterial lipopolysaccharide (LPS, Sigma-Aldrich, MO, USA) to activate cell immune response and incubated overnight at 37°C in 5% CO_2.
After incubation, DMEM media was replaced and incubated in 10 µl of 2', 7'-Dichlorofluorescein (DCF, Sigma-Aldrich, MO, USA) in PBS for 30 min at 37°C in 5% CO_2. Next, samples were washed with PBS, nuclei were stained with DAPI, and then intracellular ROS was detected using an Olympus FV3000 confocal microscope (CLSM; Olympus, Tokyo, Japan). ROS-activated DCF was imaged using an excitation wavelength of 490 nm and an emission wavelength of 520 nm. Cellular fluorescence intensity was quantified using Image J software (NIH, Maryland, USA).

4. 2. 7. *In vitro* scratch assay

The wound scratch assay was performed in a 96-well plate using an Incucyte SX5 Live-Cell Analysis Instrument (Sartorius, Göttingen, Germany) which was contained in a cell incubator (37°C, 5% CO_2). Round coverslips coated with OPP were placed into the bottom of the 96 well plates (coating surface facing upwards) then HFF-1 (ATCC, VA, USA) maintained in DMEM supplemented with 10% FBS and 1% Pen/Strep, were seeded at a density of $1x10^5$ cells/mL for 24 h. After the cell density reached 80% of confluence (24 h), uniform wound scratches were created using an Incucyte® Wound Maker 96-Tool, subsequently, wells were washed with PBS solution to remove any debris and/or free-floating cells and fresh media was added. The 96 well plate was placed into the Incucyte® instrument and images of the wound closure were taken every 6 h for 30 h.

4. 2. 8. Statistical analyses

All analysis and graphical representation were done using GraphPad Prism version 9.0.0 (121) (GraphPad Software, San Diego, CA, USA). For IL-4 and IL-6 cytokine analysis, ordinary one-way ANOVA statistical analyses followed by Bonferroni posthoc analysis were performed. To determine the mean ± SD and *p* values for ROS intensity staining, wound-healing analysis and antibacterial experiments, 2-way ANOVA followed by Bonferonni posthoc analysis was done. All experiments were performed in triplicate, and a *p*-value of less than 0.05 was deemed to be statically significant.

4. 3. Results and discussion

4. 3. 1. Chemical characterization and contact angle of OPP

Figure 4.1 shows the high-resolution C1s spectra of OPP deposited using pulse plasma (DC 50W, 500 Hz, 10 min). The XPS survey spectrum presented in Figure 4.1 A shows a strong O1s peak at 532.63 eV. This could be indicative for the retention of the OH group in the carvacrol molecule, which is the most abundant component in oregano. It also indicates the preservation of the functional groups by pulsed-wave plasma deposition. The C1s peak, shown in Figure 4.1 A can be fitted using three components. The component located at 285 eV is related to aliphatic and aromatic carbons which the one at 286.1 eV is associated with phenolic carbon atoms.[30] These groups are fragments of the monomers or recombinant compounds formed during the plasma deposition process. The component at 289 eV is assigned to COOH

peaks. [27, 31]. The Si 2s peaks at 103 eV and 150 are the substrata silica peaks of the substrate, which is detectable due to scratches occurring in the handling process.

The water contact angle (WCA) of the control group mean was 37° ± 2° and oregano-based plasma polymers were 12° ± 2°, represented in Figure 4.1 C. This indicates the hydrophilic properties of the oregano-based plasma polymer surface in accordance with the high content of OH, corroborated by chemical characterization.

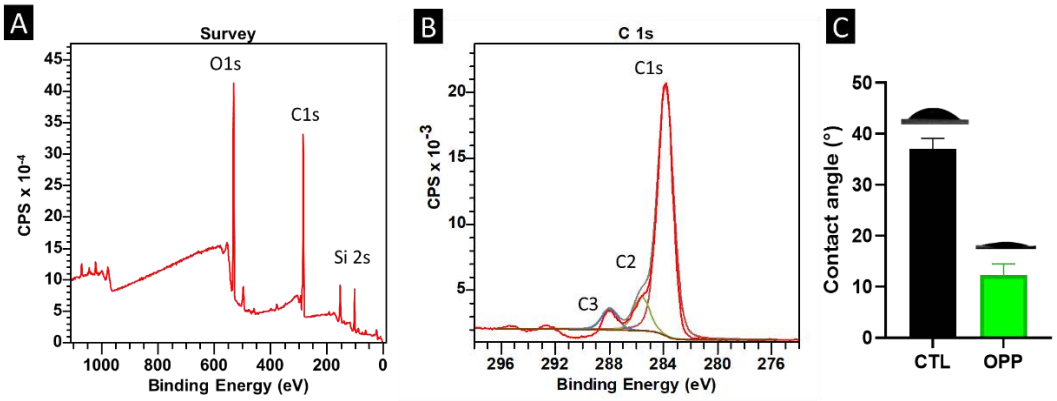

Figure 4. 1. Representative XPS survey (A) and high-resolution C1s (B) of the OPP, (C) Water contact angle of OPP. Mean ± SD, n = 3.

4. 3. 2. Cytocompatibility, adhesion and spreading of the OPP

Cell viability was evaluated at 48 h, measuring cellular metabolic activity as a marker of cell viability using an MTT assay. The cell viability of all samples was approximately 100%, without significant difference. The plot in Figure 4.2 C, shows the uncoated control coverslips and OPP. Cell adhesion and spreading of 264.7 RAW macrophages are represented by fluorescence images shown in Figure 4.1 B-D. The F actin elements are stained red (using TRITC-conjugated Phalloidin) and nuclei are stained blue (using DAPI). F-actin filaments play a crucial role in wound closure by promoting cell migration, adhesion, and proliferation.[32] Cells appear with healthy morphology on OPP and control, both show well-defined f-actin filament, a characteristic of focal adhesion. The hydrophilicity of the OPP facilitates anchorage-dependence of mammalian cells for attachment and proliferation.[33] The OPP surfaces have shown good biocompatibility, proliferation, adhesion and spreading of 264.7 RAW macrophages after 48 h of seeding.

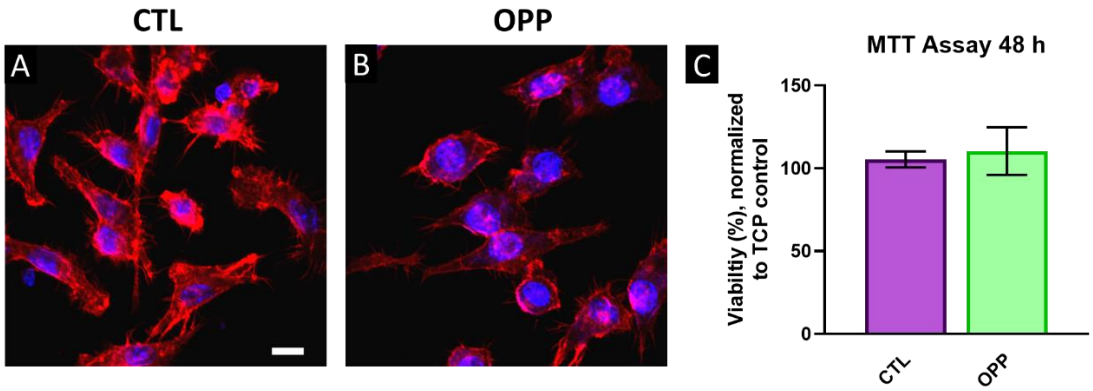

Figure 4. 2. Fluorescent confocal microscopy images of RAW macrophages treated with (A) Control and (B) OPP after 48h using Phalloidin, an actin filament dye (red) and DAPI, nuclei staining dye (blue) Scale bar represents 10 µm. (C) Cell viability of Control and OPP after 48 h. Mean ± SD, n = 3.

4. 3. 3. IL-4 and IL-6 cytokines expression by OPP

The innate immune response of RAW macrophages to OPP was evaluated by measuring the cytokine expression. The increase of IL-6 and IL-4 production is often related to macrophage activation and inflammation.[34] It has been reported that oregano has the potential to decrease IL-6 production in LPS-activated RAW cells.[21] The reduction of IL-4 was observed in asthmatic animals by *Zataria multiflora* (ZM) a compound with a high percentage of carvacrol. ZM also reduced pro-inflammatory cytokines IL-4, IL-17 and TGF-β, and increased anti-inflammatory cytokines FOXP3 and IFN-γ. [35, 36]

As shown in Figure 4.3 A, the results from ELISA analysis showed no significant difference in the expression of IL-6 on the OPP surface when compared to the control. The expression of IL-4 was significantly reduced by OPP ($p < 0.05$) (Figure 4.3 B). OPP did not induce the activation of IL-6 and IL-4 pro-inflammatory markers. This is a favorable finding in regards to wound-healing applications of OPP since the direct use of oregano extracts has previously caused irritation.[37]

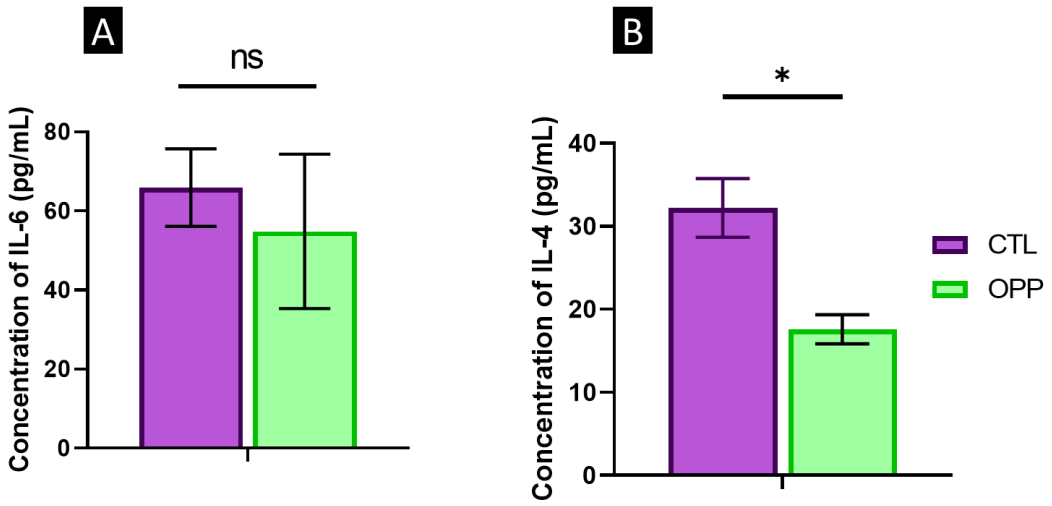

Figure 4. 3. Cytokine expression of IL-6 (A) and IL-4 (B) on Raw 264.7 Macrophages. Mean ± SD, n = 3 $p<0.05$.

4. 3. 4. Oregano-based plasma surfaces inhibit LPS-activation of ROS in RAW 264.7 macrophages

ROS-activated and non-treated RAW macrophages were incubated with OPP and control surfaces. The DCF dye was used as a fluorescent indicator to measure ROS presence in cells. [38] As seen in Figures 4.4 A-B, control and OPP samples did not show any intracellular DCF fluorescence due to ROS activation. This suggests that OPP do not induce oxidative stress or inflammation to 264.7 RAW macrophages.

Figures 4.4 C-D show an increase in intracellular ROS intensity in control samples treated with LPS, indicating inflammation and oxidative stress.[39] The ROS intensity in LPS-treated OPP surfaces remains low and similar to the non-LPS-activated control when compared to LPS-activated RAW cells ($p < 0.0001$). This result suggests that OPP may prevent the activation of macrophages through ROS inhibition when challenged with LPS. One potential mechanism could be the inactivation of the NF-κβ pathway that is ROS level dependent and regulates pro-inflammatory cytokines secretion and iNOS expression.[40],[41]

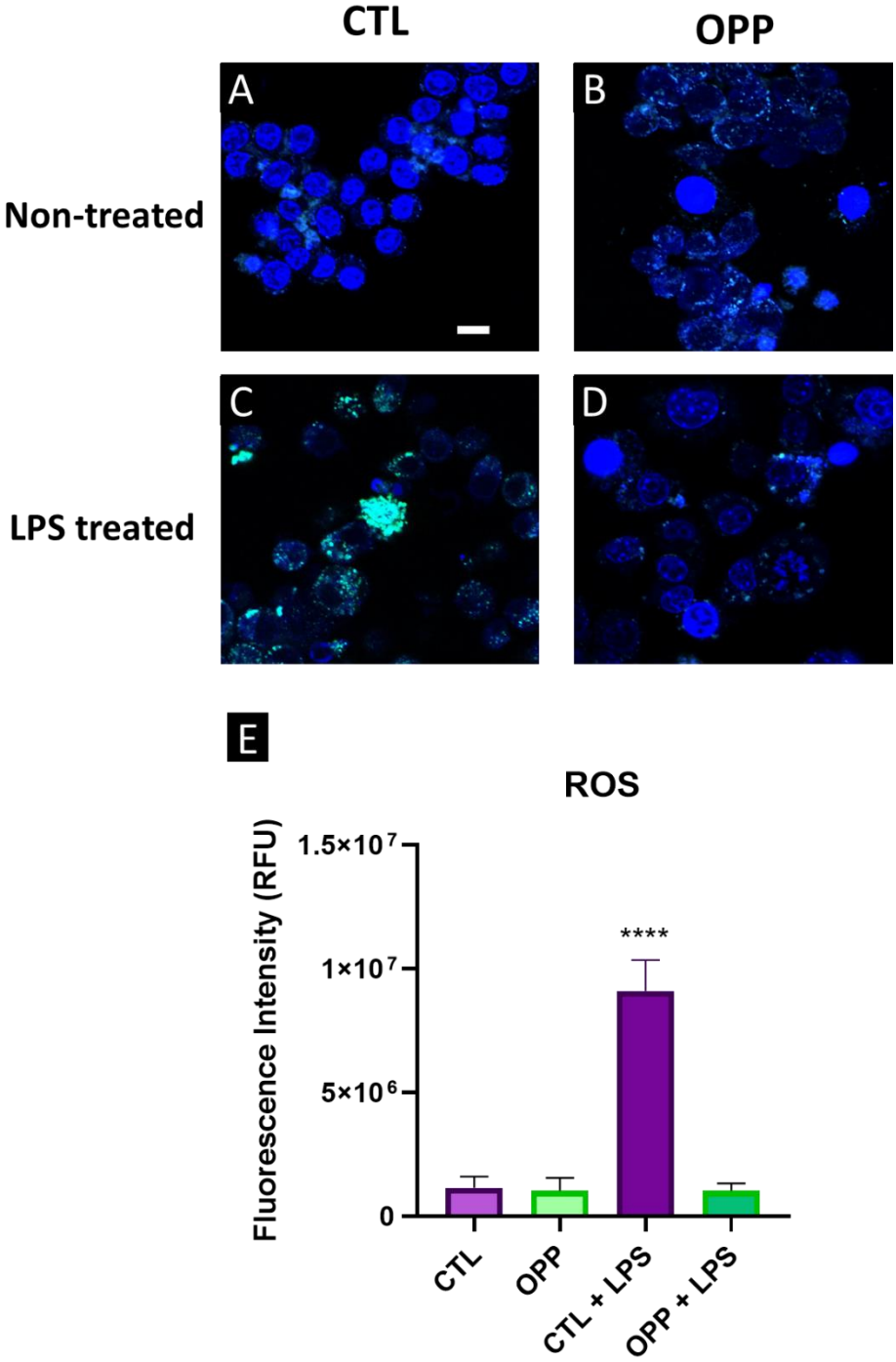

Figure 4. 4. Fluorescent confocal microscopy micrographs of RAW macrophages stained with DCF and DAPI for (A-B) Non-treated samples and (C-D) LPS-treated samples. (E) Normalised fluorescence intensities quantified using ImageJ represented as Relative Fluorescent Unit (RFU) Mean ± SD, n =3 and $p < 0.0001$.

We observed a statistically significant decrease in ROS for the LPS-activated Raw macrophage OPP samples, which indicates OPP is a ROS scavenger. Mean ± SD, $p<0.0001$, The scale bar in Figure 4.4 A represents 10 µm.

4. 3. 5. Wound-healing evaluation *in vitro*

To evaluate the influence of OPP on cell migration and proliferation, an *in vitro* scratch assay was performed. HFF-1 cells were chosen for this assay as they play a major role in wound-healing and skin regeneration. Figure 4.5 A shows three-time points after a wound was scratched on an HFF-1 monolayer seeded on control and OPP surfaces at 0, 18 and 30 h. The plot in Figure 4.5 B, shows the wound closure percentage over time of HFF-1 seeded on control and OPP surfaces. The wound closed 11.6 % faster in the case of OPP samples when compared to the control. After 18 h, OPP reaches 81.5% of closure, whereas control reaches 68.2% with a statistical difference of $p<0.05$. At 30h the wound closure for the OPP samples can be considered completed whereas the control reaches 90%. The maximum difference in wound closure occurred during the first 18h.

Fibroblast wound closure rate was estimated from scratch width measurements, shown in Figure 4.5 A. The speed of cell migration in control and OPP were 29 µm/h and 53 µm/h, respectively. A faster cell migration rate can be observed on OPP coated surfaces, which may indicate to improved wound-healing.

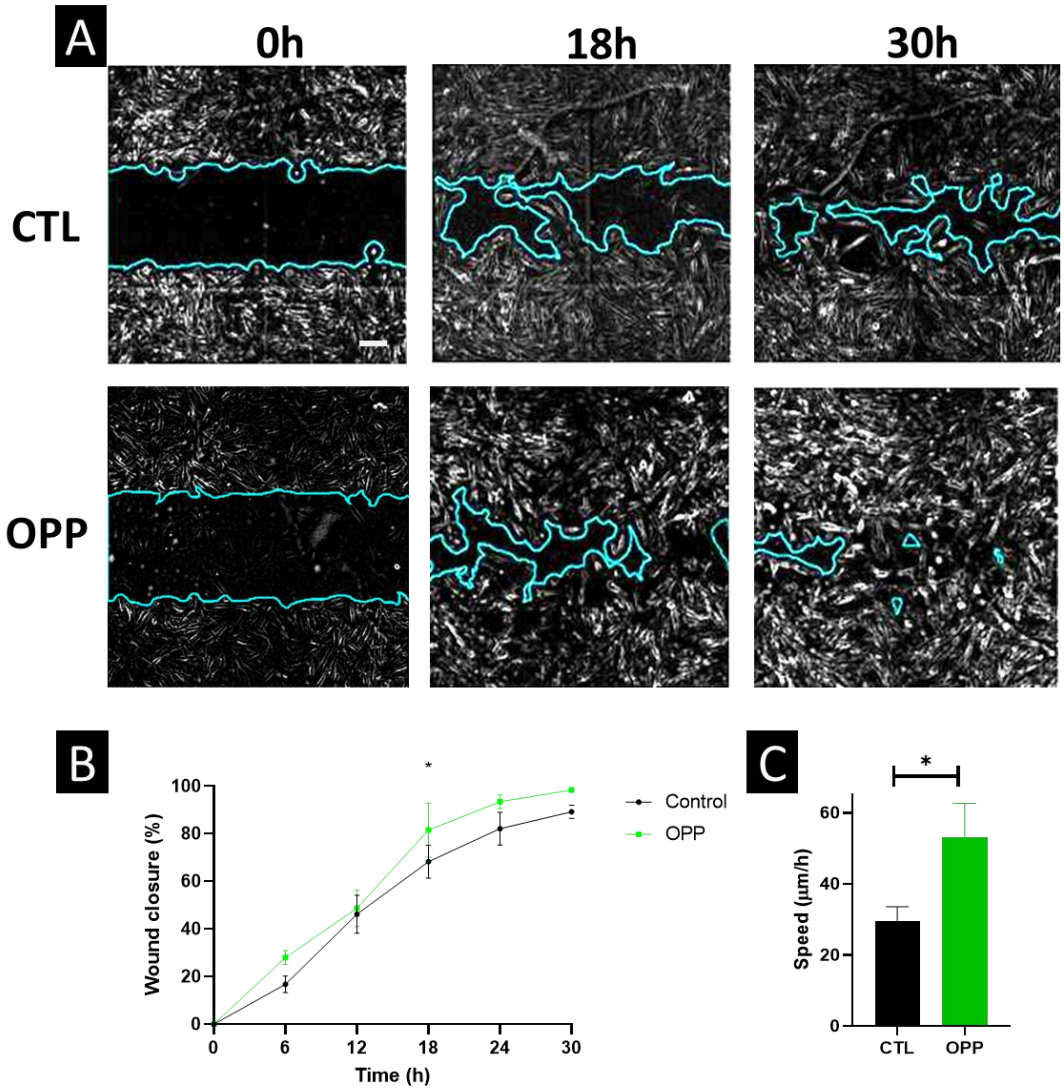

Figure 4. 5. (A) Representative images of wound scratch of CTL and OPP samples at 0h, 18h and 30h. (B) The wound closure plot in which we can observe the closure percentage of both samples every 6h. (C) Wound closure speed per hour. The scale bar in Figure 4.5 A represents 50 µm. Mean ±SD, and $p<0.05$.

4.4 Conclusion

The biocompatibility of oregano-based plasma polymer with RAW 264.7 macrophages, the first-line responders involved in the wound-healing process and defence against bacterial, viral and parasite infections is studied. Pro-inflammatory response of macrophages was not activated when in contact with OPP. This was determined by measuring the expression of IL-6 and IL-4. Importantly, the significant reduction in expression of IL-4 suggests a potential anti-inflammatory activity. Moreover, OPP did not cause any ROS activation in culture of LPS-induced macrophages and may have antioxidant and potential anti-inflammatory activity. The

wound closure rate was evaluated *in vitro* using human foreskin fibroblasts. The OPP wound closure was approximately 90% after 18h and fully closed at 30h, whereas the control samples reached 90% at 30h. Even though wound-healing is a complex process that involves a cascade of cytokines and different cell interactions, within the limitations of this study, an *in vitro* wound-healing perspective of features of OPP that are relevant to wound-healing is provided. The results suggest that oregano-based plasma polymers are strong candidates as wound-healing interfaces for dressings and bandages providing mammalian cell support, antioxidant activity, inflammation prevention, enhanced cell proliferation, together with previously demonstrated antibacterial and antifouling properties.

4. 5. Acknowledgements

Project funding (Krasimir Vasilev, Mohan Jacob, Jesus Romo-Rico, KV thanks HNMRC for for Fellowship GNT1194466 and ARC for grant DP180101254.
JG is supported by funding from Townsville Hospital and Health Services, Tropical Australian Academic Health Centre, Heart Foundation, Medical Research Future Fund and the Queensland Government. JG holds a Senior Clinical Research Fellowship from the Queensland Government, Australia.

4. 6. References

[1] R.E. Jones, D.S. Foster, M.T. Longaker, Management of Chronic Wounds—2018, JAMA : the journal of the American Medical Association 320(14) (2018) 1481-1482.
[2] G. Gurtner, P. Neligan, D.Z. Liu, Plastic surgery. Volume 1, Principles, Fourth edition ed., Elsevier, London ;, 2017.
[3] A. Hayles, R. Bright, J. Hasan, J. Wood, D. Palms, D. Barker, K. Vasilev, Dual Species Bacterial Challenge of a Biomimetic Nanostructured Surface, Advanced materials interfaces 9(32) (2022) n/a.
[4] R. Bright, A. Hayles, J. Wood, D. Palms, T. Brown, D. Barker, K. Vasilev, Surfaces Containing Sharp Nanostructures Enhance Antibiotic Efficacy, Nano letters 22(16) (2022) 6724-6731.
[5] F. Reinboldt-Jockenhöfer, Z. Babadagi, H.D. Hoppe, A. Risse, C. Rammos, A. Cyrek, C. Blome, S. Benson, J. Dissemond, Association of wound genesis on varying aspects of health-

related quality of life in patients with different types of chronic wounds: Results of a cross-sectional multicentre study, International wound journal 18(4) (2021) 432-439.
[6] V. Gribova, L. Petit, L. Kocgozlu, C. Seguin, S. Fournel, A. Kichler, N.E. Vrana, P. Lavalle, Polyarginine as a Simultaneous Antimicrobial, Immunomodulatory, and miRNA Delivery Agent within Polyanionic Hydrogel, Macromolecular bioscience 22(6) (2022) e2200043-n/a.
[7] A. Hayles, R. Bright, J. Wood, D. Palms, P. Zilm, T. Brown, D. Barker, K. Vasilev, Spiked Nanostructures Disrupt Fungal Biofilm and Impart Increased Sensitivity to Antifungal Treatment (Adv. Mater. Interfaces 12/2022), Advanced materials interfaces 9(12) (2022) 2270065-n/a.
[8] O. Bazaka, K. Bazaka, V.K. Truong, I. Levchenko, M.V. Jacob, Y. Estrin, R. Lapovok, B. Chichkov, E. Fadeeva, P. Kingshott, R.J. Crawford, E.P. Ivanova, Effect of titanium surface topography on plasma deposition of antibacterial polymer coatings, Applied surface science 521 (2020) 146375.
[9] Y. Bu, W. Zhang, S. Martin-Saldaña, A.M. Alsharabasy, M. Da Costa, L. Feng, Z. Zhang, X. Ge, C. Li, S. Lu, A. Pandit, Plant-Inspired Multifunctional Bioadhesives with Self-Healing Adhesion Strength to Promote Wound healing, Advanced materials interfaces 10(3) (2023) 2201599-n/a.
[10] B. Tao, C. Lin, X. Qin, Y. Yu, A. Guo, K. Li, H. Tian, W. Yi, D. Lei, Y. Chen, L. Chen, Fabrication of gelatin-based and Zn2+-incorporated composite hydrogel for accelerated infected wound healing, Materials Today Bio 13 (2022) 100216.
[11] K. Chae, W.Y. Jang, K. Park, J. Lee, H. Kim, K. Lee, C.K. Lee, Y. Lee, S.H. Lee, J. Seo, Antibacterial infection and immune-evasive coating for orthopedic implants, Science advances 6(44) (2020).
[12] S.V. Oopath, A. Baji, M. Abtahi, T.Q. Luu, K. Vasilev, V.K. Truong, Nature-Inspired Biomimetic Surfaces for Controlling Bacterial Attachment and Biofilm Development, Advanced Materials Interfaces 10(4) (2023) 2201425.
[13] M. Suneetha, K.M. Rao, S.S. Han, Cell/Tissue Adhesive, Self-Healable, Biocompatible, Hemostasis, and Antibacterial Hydrogel Dressings for Wound healing Applications, Advanced materials interfaces 9(13) (2022) 2102369-n/a.
[14] D.J. Charles, Oregano, in: D.J. Charles (Ed.), Antioxidant Properties of Spices, Herbs and Other Sources, Springer New York, New York, NY, 2013, pp. 449-458.
[15] X. Han, T.L. Parker, Anti-inflammatory, tissue remodeling, immunomodulatory, and anticancer activities of oregano (Origanum vulgare) essential oil in a human skin disease model, Biochimie open 4 (2017) 73-77.

[16] A. Ocaña-Fuentes, E. Arranz-Gutiérrez, F.J. Señorans, G. Reglero, Supercritical fluid extraction of oregano (Origanum vulgare) essentials oils: Anti-inflammatory properties based on cytokine response on THP-1 macrophages, Food and chemical toxicology 48(6) (2010) 1568-1575.

[17] E. Sidiropoulou, V. Marugan-Hernandez, I. Skoufos, I. Giannenas, E. Bonos, K. Aguiar-Martins, D. Lazari, T. Papagrigoriou, K. Fotou, K. Grigoriadou, D.P. Blake, A. Tzora, *In Vitro* Antioxidant, Antimicrobial, Anticoccidial, and Anti-Inflammatory Study of Essential Oils of Oregano, Thyme, and Sage from Epirus, Greece, Life (Basel) 12(11) (2022) 1783.

[18] M. Lu, T. Dai, C.K. Murray, M.X. Wu, Bactericidal Property of Oregano Oil Against Multidrug-Resistant Clinical Isolates, Front Microbiol 9 (2018) 2329.

[19] M. Hacioglu, O. Oyardi, A. Kirinti, Oregano essential oil inhibits Candida spp. biofilms, Z Naturforsch C J Biosci 76(11-12) (2021) 443-450.

[20] E.P. Gutiérrez-Grijalva, N. Leyva-López, G. Vazquez-Olivo, J.B. Heredia, Oregano as a potential source of antidiabetic agents, Journal of food biochemistry (2022) e14388-e14388.

[21] N. Leyva-López, E.P. Gutiérrez-Grijalva, J.B. Heredia, R. Ramos-Payan, L.A. Contreras-Angulo, J.R. Gonzalez-Galaviz, L.Z. Rodriguez-Anaya, Antioxidant potential, cytokines regulation, and inflammation-related genes expression of phenolic extracts from Mexican oregano, Journal of food biochemistry (2022) e14440-e14440.

[22] J. Ragi, A. Pappert, B. Rao, D. Havkin-Frenkel, S. Milgraum, Oregano extract ointment for wound healing: a randomized, double-blind, petrolatum-controlled study evaluating efficacy, J Drugs Dermatol 10(10) (2011) 1168-72.

[23] D.G. Sami, A. Abdellatif, H.M.E. Azzazy, Turmeric/oregano formulations for treatment of diabetic ulcer wounds, Drug development and industrial pharmacy 46(10) (2020) 1613-1621.

[24] M.D. Berechet, C. Gaidau, A. Miletic, B. Pilic, M. Râpă, M. Stanca, L.-M. Ditu, R. Constantinescu, A. Lazea-Stoyanova, Bioactive Properties of Nanofibres Based on Concentrated Collagen Hydrolysate Loaded with Thyme and Oregano Essential Oils, Materials 13(7) (2020) 1618.

[25] K. Yoncheva, N. Benbassat, M.M. Zaharieva, L. Dimitrova, A. Kroumov, I. Spassova, D. Kovacheva, H.M. Najdenski, Improvement of the Antimicrobial Activity of Oregano Oil by Encapsulation in Chitosan—Alginate Nanoparticles, Molecules (Basel, Switzerland) 26(22) (2021) 7017.

[26] A.u.R. Khan, K. Huang, Z. Jinzhong, T. Zhu, Y. Morsi, A. Aldalbahi, M. El-Newehy, X. Yan, X. Mo, PLCL/Silk fibroin based antibacterial nano wound dressing encapsulating oregano

essential oil: Fabrication, characterization and biological evaluation, Colloids and surfaces, B, Biointerfaces 196 (2020) 111352-111352.
[27] J. Romo-Rico, S. Murali Krishna, J. Golledge, A. Hayles, K. Vasilev, M.V. Jacob, Plasma polymers from oregano secondary metabolites: Antibacterial and biocompatible plant-based polymers, Plasma processes and polymers 19(7) (2022) n/a.
[28] A. Kumar, A. Al-Jumaili, K. Bazaka, P. Mulvey, J. Warner, M.V. Jacob, In-Situ Surface Modification of Terpinen-4-ol Plasma Polymers for Increased Antibacterial Activity, Materials 13(3) (2020) 586.
[29] S.Y. Kim, M.G. Nair, Macrophages in wound healing: activation and plasticity, Immunol Cell Biol 97(3) (2019) 258-267.
[30] C.G. Sokolik, J.-P. Lellouche, Hybrid-silica nanoparticles as a delivery system of the natural biocide carvacrol, RSC advances 8(64) (2018) 36712-36721.
[31] Database, XPS (X-ray Photoelectron Spectroscopy), XPS Spectra – Chemical Shift|Binding Energy http://techdb.podzone.net/xpsstate-e/ (2015).
[32] F. Jönsson, C.B. Gurniak, B. Fleischer, G. Kirfel, W. Witke, Immunological responses and actin dynamics in macrophages are controlled by N-cofilin but are independent from ADF, PloS one 7(4) (2012) e36034.
[33] S.M.K. Jesus Romo-Rico, Jonathan Golledge, Andrew Hayles, Krasimir Vasilev, Mohan Jacob, Plasma polymers from oregano secondary metabolites: An antibacterial and biocompatible plant-based polymers, Plasma Process Polym (2022).
[34] C. Liu, D. Chu, K. Kalantar-Zadeh, J. George, H.A. Young, G. Liu, Cytokines: From Clinical Significance to Quantification, Adv Sci (Weinh) 8(15) (2021) e2004433.
[35] M.R. Khazdair, V. Ghorani, A. Alavinezhad, M.H. Boskabady, Pharmacological effects of Zataria multiflora Boiss L. and its constituents focus on their anti-inflammatory, antioxidant, and immunomodulatory effects, Fundamental & clinical pharmacology 32(1) (2018) 26-50.
[36] S. Jalali, M.H. Boskabady, A. Haeri Rohani, A. Eidi, The effect of carvacrol on serum cytokines and endothelin levels of ovalbumin sensitized Guinea-pigs, Iranian journal of basic medical sciences 16(4) (2013) 615-619.
[37] J. Ong, R. Godfrey, B. Isaacson, P. Pasquina, D. Williams, Determining the Antibiofilm Efficacy of Oregano Gel in an Ex Vivo Model of Percutaneous Osseointegrated Implants, Microorganisms (Basel) 10(11) (2022) 2133.
[38] J.Y. Quek, R. Bright, P.R.L. Dabare, K. Vasilev, ROS-responsive copolymer micelles for inflammation triggered delivery of ibuprofen, Colloids and Surfaces B: Biointerfaces 217 (2022) 112590.

[39] Y. Wang, D.I. Adeoye, Y.J. Wang, M.G. Roper, Increasing insulin measurement throughput by fluorescence anisotropy imaging immunoassays, Analytica Chimica Acta 1212 (2022) 339942.
[40] F. Marino-Merlo, E. Papaianni, C. Frezza, S. Pedatella, M. De Nisco, B. Macchi, S. Grelli, A. Mastino, NF-κB-Dependent Production of ROS and Restriction of HSV-1 Infection in U937 Monocytic Cells, Viruses 11(5) (2019) 428.
[41] C. Tan, H. Fan, J. Ding, C. Han, Y. Guan, F. Zhu, H. Wu, Y. Liu, W. Zhang, X. Hou, S. Tan, Q. Tang, ROS-responsive nanoparticles for oral delivery of luteolin and targeted therapy of ulcerative colitis by regulating pathological microenvironment, Materials Today Bio 14 (2022) 100246.

Chapter 5

Antimicrobial graphene-based coatings for biomedical implant applications

In this chapter is focused on the deposition of graphene on CoCr substrates using RF-PECVD and *Origanum vulgare* as a Gr precursor. The presence of graphene in the CoCr-Gr sample was confirmed through various spectroscopy techniques. Biocompatibility tests showed that CoCr-Gr had similar viability, adhesion, and morphology of RAW macrophages compared to CoCr alone. CoCr-Gr also had a significant bactericidal and antifouling effect against *P. aeruginosa* and *S. aureus*. The study suggests that CoCr-Gr has potential applications as an antibacterial coating for implantable devices.

This chapter was published as: *Jesus Romo-Rico, Richard Bright, Smriti Murali Krishna, Krasimir Vasilev, Jonathan Golledge, and Mohan V. Jacob*. Antimicrobial graphene-based coatings for biomedical implant applications. Carbon trends, Volume 12, 2023. ISSN 100282, https://doi.org/10.1016/j.cartre.2023.100282.

Antimicrobial graphene-based coatings for biomedical implant applications

Graphical abstract

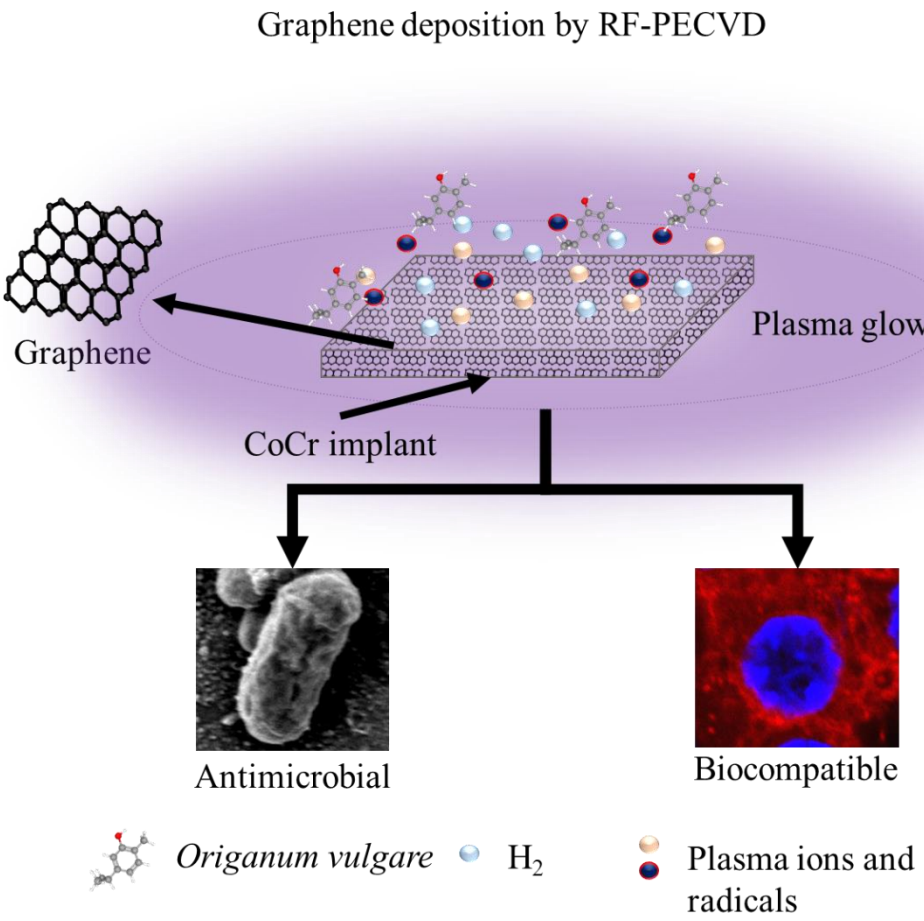

Abstract

Implant-associated infections (IAI) cause significant health issues and healthcare costs. In this research, we deposited graphene (Gr) on a medical-grade cobalt-chromium (CoCr) alloy surface by radiofrequency plasma-enhanced chemical vapor deposition (RF-PECVD) using *Origanum vulgare* as a precursor material. The deposition of Gr on the CoCr was confirmed using Raman spectroscopy and X-Ray photoelectron spectroscopy (XPS) and scanning electron microscopy (SEM). The biocompatibility and antibacterial properties of CoCr-Gr were investigated. CoCr-Gr was biocompatible and promoted cell adhesion and spreading of RAW 267.4 macrophage cells. CoCr-Gr were antibacterial against *Staphylococcus aureus* and *Pseudomonas aeruginosa* and inhibited *P.*

aeruginosa attachment. The results indicate that CoCr-Gr could be used as a potential antibacterial coating material for implantable devices.

5. 1. Introduction

Implant-associated infection (IAI) is a major global burden associated with morbidity, mortality and high healthcare cost [1, 2]. The incidence of IAI with some devices can be as high as 30% [3]. The total cost of treating IAI varies depending on the primary treatment option chosen, with debridement, antibiotics and implant retention (DAIR) resulting in the lowest cost at A$19,688, followed by excision arthroplasty at A$23,805, one-stage revision at A$26,722, and two-stage revision at A$44,744, according to a study of 114 patients who underwent a total of 178 surgical procedures for IAI treatments in Australia [4]. IAI occurs when bacteria enter the body through the implant site, attach to the device and start to form a biofilm [5]. The antibiotic resistance of a biofilm is significantly stronger than in planktonic cells and the infection becomes difficult to eradicate [6, 7]**.** The number of infections caused by antibiotic-resistant is constantly increasing, and this trend is projected to continue [8]. Therefore, the demand for developing novel coatings with enhanced properties to reduce the risk of IAI is very high [9].

Graphene-based coatings have been used in wound-healing applications [10, 11]. Studies have shown that graphene coatings can inhibit the growth of a wide range of bacteria [12, 13]. Typically, graphene oxide (GO) sheets were deposited by electrophoretic deposition on plasma electrolytic oxidation (PEO) pre-treated titanium (Ti) substrates. The GO enhanced the antibacterial activity of the PEO-Ti samples by reducing ~80% and ~100% of *Escherichia coli* and *S. aureus* viability, respectively [14]. In other studies, spark plasma sintering (SPS) was used to incorporate graphene into a magnesium alloy implant, which reduced *S. aureus* and *E. coli* viability up to 5-fold. The cytocompatibility with human mesenchymal stromal cells (hMSCs and osteogenic properties were also enhanced by graphene-modified surfaces [15].

Cobalt-chromium (CoCr) alloys are commonly used for orthopedic, dental, and cardiovascular implants [16, 17]. Despite its excellent mechanical properties, wear resistance and biocompatibility, like other metal alloys, CoCr alloys have their drawbacks [18, 19]. CoCr alloys are susceptible to bacterial infection due to contamination introduced by poor sterilization and on-sterile/handling, causing inflammation, allergic reaction and aseptic loosening [20]. Graphene has been incorporated into CoCr alloys in an attempt to enhance their properties [21]. For example, GO was electrodeposited onto medical cobalt-chromium-molybdenum (CoCrMo) alloys and coated with ε-poly-L-Lysine (ε-PLL) to endow it with

antibacterial properties. The integration of GO, as well as ε-PLL and GO/ε-PLL on CoCrMo alloys, increased antibacterial activity against *S. aureus* and *E. coli* [22].

Radiofrequency plasma-enhanced chemical vapor deposition (RF-PECVD) has been used to fabricate graphene from renewable precursors, such as plant secondary metabolites for their use in electronics applications such as sensors and organic photovoltaic cells [23]. RF-PECVD graphene derived from Pelargonium graveolens was directly deposited on silicon oxide and quartz substrates by Al-Jumaili et al. The plasma-induced fabrication of vertically oriented graphene nanowalls which were functioning as graphene knives damaged *E. coli* and *S. aureus* membranes [24].

This study aims to fabricate a graphene coating on the CoCr alloy surface by RF-PECVD using *Origanum vulgare* as a precursor material. To the best of our knowledge, the incorporation of graphene coatings into CoCr alloy surfaces by RF-PECVD using *Origanum vulgare* as a graphene precursor has not been studied yet. *Origanum vulgare* essential oil is primarily composed of volatile organic compounds such as monoterpenes and sesquiterpenes, containing a high amount of carbon that can potentially serve as a graphene precursor. Therefore, this plant was selected as a suitable source for the fabrication of graphene.

The surface was characterized by Raman, Wettability, X-ray photoelectron spectroscopy (XPS) and scanning electron microscopy (SEM). The biocompatibility of the graphene coating with mammalian cells was investigated. We also evaluated the antibacterial properties of the graphene coating against Gram-positive and Gram-negative bacteria.

5. 2. Experimental

5. 2. 1. Materials

Medical grade CoCr alloy (L605, ASTM F90, Øext = 2.5 mm, Øint = 2.28 mm) was received as a sample from Minitubes® (Grenoble, France). Origanum vulgare was purchased from Sydney Essential Oils Company (Sydney, Australia).

5. 2. 2. Synthesis of Gr on CoCr substrates

Graphene was directly deposited by RF-PECVD on CoCr substrates. Before the fabrication, the CoCr tube was flattened and cut using a diamond disk in rectangle substrates (3 × 7 mm).

CoCr substrates were sonicated and cleaned with isopropyl alcohol for 5 min and air-dried before placing them in the middle of the plasma reactor.

The custom RF-PECVD reactor is represented in Figure 5.3; it is composed of a quartz tube covered with a ceramic furnace coupled with an external heater [24, 25]. On one end of the plasma reactor, an H2 delivery system, a flask, a stopcock, and a flow meter are connected. On the other end, the quartz tube is connected to a vacuum pump. Before the Gr fabrication, the CoCr substrate were pre-treated with H2 and plasma power of 500 W at 10 sccm, and 700 °C for 1 min. A rotary pump was utilized to maintain the plasma reactor at 0.02 mbar. Origanum vulgare vapours were then introduced into the plasma reactor using the manual stopcock flow controller meanwhile the plasma discharge was kept for 4 min.

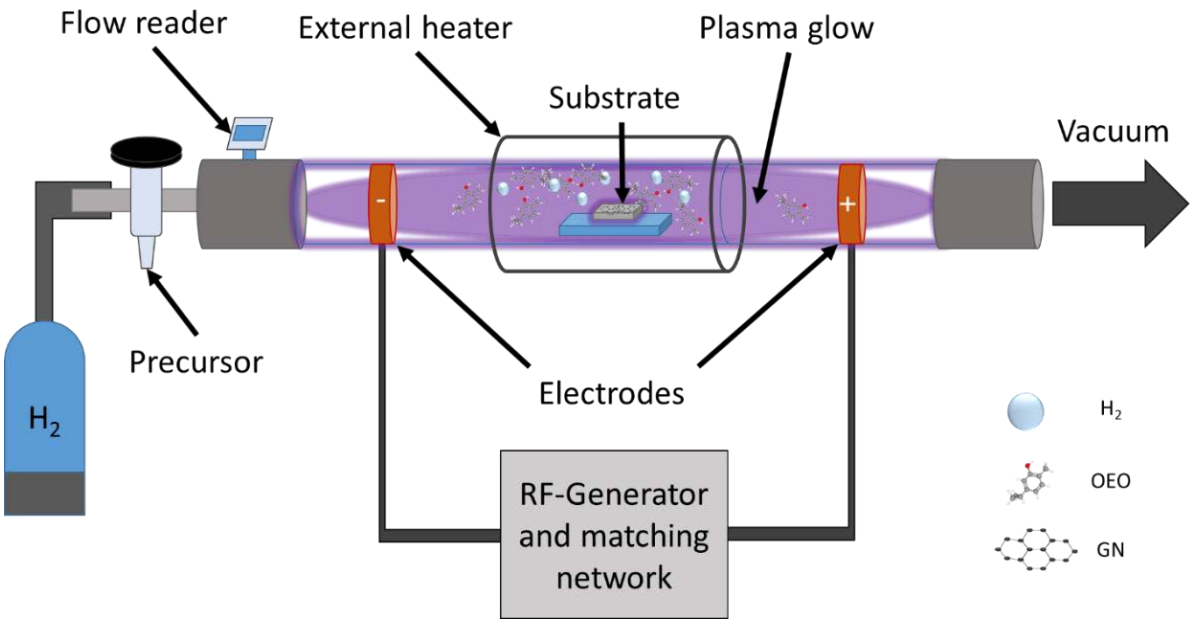

Figure 5. 3. Representation scheme of the RF-PECVD system utilized to fabricate Gr on CoCr substrate.

5. 2. 3. Raman and X-ray photoelectron spectroscopy

Raman spectroscopy was used to characterize the CoCr-Gr at room temperature with a WITec's Raman Spectrometer (WITec, Ulm, Germany). The laser wavelength utilized was, $\lambda = 532$ nm. X-ray photoelectron spectroscopy (XPS) was carried out using a Kratos AXIS Ultra DLD spectrometer (Kratos Analytical Ltd., Manchester, UK), which uses a monochromatic AlKα radiation ($h\nu = 1486.7$ eV). Data were analyzed with CasaXPS software (Casa Software Ltd., Teignmouth, UK).

5. 2. 4. Contact angle

The water contact angle (WCA) of CoCr and CoCr-Gr was determined using a sessile drop method with a KSV CAM 101 optical apparatus (KSV Instruments Ltd., Helsinki, Finland). The contact angle of an 8 µl drop of MiliQ water was measured using the CoCr and CoCr-Gr surfaces of the samples as a baseline reference.

5. 2. 5. Scanning electron microscopy

CoCr and CoCr-Gr surfaces were imaged using a Zeiss Merlin FEG-SEM, (Microscopy Australia, University of South Australia: Zeiss, Jena, Germany). The images were taken using an accelerating voltage of 2 kV, and magnifications of 10 K and 20 K.

5. 2. 6. Raw 264.7 macrophage-like cells culture

Macrophages are one of the first immune cells to interact with an implant surface and play an essential role in innate immunity, bone remodeling and wound-healing [26]. RAW 264.7 macrophage-like cells (Abelson leukemia virus-transformed cell line derived from BALB/c mice, ATCC TIB-71) were cultured in Dulbecco's modified Eagle's medium (DMEM; ThermoFisher, CA, USA) media was supplemented with 10% Fetal Bovine Serum (FBS, Life Technologies, CA, USA) plus 1% Pen/Strep (100 U/mL Penicillin and 100 µg/mL Streptomycin, Life Technologies, CA, USA) and incubated at 37 °C in 5% CO_2.

5. 2. 7. Cell viability (MTT assay)

Before the MTT (3-(4,5-Dimethylthiazol-2-yl)−2,5-diphenyltetrazolium bromide, Sigma-Aldrich, MI, USA) the assay was performed in a 24-well plate, CoCr and CoCr-Gr samples were placed into 24 well-plate and UV sterilized for 20 min. Macrophages were seeded on sample surfaces at a density of 2×10^5 cells/mL in 1 mL of RPMI supplemented with 10% Fetal Calf Serum (FCS) and 1% Pen/Strep v/v and incubated for 48 h. A working stock of MTT in PBS was prepared at 5 mg/ml, and 100 µl of MTT/PBS concentration was added into each well and then incubated for 4 h at 37 °C in 5% CO_2. Next, the solution was removed and 200 µl DMSO was added to each sample to lyse the cells. The well plate was stored in the dark for 15 min before reading its absorbance at 570 nm.

5. 2. 8. Cell adhesion and spreading

The cells were PBS-washed twice and permeabilized using 0.1% Triton X-100 diluted in 1x PBS for 5 min, then 1% BSA diluted in 1x PBS was added for 30 min. The two washing steps were repeated before TRITC-conjugated Phalloidin (FAK100 kit, Sigma-Aldrich) and PBS were added (1:1000 dilution) to the samples and incubated for 1 h. Phalloidin is a fluorescent dye used to stain actin filaments of cells, which are indicators of cell adhesion and spreading. Cell nuclei were stained incubating cells with DAPI for 5 min. Cells were washed thrice with PBS for 10 min. Then, CoCr and CoCr-Gr were mounted on microscope slides by using an antifade mounting solution. Olympus FV3000 confocal microscope (CLSM; Olympus, Tokyo, Japan) was used to take fluorescence images of each sample.

5. 2. 9. Bacterial studies

Bacteria were recovered from glycerol stocks, *S. aureus* (ATCC 25923) and *P. aeruginosa* (clinical isolate, PAO1 type; SA Pathology) and plated on tryptone soy agar plate (TSA; Oxoid, Thermofisher, MA, USA) and incubated at 37 °C for 18 h. Next, single colonies of each pathogen were inoculated into tryptone soy broth (TSB, Oxoid, ThermoFisher, MA, USA) and 5% FCS (TSBFCS; Gibco, ThermoFisher, MA, USA) and incubated at 37 °C for 18 h. Cell density was adjusted to 1×10^9 CFU/mL by measuring the absorbance at 600 nm using a NanoDrop™ 2000c (ThermoFisher, MA, USA) and incubated at 37 °C for 18 h. Finally, bacterium cultures were diluted down to 1×10^6 CFU/mL and 1 mL of each dilution was added to CoCr and CoCr-Gr.

5. 2. 10. Scanning electron microscopy of bacteria morphology

To observe *S. aureus* and *P. aeruginosa* morphology, both pathogens were cultured on the CoCr and CoCr-Gr surfaces and images using a scanning electron microscope (SEM). After inoculating the samples with *S. aureus* or *P. aeruginosa* for 24 h, the culture media was removed from each sample and washed twice with PBS to remove loosely attached bacteria. The samples were then dehydrated using increasing concentrations of ethanol (50, 75 and 100% v/v), followed by a 1:1 mix of 100% ethanol and hexamethyldisilazane (HMDS, Sigma-Aldrich, MA, USA) for 20 min, and 100% HMDS for 20 min. The samples were left to dry for 3 h and mounted on aluminium stubs (using double side carbon tape) and sputter coated with

5 nm platinum. The same SEM voltage, magnification and working distance used in the surface morphology SEM were used in these experiments.

5. 2. 11. LIVE/DEAD Bacteria assay

After the bacteria were incubated on CoCr and CoCr surfaces, a Live/Dead® BacLight™ kit (Invitrogen, ThermoFisher MA, USA) was utilized to observe and quantify the viability of the bacteria. The assay was performed according to the manufacturer's protocol. This assay uses Syto9, a green fluorescence dye that binds to live cell nucleic acids, and propidium iodide, a red fluorescence dye that stains damaged bacteria and dead cells. The samples were submerged in 1.5 µl of Syto9 (Ex/Em 480/500 nm) and 1.5 µl of Propidium Iodide (PI; Ex/Em 490/635 nm) per mL of PBS, for 15 min at RT in the dark. Thereafter, a confocal laser scanning microscope (Olympus FV3000) was used to take three random images of each sample (magnification x40). Cell viability and cell number were quantified using ImageJ software (V1.53t: NIH, MD, USA).

5. 2. 12. Statistical analyses

In the bacterial and cell viability experiments, a total of three biological replicates were conducted for each experiment. The mean and standard deviation of the replicates were plotted in GraphPad Prism (v8.3.0). To determine statistical significance, a two-way analysis of variance (ANOVA) with Sidak's multiple-comparisons test was performed using the aforementioned software.

5. 3. Results and discussion

5. 3. 1. Surface characterization

Raman spectroscopy was used to analyze the plasma-fabricated CoCr-Gr. The Raman spectra in Figure 5. 4 A highlight the presence of intense D, G, and 2D peaks of sp2 carbon structure at 1341, 1569, and 2680 cm^{-1}, respectively. These peaks are typical of graphene with high content of defects [27] The D-peak occurs at 1341 cm^{-1} due to the scattering of phonons produced by the defects on the disordered edge of the Brillouin zone. The G-peak, located at 1569 cm^{-1}, is associated with the vibrational modes of sp2-bonded carbon and the crystallinity

of the graphene. The 2D peak at 2680 cm^{-1} occurs from two phonon vibration modes and is related to the number of graphene layers [28].

The ID/IG ratio is an indicator of the structural quality of graphene. A lower ID/IG ratio indicates a higher degree of crystallinity and a more ordered structure, while a higher ID/IG ratio suggests a higher concentration of defects and disorders in the graphene material. In this study, the ID/IG ratio for the CoCr-Gr samples is 0.72, which can be associated with a few layers of graphene [29].

Figure 5. 4 C and 2 D show the XPS survey and high-resolution C1s spectra of CoCr-Gr deposited with RF-PECVD. Survey spectra in C show a strong C1s-peak located at 284.4 eV, which can be associated with the sp^2 carbon hybridization (C=C) of graphitic carbon [34]. The sp^3 hybridization of carbon at 284.9 eV corresponds to aliphatic hydrocarbon groups (C—H and C—H and C—H) [34].

These groups can be related to edges and defects in the graphite nanostructures exposed to high temperatures, it is established that Gr tends to absorb atmospheric moisture [35, 36]. A low-intensity peak related to the π-π* energy loss is located at 286.7 eV [35]. The O1s peak is observed at the binding energy of 533 eV. A shoulder peak at 531.9 eV can be attributed to C=O interactions [37]. CoCr-associated peaks, Co2p and Co 2p1/2 are located at 779.35 and 793 eV, respectively. As well as for Cr21/2 is located at 586.5 eV and Cr2p at 576.8 eV.

The SEM micrographs in Figure 5. 4 E and 2 F show the CoCr and CoCr-Gr, respectively. The CoCr control surface shows the alloy microstructure containing grain boundaries, defects and agglomerations [38]. The SEM micrographs of CoCr-Gr corroborated the presence of Gr nanosheets on the CoCr-Gr surface [39]. The CoCr-Gr micrographs show Gr in the form of nanostructures with random shapes and sizes <100 nm. There are few Gr nanosheets >100 nm. These Gr formations can be associated with the high content of defects found in the chemical characterization.

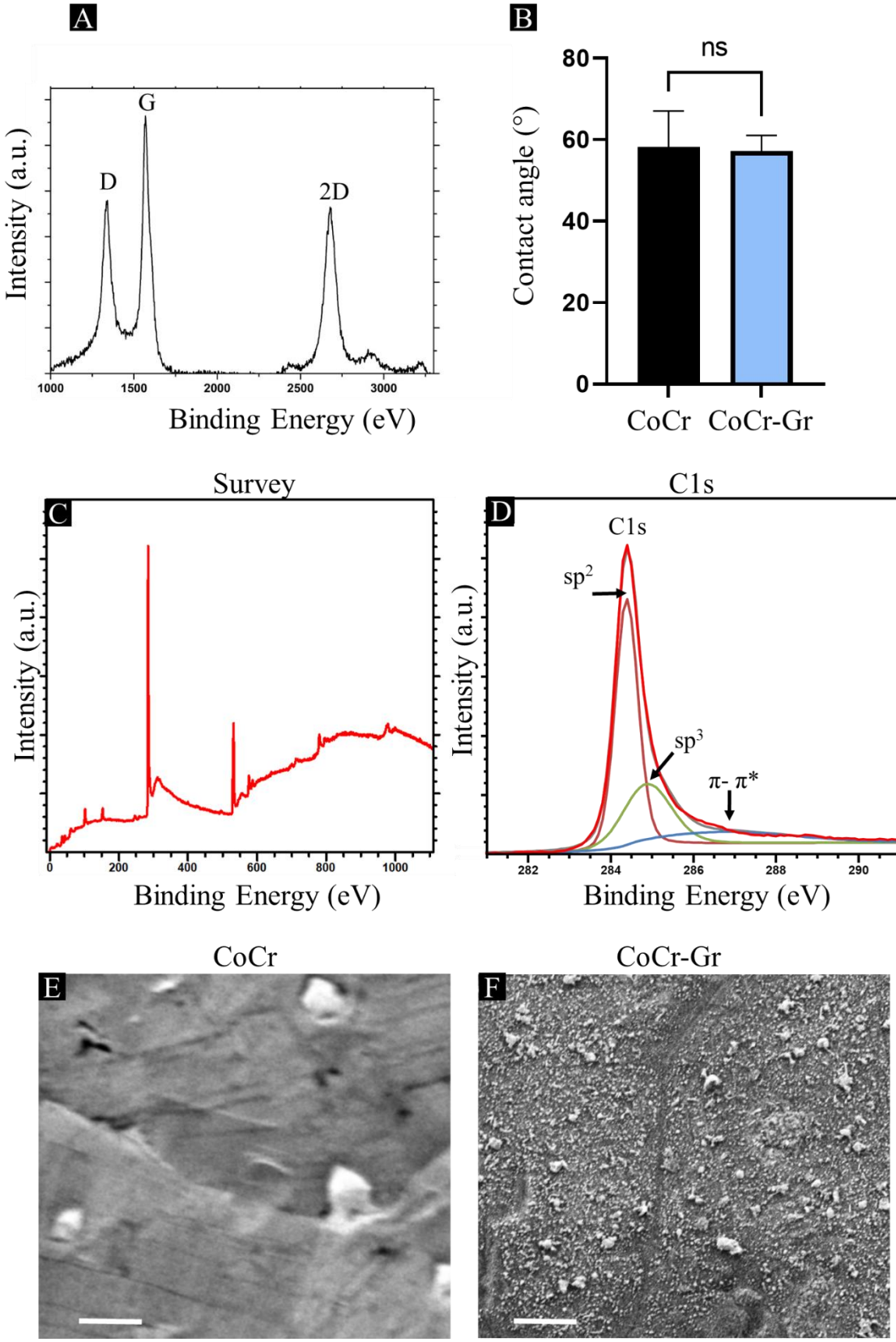

Figure 5. 4. A shows Raman spectra of CoCr-Gr, showing D, G and 2D peaks of graphene. The water contact angle of CoCr and CoCr-Gr is shown in 2 B. XPS of CoCr-Gr 2C shows normalized survey and 2 D displays high-resolution C1s spectra and hybridizations of carbon. 2 E and 2 F show SEM of CoCr and CoCr-Gr, respectively. Scale bar 1 μm.

5. 3. 2. Biocompatibility and focal adhesion of RAW macrophages on CoCr-Gr

An MTT assay was used to determine cell viability based on the conversion of the yellow tetrazolium salt MTT to purple formazan by living cells at 48 h by measuring cellular metabolic activity on RAW macrophages incubated onto CoCr and CoCr-Gr surfaces. Both samples have shown similar cell viabilities without significant difference, as it's seen in the MTT plot shown in Figure 5. 5**.** A. Figure 5. 6 B shows the corrected total fluorescence calculated using ImageJ. The fluorescence images in Figure 5. 7 C show the morphology and the actin cytoskeleton of 264.7 RAW macrophages incubated with CoCr and CoCr-Gr after 48 h. F-actin (red staining) appeared well-defined and showed normal cell spreading. F-actin filaments provide mechanical stability to the cell cytoskeleton and the cell cortex in mammalian cells and play a role in cell migration and cell adhesion [40]. DAPI (blue staining) shows the nuclei of cells with healthy morphology. Overall, there were no differences between the cytotoxicity and adhesion of RAW macrophages incubated onto CoCr and CoCr-Gr for 48 h.

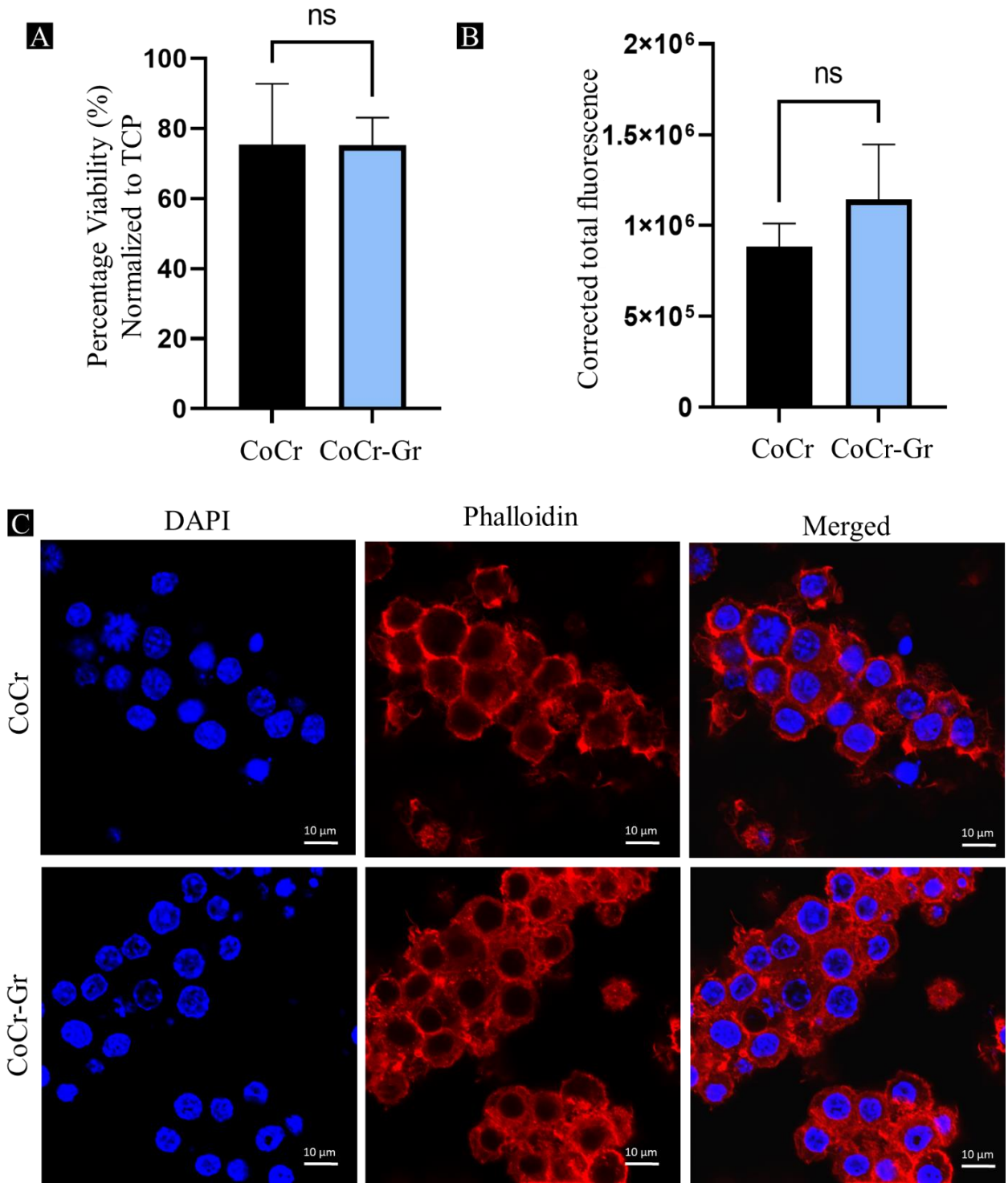

Figure 5. 8. A shows the MTT assay plot representing the cell viability of RAW macrophages CoCr and CoCr-Gr. Mean ± SD, n = 6 and B display cell fluorescence intensity. C shows morphology and focal adhesion of RAW macrophages after 48 h incubation. The scale bars represent 10 µm.

5. 3. 3. Bactericidal and antifouling effects of CoCr-Gr

The bactericidal and antifouling properties of the CoCr and CoCr-Gr were studied in cultures of *P. aeruginosa* and *S. aureus* as representative of Gram-negative and Gram-positive pathogens often causing medical device associated infections. After inoculation on the surface for 18 h adherent bacteria were stained with the well-established live/dead assay. After staining live and dead cells are represented by green and red fluorescence, respectively (Figure 5. 9. A). The bactericidal effect of CoCr-Gr was statistically significant ($p<0.0001$) against *P. aeruginosa* and *S. aureus* ($p<0.01$) when compared to CoCr control surfaces. The antifouling effect was evaluated by quantifying the attachment of bacteria onto both samples. The attachment of *P. aeruginosa* on CoCr-Gr was statistically significantly lower ($p<0.0001$) than on CoCr control surfaces but there were no significant differences in *S. aureus* attachment (Figure 5. 10. B).

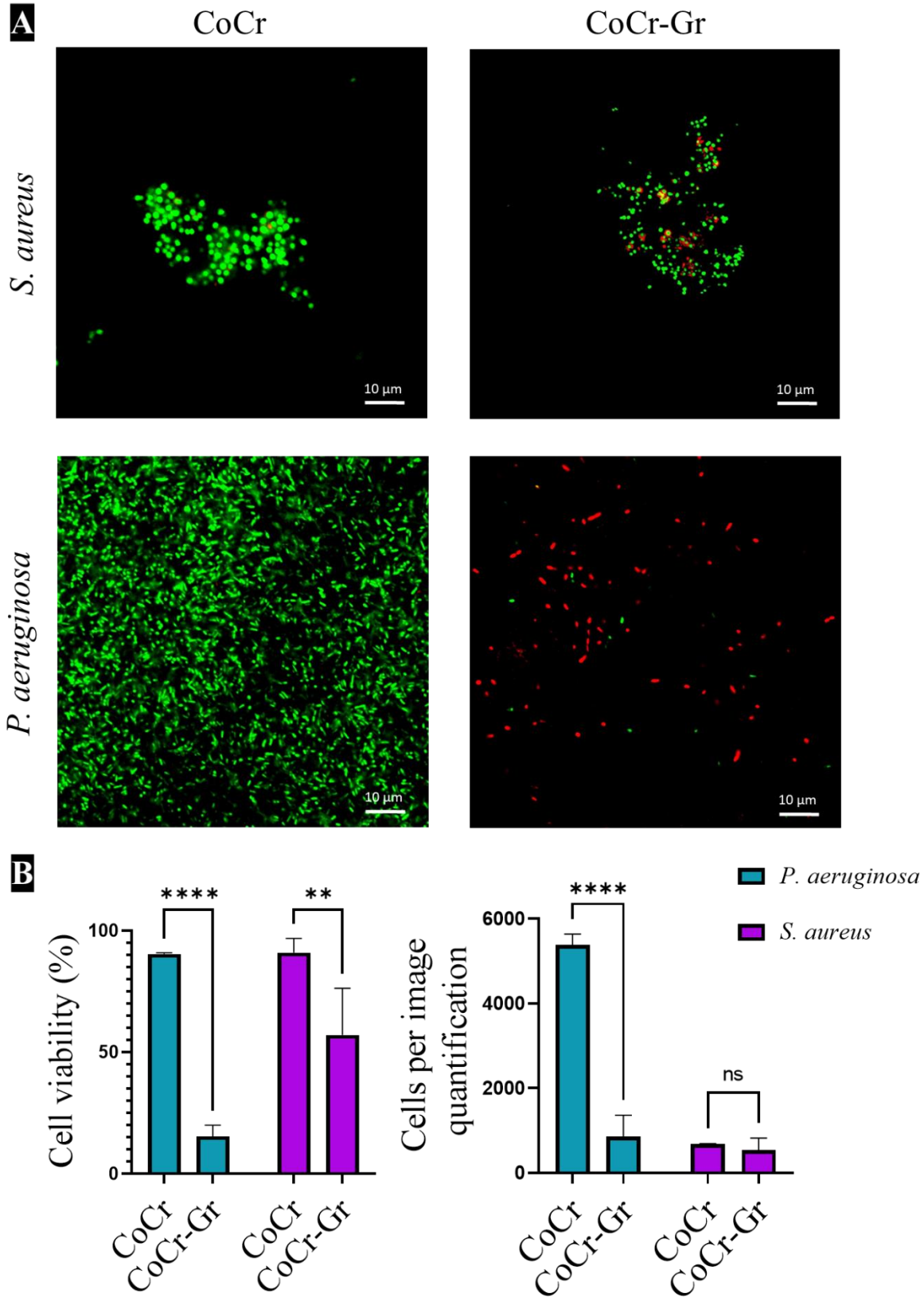

Figure 5. 11. Fluorescence microscopy images after using LIVE/DEAD staining of *S. aureus* and *P. aeruginosa* and on CoCr and CoCr-Gr are shown in 4 A. Bacterial cell viability percentage and cells per image quantification are represented in 4 B The scale bar represents 10 μm. Bar graphs are presented as mean ± SD, n = 3 **p<0.01 and ****p<0.0001.

The morphology of *S. aureus* and *P. aeruginosa* incubated in CoCr and CoCr-Gr imaged by SEM is presented in Figure 5. 7. The CoCr control samples showed healthy bacterial morphology, S. aureus appeared unaffected (A-C), whereas *P. aeruginosa* showed evidence of extracellular polymeric substances (EPS) formation, suggesting the early stage of biofilm formation [41]. In contrast, *S. aureus* and *P. aeruginosa* inoculated on the CoCr-Gr had disrupted and wrinkled cell walls, heavily affected by the Gr coating (Figure 5. 12 B and D).

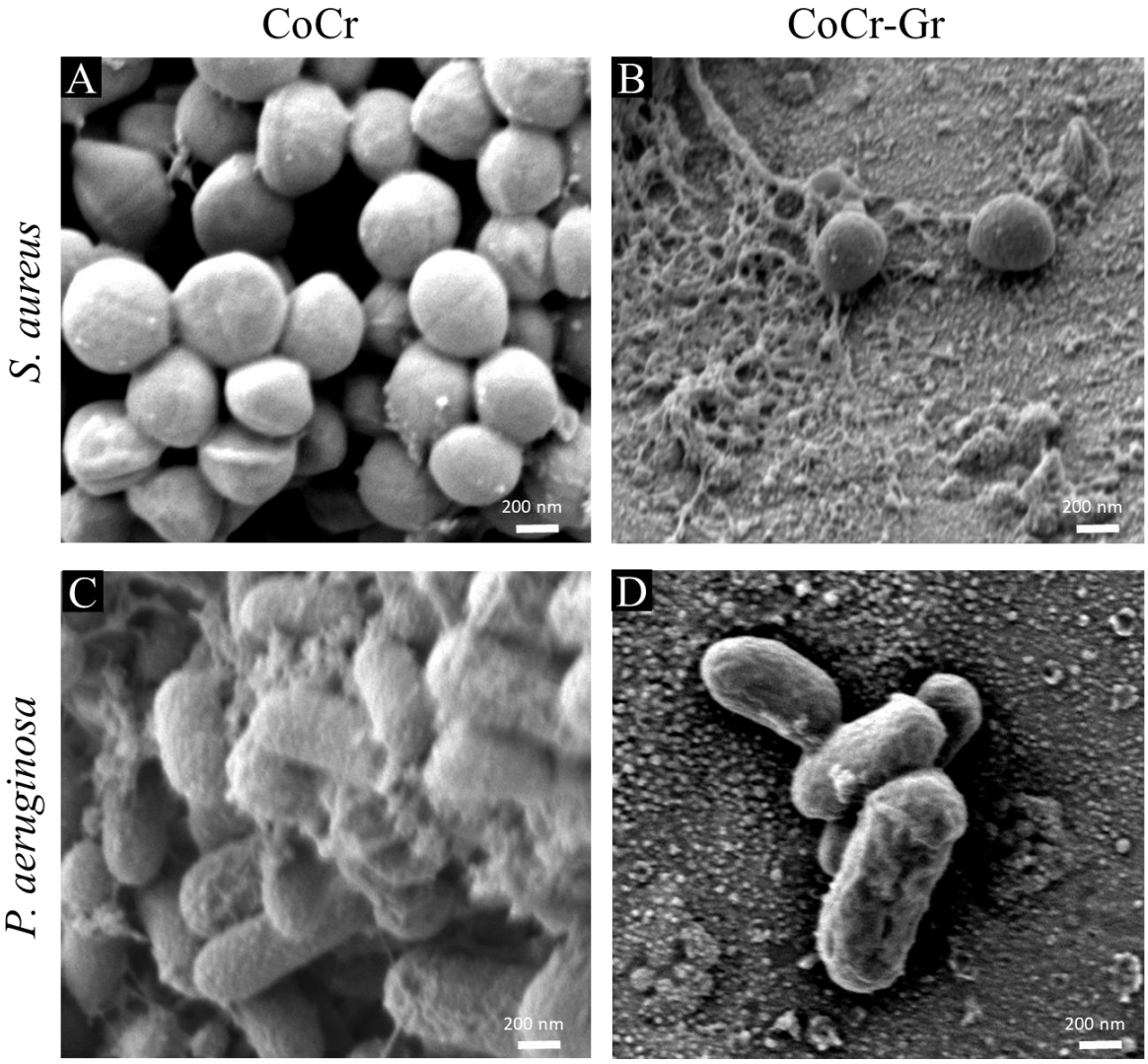

Figure 5. 13. SEM images of the bactericidal and antifouling effect of CoCr and CoCr-Gr surfaces against *P. aeruginosa* and *S. aureus*. The scale bars indicate 200 nm.

S. aureus incubated with CoCr-Gr showed a well-defined EPS connecting bacteria. One of the multiple roles of the EPS matrix is to protect bacteria against mechanical challenges. According to Tu et al. [42], sharp graphene nanosheets can extract phospholipids from bacterial Gram-negative cell membrane by hydrophobic interactions between Gr and the lipid tail of the

phospholipid. Another theory from Luan et al. [43] describes that the curvature of the graphene had a significant influence on the lipid extraction process, while Wu et al. [44] identified lipid extraction could be associated with the GO and hydrophilic head groups of lipids. However, the disruption of the Gram-negative bacterial cell wall by CoCr-Gr could be associated with the shape of the Gr, as well as potential local hydrophobic nano interactions between Gr and phospholipids.

5. 4. Conclusions

Gr was deposited on CoCr substrates using RF-PECVD and *Origanum vulgare* as a Gr precursor. Raman spectroscopy and X-ray photoelectron spectroscopy confirmed the presence of Gr in the CoCr-Gr sample which was multilayered and had a high content of defects. The plasma deposition of Gr on CoCr surfaces did not affect the hydrophilicity of the samples. The SEM microscopies showed Gr in the form of nanostructures with various nanometric shapes and sizes. The biocompatibility results demonstrated that both CoCr and CoCr-Gr had similar viability, adhesion, and morphology of RAW macrophages after 48 h of incubation. The bactericidal and antifouling effect of CoCr-Gr was significantly higher against *P. aeruginosa* compared to the control. CoCr-Gr was also bactericidal against *S. aureus*.

The rapid fabrication of Gr using RF-PECVD on a variety of substrates and a sustainable volatile source of carbon such as *Origanum vulgare* offers versatility and potential for customization in implant design and production.

Overall, the unique combination of properties exhibited by Gr coatings, including high biocompatibility, and antibacterial and antifouling properties make them a promising material for coating medical implants. However, further research is necessary to fully understand the potential of Gr coatings in the context of implant design, production, and use, and to ensure their safety and efficacy in clinical settings.

5. 5. Acknowledgements

Project funding was provided by Krasimir Vasilev, Mohan Jacob, and Jesus Romo-Rico. KV thanks NHMRC for Fellowship GNT1194466 and ARC for grant DP180101254.

JG is supported by funding from Townsville Hospital and Health Services, Tropical Australian Academic Health Centre, Heart Foundation, Medical Research Future Fund and the

Queensland Government. JG holds a Senior Clinical Research Fellowship from the Queensland Government, Australia.

5.6. References

[1] Z. Saleem, B. Godman, M.A. Hassali, F.K. Hashmi, F. Azhar, I.U. Rehman, Point prevalence surveys of health-care-associated infections: a systematic review, Pathogens and global health 113(4) (2019) 191-205.

[2] J. Sahoo, S. Sarkhel, N. Mukherjee, A. Jaiswal, Nanomaterial-Based Antimicrobial Coating for Biomedical Implants: New Age Solution for Biofilm-Associated Infections, ACS omega 7(50) (2022) 45962-45980.

[3] A. Trampuz, W. Zimmerli, Diagnosis and treatment of infections associated with fracture-fixation devices, Injury 37(2) (2006) S59-S66.

[4] K.M.D. Merollini, R.W. Crawford, N. Graves, Surgical treatment approaches and reimbursement costs of surgical site infections post hip arthroplasty in Australia: a retrospective analysis, BMC Health Services Research 13(1) (2013) 91.

[5] R. Bright, A. Hayles, J. Wood, N. Ninan, D. Palms, R.M. Visalakshan, A. Burzava, T. Brown, D. Barker, K. Vasilev, Bio-Inspired Nanostructured Ti-6Al-4V Alloy: The Role of Two Alkaline Etchants and the Hydrothermal Processing Duration on Antibacterial Activity, Nanomaterials (Basel, Switzerland) 12(7) (2022) 1140.

[6] A.F.P. Carreiro, J.A. Delben, S. Guedes, E.J.D. Silveira, M.N. Janal, C.E. Vergani, S. Pushalkar, S. Duarte, Low-temperature plasma on peri-implant–related biofilm and gingival tissue, Journal of periodontology (1970) 90(5) (2019) 507-515.

[7] T.-F.C. Mah, G.A. O'Toole, Mechanisms of biofilm resistance to antimicrobial agents, Trends in Microbiology 9(1) (2001) 34-39.

[8] A.G. Emelianova, N.V. Petrova, C. Fremez, M. Fontanié, S.A. Tarasov, O.I. Epstein, Therapeutic potential of highly diluted antibodies in antibiotic-resistant infection, European Journal of Pharmaceutical Sciences 173 (2022) 106161.

[9] A. Hayles, J. Hasan, R. Bright, D. Palms, T. Brown, D. Barker, K. Vasilev, Hydrothermally etched titanium: a review on a promising mechano-bactericidal surface for implant applications, Materials Today Chemistry 22 (2021) 100622.

[10] S. Beyranvand, Z. Pourghobadi, S. Sattari, K. Soleymani, I. Donskyi, M. Gharabaghi, W.E.S. Unger, G. Farjanikish, H. Nayebzadeh, M. Adeli, Boronic acid functionalized graphene platforms for diabetic wound healing, Carbon 158 (2020) 327-336.

[11] M. Shahnawaz Khan, H.N. Abdelhamid, H.-F. Wu, Near infrared (NIR) laser mediated surface activation of graphene oxide nanoflakes for efficient antibacterial, antifungal and wound healing treatment, Colloids and Surfaces B: Biointerfaces 127 (2015) 281-291.

[12] S. Pandit, Z. Cao, V.R.S.S. Mokkapati, E. Celauro, A. Yurgens, M. Lovmar, F. Westerlund, J. Sun, I. Mijakovic, Vertically Aligned Graphene Coating is Bactericidal and Prevents the Formation of Bacterial Biofilms, Advanced materials interfaces 5(7) (2018) 1701331-n/a.

[13] S.Y. Bhong, N. More, M. Choppadandi, G. Kapusetti, Review on carbon nanomaterials as typical candidates for orthopaedic coatings, SN Applied Sciences 1(1) (2018) 76.

[14] A. Mazinani, M.J. Nine, R. Chiesa, G. Candiani, P. Tarsini, T.T. Tung, D. Losic, Graphene oxide (GO) decorated on multi-structured porous titania fabricated by plasma electrolytic oxidation (PEO) for enhanced antibacterial performance, Materials & design 200 (2021) 109443.

[15] N. Safari, N. Golafshan, M. Kharaziha, M. Reza Toroghinejad, L. Utomo, J. Malda, M. Castilho, Stable and Antibacterial Magnesium–Graphene Nanocomposite-Based Implants for Bone Repair, ACS biomaterials science & engineering 6(11) (2020) 6253-6262.

[16] B. Singh, G. Singh, B.S. Sidhu, *In vitro* investigation of NbTa alloy coating deposited on CoCr alloy for biomedical implants, Surface and Coatings Technology 377 (2019) 124932.

[17] M.C. Garcia-Mendez, V.H. Urrutia-Baca, C.A. Cuao-Moreu, E. Lorenzo-Bonet, M. Alvarez-Vera, D.M. Ortiz-Martinez, M.A. de la Garza-Ramos, *In Vitro* Biocompatibility Evaluation of a New Co-Cr-B Alloy with Potential Biomedical Application, Metals (Basel) 11(8) (2021) 1267.

[18] B. Stojanović, C. Bauer, C. Stotter, T. Klestil, S. Nehrer, F. Franek, M. Rodríguez Ripoll, Tribocorrosion of a CoCrMo alloy sliding against articular cartilage and the impact of metal ion release on chondrocytes, Acta Biomaterialia 94 (2019) 597-609.

[19] K. Shukla, A.A. Sugumaran, I. Khan, A.P. Ehiasarian, P.E. Hovsepian, Low pressure plasma nitrided CoCrMo alloy utilising HIPIMS discharge for biomedical applications, Journal of the Mechanical Behavior of Biomedical Materials 111 (2020) 104004.

[20] N.A. Hodges, E.M. Sussman, J.P. Stegemann, Aseptic and septic prosthetic joint loosening: Impact of biomaterial wear on immune cell function, inflammation, and infection, Biomaterials 278 (2021) 121127.

[21] A. García-Argumánez, I. Llorente, O. Caballero-Calero, Z. González, R. Menéndez, M.L. Escudero, M.C. García-Alonso, Electrochemical reduction of graphene oxide on biomedical grade CoCr alloy, Applied surface science 465 (2019) 1028-1036.

[22] J. Guo, G. Cao, X. Wang, W. Tang, W. Diwu, M. Yan, M. Yang, L. Bi, Y. Han, Coating CoCrMo Alloy with Graphene Oxide and ε-Poly-L-Lysine Enhances Its Antibacterial and Antibiofilm Properties, International journal of nanomedicine 16 (2021) 7249-7268.
[23] M.S.A. Kamel, C.T. Stoppiello, M.V. Jacob, Single-step, catalyst-free, and green synthesis of graphene transparent electrode for organic photovoltaics, Carbon 202 (2023) 150-158.
[24] A. Al-Jumaili, M.A. Zafar, K. Bazaka, J. Weerasinghe, M.V. Jacob, Bactericidal vertically aligned graphene networks derived from renewable precursor, Carbon Trends 7 (2022) 100157.
[25] A. Al-Jumaili, P. Mulvey, A. Kumar, K. Prasad, K. Bazaka, J. Warner, M.V. Jacob, Eco-friendly nanocomposites derived from geranium oil and zinc oxide in one step approach, Sci Rep 9(1) (2019) 5973.
[26] Z. Sheikh, P.J. Brooks, O. Barzilay, N. Fine, M. Glogauer, Macrophages, Foreign Body Giant Cells and Their Response to Implantable Biomaterials, Materials 8(9) (2015) 5671-5701.
[27] M.Y. Svavil'nyi, V.Y. Panarin, A.A. Shkola, A.S. Nikolenko, V.V. Strelchuk, Plasma Enhanced Chemical Vapor Deposition synthesis of graphene-like structures from plasma state of CO2 gas, Carbon 167 (2020) 132-139.
[28] Z. Muhammad Adeel, L. Yang, A. Scarlett, V.J. Mohan, Electrochemical sensing of oxalic acid using silver nanoparticles loaded nitrogen-doped graphene oxide, Carbon trends 8 (2022) 100188.
[29] M.A. Zafar, M.V. Jacob, Synthesis of free-standing graphene in atmospheric pressure microwave plasma for the oil-water separation application, Applied Surface Science Advances 11 (2022) 100312.
[30] K.-Y. Law, Definitions for Hydrophilicity, Hydrophobicity, and Superhydrophobicity: Getting the Basics Right, The journal of physical chemistry letters 5(4) (2014) 686-688.
[31] M. Ramiasa-MacGregor, A. Mierczynska, R. Sedev, K. Vasilev, Tuning and predicting the wetting of nanoengineered material surface, Nanoscale 8(8) (2016) 4635-4642.
[32] L. Lv, Y. Xie, K. Li, T. Hu, X. Lu, Y. Cao, X. Zheng, Unveiling the Mechanism of Surface Hydrophilicity-Modulated Macrophage Polarization, Advanced healthcare materials 7(19) (2018) e1800675-n/a.
[33] R.M. Visalakshan, M.N. MacGregor, S. Sasidharan, A. Ghazaryan, A.M. Mierczynska-Vasilev, S. Morsbach, V. Mailänder, K. Landfester, J.D. Hayball, K. Vasilev, Biomaterial Surface Hydrophobicity-Mediated Serum Protein Adsorption and Immune Responses, ACS Applied Materials & Interfaces 11(31) (2019) 27615-27623.

[34] C.G. Sokolik, J.-P. Lellouche, Hybrid-silica nanoparticles as a delivery system of the natural biocide carvacrol, RSC advances 8(64) (2018) 36712-36721.
[35] Database, XPS (X-ray Photoelectron Spectroscopy), XPS Spectra – Chemical Shift|Binding Energy http://techdb.podzone.net/xpsstate-e/ (2015).
[36] J. Romo-Rico, S. Murali Krishna, J. Golledge, A. Hayles, K. Vasilev, M.V. Jacob, Plasma polymers from oregano secondary metabolites: Antibacterial and biocompatible plant-based polymers, Plasma processes and polymers 19(7) (2022) n/a.
[37] J.H. María, M. Denise, B. Igor, N. Victor, O.-I. Gonzalo, Chemical Changes of Graphene Oxide Thin Films Induced by Thermal Treatment under Vacuum Conditions, Coatings (Basel) 10(2) (2020) 113.
[38] J. Augustyn-Pieniazek, A. Lukaszczyk, R. Zapala, Microstructure and Corrosion Resistance Characteristics of Cr-Co-Mo Alloys Designed for Prosthetic Materials, Archives of metallurgy and materials 58(4) (2013) 1281.
[39] M.V. Jacob, R.S. Rawat, B. Ouyang, K. Bazaka, D.S. Kumar, D. Taguchi, M. Iwamoto, R. Neupane, O.K. Varghese, Catalyst-Free Plasma Enhanced Growth of Graphene from Sustainable Sources, Nano Letters 15(9) (2015) 5702-5708.
[40] Y.-L. Fan, H.-C. Zhao, B. Li, Z.-L. Zhao, X.-Q. Feng, Mechanical Roles of F-Actin in the Differentiation of Stem Cells: A Review, ACS biomaterials science & engineering 5(8) (2019) 3788-3801.
[41] L. Kirchhoff, D. Arweiler-Harbeck, J. Arnolds, T. Hussain, S. Hansen, R. Bertram, J. Buer, S. Lang, J. Steinmann, B. Höing, Imaging studies of bacterial biofilms on cochlear implants-Bioactive glass (BAG) inhibits mature biofilm, PloS one 15(2) (2020) e0229198-e0229198.
[42] Y. Tu, M. Lv, P. Xiu, T. Huynh, M. Zhang, M. Castelli, Z. Liu, Q. Huang, C. Fan, H. Fang, R. Zhou, Destructive extraction of phospholipids from Escherichia coli membranes by graphene nanosheets, Nat Nanotechnol 8(8) (2013) 594-601.
[43] B. Luan, T. Huynh, R. Zhou, Complete wetting of graphene by biological lipids, Nanoscale 8(10) (2016) 5750-5754.
[44] L. Wu, L. Zeng, X. Jiang, Revealing the Nature of Interaction between Graphene Oxide and Lipid Membrane by Surface-Enhanced Infrared Absorption Spectroscopy, Journal of the American Chemical Society 137(32) (2015) 10052-10055.

Chapter 6

Conclusion

Chronic wounds are a significant healthcare challenge, impacting the quality of life of patients and posing a substantial burden to healthcare systems worldwide. Biofilms and antibiotic-resistant bacteria are factors that complicate chronic wounds. Moreover, oxidation and inflammation can impair wound-healing. Antioxidants, as physical barriers that neutralize ROS, hold promise in reducing inflammation and preventing the activation of pro-inflammatory cytokines and pathways. Addressing these challenges requires a multidisciplinary approach and continued research to improve the management of chronic wounds.

Chronic inflammation, oxidative stress, and bacterial infection are known to cause delayed wound-healing. Therefore, targeting these factors is essential for effective wound-healing. The development of plasma coatings for medical applications has been a subject of growing interest in recent years. In this research project, RF plasma coatings derived from oregano secondary metabolites were designed and investigated for their potential use in wound-healing and implant coatings. The use of plasma polymer films, specifically oregano-based plasma polymers, have shown promising results in addressing these factors, exhibiting antioxidant, anti-inflammatory, antibacterial, and biocompatible properties.

Literature review on the potential application of PSMs-based polymers is carried out and reported in Chapter 2. Based on the analysis it is found that delayed wound-healing can be caused by chronic inflammation, oxidative stress, and bacterial infection. To effectively promote wound-healing, it is important to target these factors by downregulating pro-inflammatory cytokines and ROS and protecting against bacterial infection and biofilm formation. PSMs have been shown to have antioxidant, anti-inflammatory, and antibacterial properties, and can be incorporated into wound dressings using various polymerization techniques, including radiofrequency plasma enhanced chemical vapor deposition. However, further clinical studies are needed to test the *in vivo* wound-healing properties of PSMs-based wound dressings. Despite these challenges, the potential applications of PSMs in wound dressings are promising.

Plasma polymer films were successfully developed from oregano monomer using RF-PECVD at various RF power levels, and the procedures and properties of the oregano-based plasma polymer thin films are reported in Chapter 3. The resulting PP-OSMs exhibited hydrophilic

and superhydrophilic surfaces and retained functional groups from the oregano monomer. Coating leachate of the PP-OSMs modified the pH of the media used. PP-OSMs exhibited bactericidal and antifouling properties against Gram-negative *P. aeruginosa* and Gram-positive *S. aureus*, respectively. In addition, the PP-OSMs was found to support the growth and proliferation of fibroblasts without causing significant cytotoxicity. The adhesion and spread of fibroblasts on PP-OSMs were also observed. These findings suggest that PP-OSMs has potential applications in medical fields, particularly in wound dressings where antibacterial and biocompatible properties are essential.

In chapter 4 the wound-healing properties of an oregano-based plasma polymer (OPP) is reported. It has been found that oregano-based plasma polymer (OPP) is biocompatible with RAW 264.7 macrophages, as it did not activate a pro-inflammatory response and did not cause ROS activation. In fact, OPP showed potential antioxidant activity in LPS treated RAW 264.7 macrophages. *In vitro* wound-healing assay showed that OPP accelerated the closure rate of human foreskin fibroblasts, which reached 90% closure after 18 hours and full closure after 30 hours. This suggests that OPP has potential as a wound-healing interface for dressings and bandages, as it provides mammalian cell support, antioxidant activity, inflammation prevention, enhanced cell proliferation, antibacterial and antifouling properties. However, further research is needed to fully understand the mechanism of action and effectiveness of OPP in wound-healing, and to validate these findings in *in vivo* models.

The manufacturing of high-quality Graphene (Gr) from *Origanum vulgare* carbon source on CoCr substrates using RF-PECVD is reported in chapter 5. The presence of graphene in the CoCr-Gr sample was confirmed using Raman spectroscopy and X-ray photoelectron spectroscopy. The SEM microscopies revealed that graphene was present in the form of nanostructures with a variety of nanometric shapes and sizes. The biocompatibility results of CoCr-Gr were investigated, and it was found that both CoCr and CoCr-Gr had similar viability, adhesion, and morphology of RAW macrophages after 48 hours of incubation. Additionally, the bactericidal and antifouling effect of CoCr-Gr was significantly higher against *P. aeruginosa* when compared to the control. Furthermore, CoCr-Gr was also found to be bactericidal against S. aureus. Overall, the results of this study suggest that CoCr-Gr has promising potential as an antibacterial coating material for implantable devices.

In conclusion, this research project has explored the potential applications of various plasma polymer films for medical purposes, particularly in wound dressings and implantable devices. The literature review in chapter 2 highlighted the importance of targeting chronic inflammation, oxidative stress, and bacterial infection to promote wound-healing, and

suggested that PSMs-based polymers have promising antioxidant, anti-inflammatory, antibacterial and wound-healing properties. Chapters 3 and 4 investigated the properties of oregano-based plasma polymer films, and found that they exhibit antibacterial and biocompatible properties, as well as potential antioxidant and wound-healing properties. Chapter 5 explored the potential of plasma fabricated graphene from *Origanum vulgare* as an antibacterial coating material for implantable devices. Graphene deposited on CoCr substrates had significant bactericidal and antifouling properties. Overall, this research project highlights the potential of using oregano for developing plasma polymer films and graphene as materials for medical applications and provides a foundation for future studies to further investigate and develop these materials for use in medical devices. This research not only assisted in developing procedures for developing sustainable biomaterials but also find added values to the agricultural produce.

6. 1. Future work

The studies presented in these chapters highlight the potential of plasma polymer films and graphene as materials for medical applications, particularly in wound dressings and implantable devices. However, there is still a need for further research to fully understand the mechanisms of action and effectiveness of these materials *in vivo*.

Future studies could investigate the *in vivo* wound-healing properties oregano-based wound dressings and explore their potential as alternatives to traditional wound dressings. Further research could investigate the use of PSMs-based wound dressings in combination with other materials to enhance their wound-healing properties. In addition, the long-term stability and wound-healing properties of these films *in vivo* would be an interesting topic of study.

Other studies could focus on investigating the immune response of cells when interacting with CoCr-Gr coatings as well as with animal models.

All the mentioned recommendations are with the aim of eventually translating these findings into clinical applications.

Overall, the potential of plasma polymer films and graphene as materials for medical applications is promising, and further research could lead to the development of novel and effective medical devices and treatments.